University of Alberta

An RGD-Containing-Polymer to Promote Local Bone Regeneration

by

Erin Elizabeth Smith ©

A thesis submitted to the Faculty of Graduate Studies and Research in partial fulfillment of the requirements for the degree of Master of Science

Department of Biomedical Engineering

Edmonton, Alberta

Spring, 2002

National Library of Canada
Acquisitions and Bibliographic Services
395 Wellington Street
Ottawa ON K1A 0N4
Canada

Bibliothèque nationale du Canada
Acquisitions et services bibliographiques
395, rue Wellington
Ottawa ON K1A 0N4
Canada

Your file Votre référence

Our file Notre référence

The author has granted a non-exclusive licence allowing the National Library of Canada to reproduce, loan, distribute or sell copies of this thesis in microform, paper or electronic formats.

L'auteur a accordé une licence non exclusive permettant à la Bibliothèque nationale du Canada de reproduire, prêter, distribuer ou vendre des copies de cette thèse sous la forme de microfiche/film, de reproduction sur papier ou sur format électronique.

The author retains ownership of the copyright in this thesis. Neither the thesis nor substantial extracts from it may be printed or otherwise reproduced without the author's permission.

L'auteur conserve la propriété du droit d'auteur qui protège cette thèse. Ni la thèse ni des extraits substantiels de celle-ci ne doivent être imprimés ou autrement reproduits sans son autorisation.

0-612-69760-6

Canada

University of Alberta

Library Release Form

Name of Author: Erin Elizabeth Smith

Title of Thesis: An RGD-containing Polymer to Promote Local Bone Regeneration

Degree: Master of Science

Year this Degree Granted: 2002

Permission is hereby granted to the University of Alberta Library to reproduce single copies of this thesis and to lend or sell such copies for private, scholarly or scientific research purposes only.

The author reserves all other publication and other rights in association with the copyright in the thesis, and except as herein before provided, neither the thesis nor any substantial portion thereof may be printed or otherwise reproduced in any material form whatever without the author's prior written permission.

15/04/01

15/04/02.

Erin Elizabeth Smith
4826 Petworth Road
R.R. #1 Harrowsmith, ON
K0H 1V0

University of Alberta

Faculty of Graduate Studies and Research

The undersigned certify that they have read, and recommend to the Faculty of Graduate Studies and Research for acceptance, a thesis entitled An RGD-containing Polymer to Promote Local Bone Regeneration submitted by Erin Elizabeth Smith in partial fulfillment of the requirements for the degree of Master of Science.

Dr. H. Uludag (Supervisor)
Department of Chemical & Materials Engineering

Dr. L. McGann (Committee Member)
Department of Laboratory Medicine & Pathology

Dr. Z. Xu (Committee Member)
Department of Chemical & Materials Engineering

Date: April 12/02

ABSTRACT

The ultimate goal of this thesis was to design a biomaterial to enhance cell adhesion while retaining BMP-2 at a coinjected site, resulting in increased local osteoinductive activity. Peptides containing the Arginine-Glycine-Aspartic Acid sequence were conjugated to thermoreversible N-isopropylacrylamide (NiPAM) copolymers via protein-reactive N-acryloxysuccinimide (NASI) groups. ^{1}H-NMR was used to confirm successful conjugation. The peptide/polymer yield in the conjugates was directly correlated to the concentration of peptide in the conjugation reaction, decreasing from 3.8 to 0.7 peptides/polymer chain as the peptide concentration decreased from 2.5 to 0.5 mg/mL. The conjugation efficiency was determined to be ~8.5% using Reverse Phase High Pressure Liquid Chromatography (RP-HPLC). C2C12 cell adhesion to RGD-conjugated polymer surfaces was significantly higher than adhesion on NiPAM/NASI surfaces and was morphologically comparable to adhesion on TCPS control surfaces. The increased adhesion on the RGD-conjugated surfaces was directly correlated to the peptide surface density (max. ~3.4 nmol/cm^2). BMP-2 treatment induced osteoblastic differentiation in C2C12 cells (as assessed by the induction of ALP activity) in a dose dependent manner. In the absence of BMP-2 treatment, cells cultured on RGD-conjugated surfaces expressed higher levels of ALP activity than those cells cultured on TCPS surfaces, indicating that the conjugated RGD sequence induces osteoblast activity in C2C12 cells without the need for BMP-2 treatment. The RGD-containing polymers offer a viable biomaterial for local bone regeneration *in vivo*.

ACKNOWLEDGEMENTS

The author gratefully acknowledges the materials generously provided by Dr. Civetilli (University of Washington, St. Louis, MO) and Dr. Sebald (Universitait Wurzburg, Wurzburg, Germany). I would like to thank Dr. Somayaji (University of Alberta) for his skillful technical assistance with NMR analysis and Dr. McGann (University of Alberta) for allowing me the use of his tissue culture facilities, and for his guidance. I would also like to thank Dr. Xu and Dr. Snyder (University of Alberta) for their feedback on the writing and presentation of this thesis. In addition, I would like to acknowledge the Canadian Institutes of Health Research (CIHR), whose support and grant funding made this research possible.

I would also like to thank my supervisor, Dr. Uludag for his knowledge and expertise, as well as his guidance and patience. Finally, I would like to thank Sebastien, Asif, and Jennifer, for their feedback, continued support and friendship. I have learned a great deal from all of you. Best wishes and good luck.

TABLE OF CONTENTS

INTRODUCTION 1

PROJECT RATIONALE 22

EXPERIMENTAL

A. Materials 26
B. Polymer Synthesis and Characterization 27
C. Quantifying RGD-Containing Peptide-Polymer Conjugation 29
D. Coating Techniques to Obtain RGD-Containing Surfaces 31
E. Cell Attachment to Polymer Films 33
F. Cell Response to BMP-2 35
G. Experimental Designation 36

RESULTS & DISCUSSION

Phase I: Creating an RGD-containing-polymer

A. Quantifying Peptide-Polymer Conjugation Using NMR 37
B. Quantifying Peptide-Polymer Conjugation Using RP-HPLC 43
C. Hydrolysis and Stability of the Peptide-Polymer Conjugation Reaction 47

Phase II: Confirming Bioactivity of Conjugated RGD Sequence

A. C2C12 Cell Attachment to NiPAM/NASI Copolymer Using Hemacytometer 50
B. C2C12 Cell Attachment to NiPAM/NASI Copolymer Using Coulter Counter 52
C. Effects of Cell Density on Cell Attachment to NiPAM/NASI Copolymer 56
D. C2C12 Cell Attachment to RGD-containing Copolymers 58
   I. Single Coat 59
   II. Bulk Coat 60
   III. Two-Coat 61
   IV. Surface Conjugation 63
E. Cell Attachment by MTT Assay 68
F. The Effects of Different Polymers on C2C12 Cell Attachment 73
G. Effectiveness of Techniques to Quantify Cell Adhesion 77
H. GRGDS-Dose Dependent Cell Attachment 82
I. Cell Density Effects on Cell Growth on Polymer Films 87
J. Non-Specific Adhesion Studies 90

Phase III: Cell Response to BMP-2 When Cultured on RGD-containing Polymers

A. C2C12 Cell Response to BMP-2 93
B. Cell Response to BMP-2 When Cultured on GRGDS-Conjugated Surfaces 101
C. Cell Density Effects on Cell Response to BMP-2 104

CONCLUSIONS 110

FUTURE DIRECTION 112

REFERENCES 114

APPENDICES

A. ^{1}H-NMR Spectra 121

LIST OF TABLES

INTRODUCTION

Table 1	Cellular Response Studies Using NiPAM Polymers	12
Table 2	Cellular Response Studies Incorporating RGD into Biomaterials	18

EXPERIMENTAL

Table 3	NiPAM Copolymer Compositions	29
Table 4	RP-HPLC Elution Conditions	30
Table 5	Surface Coating Techniques	32

RESULTS & DISCUSSION

Table 6	^{1}H-NMR Spectra Analysis for Arginine, Glycine, and Aspartic Acid and the RGD tripeptide	39
Table 7	Initial RP-HPLC studies to characterize materials and conjugation reaction efficiency	43
Table 8	RP-HPLC quantification of GYRGDS conjugation efficiency	44
Table 9	C2C12 cell adhesion to TCPS and NiPAM/NASI surfaces	50
Table 10	Cell density effects on cell adhesion to NiPAM/NASI surfaces	57
Table 11	Cell adhesion to RGD-conjugated surfaces, applied using the 'Bulk Coat' Technique	60
Table 12	Cell adhesion to RGD-conjugated surfaces, applied using the 'Two-Coat' Technique, modified to use HBSS as the solvent	63
Table 13	Cell adhesion to GYRGDS-conjugated surfaces, applied using the 'Surface Conjugation' Technique	65
Table 14	Cell response to RGD incorporation into biomaterials at varying peptide surface densities	67
Table 15	MTT assay quantified cell adhesion to GYRGDS-conjugated Surfaces	72
Table 16	BMP-2 induced ALP activity in C2C12 cells	95

LIST OF FIGURES

INTRODUCTION

Figure 1	Chemical structure of NiPAM (A) and NASI (B) monomers	10
Figure 2	Chemical structure of RGD tripeptide	16

RESULTS & DISCUSSION

Figure 3	Schematic presentation of peptide/polymer conjugation reaction	38
Figure 4	^{1}H-NMR spectrum for NiPAM/NASI polymer	42
Figure 5	^{1}H-NMR spectrum for RGD-containing NiPAM/NASI polymer	42
Figure 6	Photographs illustrating C2C12 cell adhesion on TCPS (A) and NiPAM/NASI (B) surfaces	52
Figure 7	Cell adhesion to TCPS and NiPAM/NASI surfaces	53
Figure 8	Cell adhesion to RGD-conjugated surfaces created using the 'Two-Coat' technique	62
Figure 9	Photographs illustrating cell adhesion on GRGDS-conjugated surfaces (A), as compared to TPCS (B) and NiPAM/NASI (C)	65
Figure 10	Comparison of cell adhesion data obtained using the Coulter Counter (top) and MTT assay (bottom) methods	71
Figure 11	Cell adhesion to JY-2 NiPAM/NASI polymer surface and GYRGDS-conjugated surfaces using the JY-2 polymer	74
Figure 12	Cell adhesion to various NiPAM copolymers and NiPAM copolymers modified to contain the RGD sequence	76
Figure 13	Photographs illustrating cell adhesion on TCPS (A) and NiPAM/EMA (B) surfaces	77
Figure 14	GRGDS dose dependent cell adhesion	84
Figure 15	Cell proliferation on polymer films at high (A) and low (B) seeding densities	88
Figure 16	Non-specific cell adhesion to GRGES-conjugated surfaces	91
Figure 17	Photographs illustrating adhesion to GRGES-conjugated (A) and GRGDS-conjugated (B) surfaces	92
Figure 18	BMP-2 induced ALP activity in C2C12 cells	97
Figure 19	BMP-2 dose dependent response in ALP activity expressed by C2C12 cells	99
Figure 20	Effects of the cell seeding density on the cell response to BMP-2 treatment	106
Figure 21	Effects of BMP-2 treatment on the cell metabolic activity	108

APPENDIX A 121

Figure A1	^{1}H-NMR spectrum for Glycine (Aldrich)	122
Figure A2	^{1}H-NMR spectrum for Arginine (Aldrich)	122
Figure A3	^{1}H-NMR spectrum for Aspartic Acid (Aldrich)	123
Figure A4	^{1}H-NMR spectrum for RGD, obtained in our lab.	124

ABBREVIATIONS

BMP:	Bone Morphogenetic Protein
ECM:	Extracellular Matrix
LCST:	Lower Critical Solution Temperature
MW:	Molecular Weight
NiPAM:	N-isopropylacrylamide
NASI:	N-acryloxysuccinimide
MMA:	methylmethacrylate
EMA:	ethylmethacrylate
TCPS:	Tissue Culture Polystyrene
R:	Arginine
G:	Glycine
D:	Aspartic Acid
S:	Serine
Y:	Tyrosine
E:	Glutamic Acid
NMR:	Nuclear Magnetic Resonance
RP-HPLC:	Reverse-Phase High Pressure Liquid Chromatography
MTT:	3-(4,5-dimethyl-thiazol-2-yl)-2,5-diphenyl-tetrazolium bromide
ALP:	Alkaline Phosphatase
PNP:	p-Nitrophenol Produced
FBS:	Fetal Bovine Serum
HBSS:	Hank's Balanced Salt Solution

INTRODUCTION

The human body is an incredible phenomenon. It is composed of a vast interconnected network of organs, tissues, cells and proteins. The functioning of the human body is the single most complex and mysterious thing known to mankind. Perhaps the biggest mystery is the body's ability to regenerate and repair itself, to a certain extent; like many other tissues, our bones are constantly in a cycle of renewal. Unfortunately, nothing lasts forever and for a variety of reasons, be they accidental, illness or age-related, at some point the cycles of renewal slow down and become less efficient and the body begins to deteriorate. The field of Biomedical Engineering incorporates the study of these cycles with the technology and innovation of engineering; it is the pursuit of developing techniques that will aid the human body in its infinite quest to repair itself.

Bone Tissue Engineering: Past, Present and Future

Osteoporosis is a common disease amongst today's elderly society, becoming more predominant in older women especially. It is characterized by a systemic reduction in bone mineral density caused by an imbalance in the activity between osteoclast and osteoblast cells. This is to say that bone is resorbed by the osteoclasts faster than the osteoblasts can deposit it naturally at the specific site, resulting in bone with reduced mineral mass [1]. While these specific processes will not be discussed in further detail here, a thorough account of the basic biology of bone formation and repair is available through other sources [2]. The systemic imbalance results in local defects in bones

throughout the body and as such, osteoporotic patients are prone to bone fractures. Although the disease is systemic, it is the consequences of individual local defects (fractures) that are the cause of so much pain and discomfort for many of our elders.

Traditional treatment for these osteoporotic patients, and others who suffer from a sudden bone fracture, due to excessive loss of mineral mass, has been bone tissue transplantation, i.e. bone grafting. Studies have shown that autogenic (tissue from patient) and allogenic (tissue from bone banks) bone grafting are effective methods of replacing lost bone mass [2]. Unfortunately, there are still many issues to be resolved before bone-grafts will be deemed a complete success. Tissue mortality and sterility (autografts), and disease transmission and immunogenicity (allografts) are some of the significant issues at hand. Another widely studied area of treatment involves the use of therapeutic agents, such as estrogen, bisphosphonates, and calcitonin, all of which have the ability to slow the bone resorption systemically (i.e. throughout the body), thus eliminating the imbalance. These agents are used for systemic therapy, which, unfortunately doesn't provide an ideal solution. These methods are effectively able to prevent any further bone loss, but there are no current treatments, which are able to restore the bone mass that has already deteriorated [3].

We have entered into a new era of medicine, where the focus is not only preventative, but regenerative as well. Bone Tissue Engineering has become a significant area of research, offering many opportunities for employment and receiving substantial amounts of funding from a variety of sources. As discussed elsewhere [2], there are three main areas of research within the field of Bone Tissue Engineering. These are (i) local bone regeneration, (ii) engineering biomaterial-bone interfaces to enhance integration of

biomaterial implants, and (iii) reversal of systemic degeneration in bone structure. The primary focus of the Bone Tissue Engineering field and incidentally, the focus of these writings, is local bone regeneration, i.e. regenerating bone at a specific skeletal site where, due to disease, trauma and/or bone removal, the bone integrity has been significantly compromised. The experimental regenerative techniques currently experiencing the most success, naturally, incorporate the three critical components of real bone: viable cells, an extracellular matrix (ECM) to support them, and growth factors to supplement them.

Role of Bone Morphogenetic Proteins in Regenerating Bone Tissue

A new class of drugs has evolved, which show excellent potential to stimulate new bone formation. They are based on protein growth factors (GF), which are endogenous proteins that have been shown to be effective in stimulating bone regeneration [4]. One such example of this new class of drugs is Bone Morphogenetic Proteins (BMP), whose ability to stimulate local bone regeneration is being assessed in clinical trials. BMP is critical to bone formation because of its effect on noncommitted, pluripotent cells at the implant site. It provides the primary signal for these cells to differentiate into osteoblasts, which are bone-depositing cells [5]. Recombinant forms of BMP (in particular BMP-2 and BMP-7) have been shown to induce healing of segmental defects in a number of species, including nonhuman primates [6-8], as well as in humans [9,10]. However, not all BMP-containing devices have yielded successful bone regeneration; reasons for this failure may be related to the fact that BMPs are lost at the implant site quickly [11].

The lack of optimal matrices for controlled, sustained BMP delivery at the site of implantation is believed to be largely responsible for the failure of BMP therapy. Numerous studies have shown that the osteoinductive activity at a particular injection site is directly correlated to the concentration of injected BMP retained at that site [2,5,14, 16]. A carrier able to effectively retain more of the drug at the site of injection would reduce the dosage required, thereby lowering costs incurred, while also reducing overall levels of drug in the subject, which could possibly migrate to other sites. The use of a bone-targeting strategy would eliminate misguided deposition of the drug and ideally, the undesirable side-effects, while still delivering the BMP to an intended site, where it can effectively stimulate bone formation. A biomaterial carrier would effectively mimic an ECM, providing a controllable matrix to support sustained BMP delivery at a local site of administration.

Biomaterial Carriers for Advanced Drug Delivery

Various biomaterials have been developed and employed in studies to accelerate natural occurring phenomena involved in the healing process. The beneficial attributes and functions of natural materials are maintained and combined with synthetic materials to create biomaterials. These biomaterials are specifically engineered to make use of the necessary natural biology but allow it to be controlled and manipulated through the use of lower cost, easily duplicated, synthetic materials [13].

There are a variety of biomaterials currently being used for drug delivery applications. For a carrier to successfully deliver therapeutic agents resulting in bone regeneration, it needs to be conducive to cell recruitment, attachment, expansion,

differentiation and the interactions of the cellular elements with ECM proteins. When designing the optimal carrier system, some of the critical characteristics to consider should include surface chemistry, surface charge, surface texture, pore size range, void volume, biodegradation rates, hydrophobicity and hydrophilicity, crystallinity, and release kinetics of incorporated molecules (if any) such as growth factors [14]. Many of the successful biomaterial carriers share common characteristics. However, there is no one single trait or a single universal carrier that will be suitable for all tissue engineering applications; most carriers will need to be uniquely engineered for each specific application. It is very difficult to categorize all the different biomaterials currently employed in drug delivery applications and rank their effectiveness. This is not possible because of the different evaluation techniques used for the performance of biomaterials. There is, however, a division in their mode of delivery. Traditional biomaterials (i.e. those which have been in use for 10 years or more) are typically implanted, while the newer generations also include those that can be injected.

Typically, the implantable carriers are used as osteoconductive scaffolds, i.e. scaffolds that allow ingrowth of osseous tissue, while stimulating its regeneration at the site. Biomaterials used for this purpose include bovine collagen, demineralized bone matrix, calcium phosphate ceramics, bioglasses, organoapatites, polylactide (PL) homopolymers, poly(lactide-co-glycolide) polymers (PLG), polyanhydrides, organophosphates, and polyphosphazenes, as reviewed by S.R. Winn et al. [14]. All of these have experienced some degree of success: collagen is the major protein in bone, making it an ideal choice; PL and PLG polymers are also proven to be safe, effective and biodegradable, the combination of which defines biocompatibility. Unfortunately, there

are drawbacks associated with each material. As examples, calcium alginate is immunogenic and relatively nondegradable, while copolymers of poly(ethylene oxide) (PEO) and poly(propylene oxide) (PPO) lack structural integrity and do not allow cell attachment [17]. In the cases of virtually all biomaterials, 'batch' variations may unexpectedly alter the desired cellular response. There may be unwanted contaminants, residuals or byproducts from polymerization processes, such as solvents and catalysts, as well as variations in crystallinities within the same polymer, which will influence both the biocompatibility and biodegradation and ultimately, their effectiveness for a biological response [14]. Regardless of their successes and failures, all of these biomaterials are associated with one common significant drawback: they are *implantable* carriers, which requires that they be *surgically implanted*. The need to eliminate undesirable, invasive surgical procedures has lead to the exploration of injectable biomaterials. As an attractive alternative to implants, the injectable mode of delivery is less invasive and more attractive for the target population, i.e. the elderly.

The injectable biomaterials need to be intelligent. They should not only be soluble in aqueous systems (allowing them to be injectable), but they must retain the proteins at the site of injection. Thermoreversible biomaterials offer on such possibility: these temperature-responsive, 'smart' polymers are able to respond to small stimuli (in this case, temperature) with large property changes (in this case, solubility). They are employed in many different forms, including dissolved in aqueous solutions, adsorbed or grafted on aqueous-solid interfaces, or crosslinked in the form of hydrogels [15]. In addition to temperature, they can be engineered to respond to a variety of environmental stimuli, such as radiation and pH, and in many cases, this response is reversible – a trait

which makes these materials doubly smart. They are used in numerous applications, such as enzyme recycling, antibody recovery, immunoassays, and of course, drug delivery [15]. Perhaps the most appealing type of these polymers, for use in drug delivery, are those whose critical stimulus is temperature. Temperature sensitive polymers have the ability to undergo a phase change from a soluble system to insoluble, allowing them to entrap a co-injected biological molecule, once stimulated. Temperature induced changes allow for a simple, clean and effective carrier for sustained release of a particular therapeutic agent, without the need to introduce exogenous molecules to the polymer system. Therefore, in practice, one can combine the protein and the biomaterial in a laboratory setting, store it at low temperature (e.g. fridge), inject it and observe as a phase change occurs, encapsulating the protein at physiological temperature.

The behavioral properties of thermoresponsive polymer systems are dependant upon one very significant characteristic – the lower critical solution temperature (LCST). The LCST is the temperature at which the polymers exhibit a reversible phase change, i.e. below the LCST, the polymer is soluble in water-based solvents and above the LCST it exhibits phase separation insolubility and in some cases, precipitation. Manipulating a polymer system to exhibit a desired LCST has become a relatively simple task; copolymerization with a more hydrophilic monomer will increase the LCST and copolymerization with a more hydrophobic monomer will lower it [15]. The LCST phenomenon makes thermoresponsive polymers very attractive for *in vivo* applications; this material is designed so that it may be injected in the liquid form to a specific site, where it will become insoluble at the physiological temperature [5]. The experimental work described later in these writings makes use of such a polymer, with the idea of

creating a three-dimensional gel matrix at a specific injection site, where bone will form *in situ*.

Typically, a thermoresponsive polymer in an aqueous solution will collapse above its LCST, forming micellar-like structures. The water will be excluded from the polymer, converting it from hydrophilic to hydrophobic. Since many drugs are hydrophobic in nature, as the polymer collapses, it encapsulates the drug within itself; this has proven to be very effective in a number of applications. For example, Chung et al. were able to show that N-isopropylacrylamide (NiPAM) was also an effective biomaterial for drug delivery [18-20]. Their studies show that NiPAM micelles encapsulating adriamycin (ADR) exhibited higher cytotoxic activity than free ADR above LCST, but were lower than free ADR below LCST. NiPAM can effectively and selectively release a co-injected drug, making it an excellent biomaterial choice for drug delivery applications. The drug is protected within the hydrophobic core of the polymer micelles while still retaining its active/passive targeting mechanisms (if any) and overall bioactivity. Retention of the drug's viable bioactive characteristics throughout modification is a crucial consideration for any application involving biomolecules.

In addition to physical entrapment, it is possible to use crosslinking agents to conjugate therapeutic molecules to these polymers and, in many cases, this is an effective way of obtaining successful sustained drug delivery. Naturally, crosslinked drugs stay at the injection site if the biomaterial is also retained at this site. However, the use of crosslinkers requires an extra step during the process of drug delivery and, in some cases, may require complicated chemistry. As well, with every additional step in the procedure, the possibility of altering the bioactivity is increased, and can cause non-

specific modification to the biomolecule. Fortunately, there are ways to avoid using crosslinking agents altogether. Many of the therapeutic agents used for bone tissue engineering are proteins in nature and as such, contain a variety of reactive functional groups (such as amine and thiol moieties), which are amenable for modification in these types of applications. There are a number of protein-reactive monomer units, which have, in recent years been incorporated into smart polymers to prepare pre-activated materials. The most well known monomers are amino-reactive epoxide, maleic anhydride and succinimide esters, and thiol-reactive vinylsulfone and maleimide [21]. As with most biomaterial applications, the choice of monomer unit depends on the protein that it is to be conjugated with, and the chemistry is unique for each specific reaction. A thorough understanding of the properties and reaction kinetics of all materials involved will allow for the optimization of the conjugation process and improved specificity and reactivity of the evolved system. For most protein-polymer conjugate systems, in addition to controlling the protein delivery kinetics, the polymer is also responsible for mediating the cellular response upon injection [22].

In the specific case of thermoresponsive polymers, the hydrophobicity of the polymers has an enormous impact on the polymer's compatibility with cells; cells will only adhere to certain surfaces and will detach if that environment changes, as many different researchers have shown [19, 23-27]. These studies have confirmed that cells adhere well to moderately hydrophobic or ionic surfaces (tissue culture polystyrene (TCPS), silicon, silicone rubber (SR), polyethylene oxide (PEO)), but do not adhere well to hydrophilic, nonionic surfaces (polyethylene glycol (PEG), polyacrylamide (PAAm), polyvinylpyrrolidone (PVP), polyethylene terephthalate (PET)). These results are most

likely related to the protein adsorption characteristics of the different surfaces. Cells do not bind directly to synthetic materials. Hydrophobic polymers, on the other hand, readily adsorb serum proteins and hydrophilic polymers do not, to the extent that they are used to inhibit protein adsorption [27]. The water content of a hydrogel is also thought to play a major role in deciding which surfaces cells will adhere to. Materials with a high water content are too soft to withstand the mechanical forces involved in cell attachment [23] and high water content is protein repulsive.

When it comes to cell attachment to biomaterials, thermoresponsive polymers provide an interesting surface for cell attachment: their hydrophilicity/hydrophobicity in any given situation depends on the temperature. One of the most widely studied thermoresponsive polymers is NiPAM. It has an LCST of 32 °C in water and has been shown to successfully copolymerize with protein reactive N-acryloxysuccinimide (NASI) monomers [21,22]. Chemical structures of NiPAM and NASI are illustrated in Figures 1A and 1B, respectively:

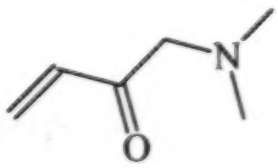

A

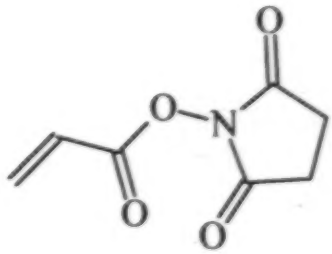

B

Figure 1 – The chemical structure of the NiPAM (A) and NASI (B) monomer units are illustrated here. The succinimde ester (in the NASI monomer) is the amine-reactive moiety where protein conjugation can take place.

Members of this lab group have also been able to show that NiPAM/NASI copolymers mixed or conjugated with BMP are able to effectively increase BMP retention at the local injection site [2]. There has been no studies done on the compatibility of cells with NiPAM-based biomaterials in this lab. Numerous other studies done using a variety of copolymers of NiPAM show that for a given polymer, the cellular response, i.e. the biocompatibility of the material, will vary somewhat with the cell type (Table 1).

Table 1 – Cellular Response Studies Using NiPAM Polymers

Study	Polymer	Cell Type	Observed Response
[17]	NiPAM-co-AA/ NiPAM Hydrogels	BAC	**Morphology:** Cells in 3-D hyrogels maintained characteristic round shape, while cells on 2-D TCPS caused dedifferentiation to fibroblastic morphology **ECM production:** Both hydrogels showed ECM deposition, indicating sustained cell viability; cells in NiPAM hydrogel were farther apart, due to more ECM being synthesized and secreted (closer resemblance to native articular cartilage) – this could, however be due to longer culture time in NiPAM.
[23]	NiPAM/NTBAM	NRK 49F	**Reversible attachment:** Adhesion to NiPAM/NTBAM surfaces was 4 times lower than on TCPS and was present in patches or as single cells. Cell patches adhered to polymer surfaces detached in sheets upon cooling below LCST, without trypsin.
[24]	NiPAM/AA	MF STO	**Protein Adsorption:** NiPAM/AA grafted surfaces inhibited albumin adsorption, but did not affect fibronectin adsorption. No significant difference in adsorption below LCST. **Reversible attachment:** In serum-free media, NiPAM/AA surfaces slightly increased cell spreading, as did fibronectin adsorption, whereas albumin adsorption decreased it. Cells on all surfaces, except those adhered to NiPAM/AA preadsorbed with fibronectin, albumin or serum, detached immediately, when cooled below LCST. Therefore, adhesion is regulated more by adhesion factor protein than physiochemical properties of polymer.
[25]	NiPAM/CCMS	BAE & RPE	**Morphology:** Both cell types grew to confluence on all surfaces and cell growth and morphologies appeared identical to TCPS. Respective Morphologies were retained when subcultured after detachment. **Reversible attachment:** Cells detached in sheets from both polymer surfaces upon cooling below LCST, but did not detach from TCPS.
[26]	NiPAM	HBM	**Reversible attachment:** Temperature change did not affect cell attachment or morphology on TCPS surfaces. Cells adhered to polymer surface (xx x/cm^2) decreased in size and detached upon cooling below LCST. Increased culture time on polymer surfaces increased adhesion strength, thereby decreasing number of cells to detach below LCST. Typical HBM morphology was retained in all cases, when replated on TCPS.

Polymers: NiPAM - N-isopropyl acrylamide; AA - acrylic acid; PBMA - poly(butylmethacrylate); NTBAM - N-t-butyl acrylamide; CCMS - 4-(N-cinnamoylcarbamide)methylstyrene **Cells:** BAC - bovine articular chondrocytes; BAE - bovine aortic endothelium; MF STO - mouse fibroblast STO cells; RPE - human retinal pigmented epithelium; HBM - human blood monocytes;

Although all of these studies found that the various NiPAM copolymers did in fact support adhesion, it was typically in clumps or individual cells, without much spreading [17,23-26]. As well, when compared to tissue culture polystyrene (TCPS) surfaces, cell adhesion on NiPAM surfaces was decreased significantly, and in the study of Collier et al, the size of the cells also decreased. Studies conducted by Rollason et al. Chen et al, Horst et al and Collier et al, show that the majority of cells adhered to the polymer surfaces detached in sheets upon cooling to temperatures below the LCST. These studies also showed that cell morphology was retained after subsequent replating, making thermoreversible attachment a very useful technique for harvesting sheets of differentiated cells intact, without the need for trypsin or other proteolytic enzymes.

The cellular preferences to specific surfaces appeared to be the limiting factor of all carriers; some cell types adhered and proliferated on NiPAM surfaces, but not all. Since an osteoinductive event is dependent on the presence of the responding cell population, increasing the local cell population will increase the regeneration at that site [16]. This leads us to the notion of modifying the NiPAM polymer to contain a bioactive moiety, which will enhance adhesion and promote differentiation of virtually any cell type. Members of this group have previously shown that BMP will effectively induce osteoblastic differentiation when the appropriate cells are present, i.e. when implanted into the muscle site in rats [5]. Therefore, the ideal BMP carrier needs to not only control BMP retention at a site, but also recruit cells to the desired regeneration site. A through understanding of the cell-surface interactions responsible for anchorage-dependant cell adhesion to these biomaterial surfaces will be necessary to design an optimal carrier for BMP delivery.

The Role of the Arginine-Glycine-Aspartic Acid (RGD) Tripeptide in Cell Adhesion

As discussed in the previous section, the presence of an ECM is critical for cells to adhere, proliferate and differentiate; therefore, naturally, a biomaterial carrier must effectively mimic an ECM in order to be successful. Cell development and function is, in part mediated by a complex series of cell-cell and cell-ECM interactions, acting through a variety of ECM proteins and their corresponding cell surface receptors. Integrins represent a major family of cell-surface receptors that facilitate the adhesion between cells and the surrounding ECM [13]. Interactions between integrins and their ligands have been linked to many cellular processes including proliferation, differentiation, survival, motility, embryogenesis and apoptosis [28]. After the initial ligand binding, integrins form linkages to the cytoskeleton and regulate signal transmission. There is a significant amount of redundancy associated with ligand specificity between the different types of integrins. Consequently, a single integrin has the potential to elicit a variety of different cellular responses, depending on the type of integrin receptor expressed, the developmental stage of the cell and according to the composition of the surrounding ECM [13].

There are several ECM proteins, which play important roles in cell function and development, not the least of which, are adhesion proteins. Adhesion is the first and perhaps most critical function that a cell must achieve; in the case of osteoblasts, adhesion triggers a variety of specific biochemical functions within the cell, including proliferation, migration, production and deposition of mineralized matrix [29]. Examples of these proteins include fibronectin, vitronectin, fibrinogen and collagen [30, 31]; some

are also found in blood, plasma and many other biological fluids. Adhesion proteins are important for cell adhesion to occur on natural surfaces, but they are absolutely critical in mediating adhesion to biomaterial surfaces. Many people supplement their *in vitro* tissue culture medium with serums, such as fetal bovine serum (FBS), because many types of serum contain a variety of the ECM proteins necessary for cell function and development.

Adhesion proteins have been used for Tissue Engineering purposes, the most common usage being to immobilize them to the material surface, where they form an adherent monolayer. As the proteins are adsorbed, the nearby water molecules are released, and the material interface exhibits an entropic gain, thereby reducing the free energy of the system [13]. Studies have shown that the adsorbed protein layer increases subsequent cell adhesion to the material surfaces, and this has become a common practice in designing biomaterials that are capable of directing desired cell behavior [13,28]. By immobilizing or grafting certain proteins and other biomolecules onto a material, it is possible to mimic the environment within the ECM, providing a multifunctional cell adhesive surface. Unfortunately, these proteins are fairly large (molecular weight (MW) >50,000 kD) and as such, are subject to denaturation and degradation when used therapeutically *in vivo*, and are therefore not suitable for long-term applications [1].

The integrin receptors bind to relatively small domains on their respective adhesion protein ligands and fortunately, these domains can be mimicked by synthetic oligopeptides. The oligopeptides can be prepared as linear sequences of as cyclic peptides. A synthetic oligopeptide (<1000 Da) behaves very similarly to a >100,000 Da protein in its binding affinity for the corresponding integrin receptor [13], while offering many advantages over their larger protein counterparts. Due to their smaller size, these

short peptide sequences can be incorporated at much higher concentrations than their parent proteins. Their simple, synthetic nature also allows for straightforward chemistry for incorporation into biomaterials [32]. In addition, the short peptides have proven to be relatively stable and much cheaper and easier to obtain and reproduce than the larger proteins [1], making them a much more effective and efficient alternative for enhancing cell adhesion on a surface.

The most widely studied cell adhesion sequence is the arginine-glycine-aspartic acid (RGD) tripeptide (Figure 2):

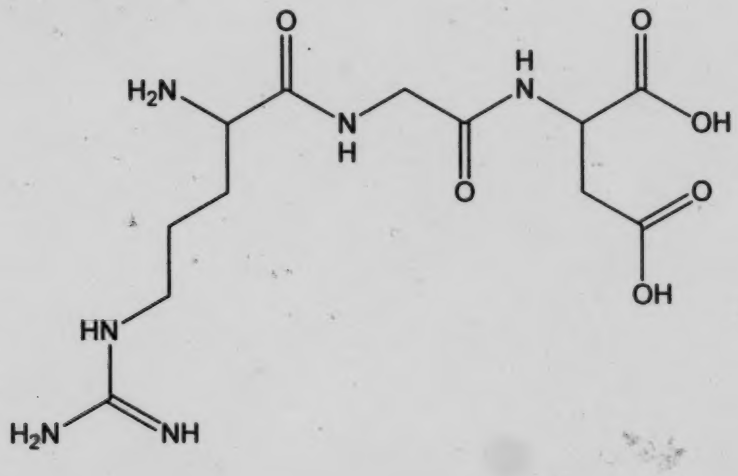

Figure 2 – The chemical structure of the minimal RGD peptide is shown here. While other RGD-containing peptides are discussed in this report and used in these studies, their structures are not herein illustrated.

RGD is contained within the cell binding domain of fibronectin and is common to several other ECM adhesion proteins. These proteins include vitronectin, laminin A, collagen I and thrombospondin [13]. RGD and other oligopeptides have been incorporated into biomaterials to enhance adhesion, spreading and higher functions in a variety of cell types, including fibroblasts, bovine pulmonary artery endothelial cells

(BPAE), bovine aortic endothelial cells (BAE) and human umbilical vein endothelial cells (HUVEC) [34]. The presence of the peptides results in direct adhesion to the material, thus eliminating the need for adsorbed proteins altogether. Studies reviewed by Hubbell show that the RGD ligand alone was sufficient to support morphologically complete cell spreading in a dose dependant manner. These studies also show that a variable surface density of immobilized RGD peptides elicits different cellular migratory responses, resulting in variable rates of proliferation. For example, low adhesion strength is thought to be a result of less than optimum ligand surface density, while a high density may inhibit the ability of a cell to migrate on the surface [13].

Various techniques, such as adsorption, covalent incorporation at the surface and covalent incorporation, have been used to incorporate RGD-containing peptides into numerous different biomaterials. In virtually all cases, cell adhesion and spreading was increased due to the presence of the RGD peptide (Table 2), which is just as effective as an adsorbed layer of more native proteins.

Table 2 – Cellular Response Studies Incorporating RGD into Biomaterials

Study	Surface	Peptide	Attachment Technique	Cell Type	Critical Observation
[29]	Glass	RGDS/ RDGS	Covalent immobilization	NRCO/ BPAE/ RSF	**Competitive Inhibition**: RGDS surface significantly increased cell adhesion. Preincubation of NRCO with RGDS resulted in decreased subsequent adhesion to RGDS-modified surfaces.
[30]	PS/ PEO	GRGDSY	Immobilization via PEO tether	NIH 3T3	**Peptide coupling reaction**: 11% efficient. **Morphology**: RGDS-treated surfaces increased cell spreading 350 %, when compared to untreated surfaces.
[32]	PEG	YRGDS/ YRDGS	Copolymerization of acrylated peptide or acrylated-PEG-peptide	HFF	**Immobilization Technique**: Cells adhered non-specifically to gels containing peptide incorporated via a linkage lacking a PEG spacer arm (i.e. YRDGS was similarly effective as YRGDS), while adhesion to gels with peptides incorporated via spacers was specific and in a dose dependant manner. **Competitive Inhibition**: Preincubation of cells with soluble YRGDS completely inhibited spreading. **Morphology**: YRGDS increased spreading and creation of F-actin stress fiber network of HFF in dose dependant manner. Cells on YRDGS-containing surfaces were morphologically the same as surfaces without peptide.
[33]	Quartz/ SiO_2	RGD/ RGE	Immobilization via heterobifunctional crosslinker	RCO	**Cell Detachment**: Radial flow apparatus (RFA) used to show that higher interfacial shear stresses were required to detach cells from RGD surfaces, as compared to RGE surfaces. **Morphology**: Cells on clean and RGE surfaces remained round while cells on RGD surfaces spread and exhibited a much higher mean area of coverage. **Degree of Focal Contact**: RGD surfaces showed spread cells with cell processes, like characteristic canalicular projections; RGE and clean surfaces lacked focal contact regions.

Study	Surface	Peptide	Attachment Technique	Cell Type	Critical Observation
[34]	Glass	RGDS/ RGES	Immobilization to aminophase glass	HASMC/ HUVEC/ HDF/ SHR	**ECM production**: Dose dependent - Higher concentrations of RGDS produced more initial adhesion but less ECM on a per cell basis (HASMC, HUVEC, & HDF), than the lower concentrations. In contrast, RGES surfaces had less adhesion but more ECM production, for SHR & BAEC cells.
[35]	PEGMA/ MPEGMA; PMMA	GRGDSP	Solution coupling to PEGMA units	NR6	**Competitive Inhibition:** All cells detached from RGD-bearing surfaces within 1 hour of adding soluble GRGDSP. **Dose Response**: Number and morphology of cells adhered to RGD-latex-comb surfaces was modulated by the surface density of the RGD beads.
[36]	Silica	RGDC/ YIGSR	Immobilization via heterobifunctional crosslinker	HUVEC	**Competitive Inhibition**: Preincubation of cells with soluble RGDC decreased HUVEC adhesion significantly in dose dependant manner. **Selectivity**: Preincubation of cells with soluble YIGSR had no effect on adhesion to RGDC surfaces. Silica surface with BSA (5%) coating served as negative control to ensure RGDC adhesion is specific to RGD sequence.
[37]	PEG-NHS-ACRL/ LGPA	RGDS	Copolymerization, then grafted into hydrogel network	HDF/ RASMC	**Dose Dependant Migration:** HDF migrated to LGPA-RGD hyrogels with 71% efficiency, as compared to collagen controls. Migration of RASMC through RGDS-containing hydrogels was dose dependant to an intermediate concentration of 2.8umol/mL RGD; no migration was observed at higher RGD concentration.

Peptides: R – Arginine; G – Glycine; D – Aspartic Acid; E – Glutamic Acid; S – Serine; Y – Tyrosine; P – Proline; C – Cysteine; I – Isoleucine; **Polymers:** S - styrene; PS - polystyrene; PEO - polyethylene oxide; P/MMA - methyl methacrylate; PEG - poly(ethylene glycol) diacrylate; MPEGMA - methoxy PEGMA comb polymer; **Cells:** NRCO - neonatal rat calvarial osteoblasts; BPAE - bovine pulmonary artery endothelial cells; RSF - rat skin fibroblasts; LL - lymphoid leukemia L1210 cells; HFF - human foreskin fibroblasts; RCO - rat calvaria osteoblasts; HASMC - human aortic smooth muscle cells; HUVEC - human umbilical vein endothelial cells; HDF - human dermal fibroblasts; SHR - spontaneously hypertensive rat thoracic aorta cells; BAEC - bovine pulmonary artery endothelial cells; NR6 - NR6 fibroblasts; BSA - bovine serum albumin (protein); RASMC - rat aortic smooth muscle cells;

The enhanced cell adhesion and spreading was shown to be RGD-dose dependent, by Hern et al. [32], and Gobin et al [37]. Competitive inhibition studies using non-specific peptides [29,34], such as arginine-glycine-glutamic acid (RGE), or soluble forms of RGD-containing peptides [35,36], such as arginine-glycine-aspartic acid-cysteine (RGDC), were effective in showing the selectivity and effectiveness of RGD in these applications.

RGD has also proven to be effective in bone-specific applications. Osteopontin (OP) is a protein, which is synthesized by osteoblasts and is localized at regions where osteoclasts are attached to the bone surface. Bone sialoprotein (BSP) is another osteoblast-derived protein localized in the bone matrix, but is only expressed at late stages of differentiation. Both of these non-collagenous proteins are involved in cell-matrix attachment via cell-surface integrins; they both bind tightly to hydroxyapatite, and without coincidence, they both contain the RGD sequence within their cell binding regions [33]. Rezania et al. were able to use the attachment signals originating from the RGD peptide to modulate osteoblast attachment and differentiation. They were able to prove the theory that RGD peptides grafted to a metal oxide surface (quartz or SiO_2) were able to preferentially recruit osteoblasts, thereby increasing the rate of integration of the implant with the surrounding tissue [33].

The adhesion proteins found in ECM, blood, plasma and serum form an integral component of the cell-surface interaction mechanisms, through which normal cell function and development occur. The smaller oligopeptides, such as RGD, which have the ability to mimic the specific binding sequences of these adhesion proteins, have proven to be a more effective and cost efficient alternative to enhance cell adhesion and

spreading in a variety of applications. The new era of regenerative medicine calls for proactive biomaterials designed to elicit specific desirable responses from surrounding cells. RGD can be used to create such biomaterials, which will selectively and specifically support and enhance osteoblast adhesion on any given surface.

PROJECT RATIONALE

This project was performed with the ultimate goal of designing and developing a biomaterial carrier, which would effectively deliver BMP to a desired injection site, while supporting and enhancing osteoblast adhesion and differentiation. This was to be achieved by grafting peptides containing the biomimetic RGD sequence onto thermoreversible polymers and co-injecting these RGD-containing polymers with BMP-2. Members of this group have successfully conjugated therapeutic proteins to thermoreversible NiPAM copolymers for drug delivery and tissue engineering applications [5,12,21,22,47]. Other researchers have shown that incorporating the RGD moiety into or onto various other types of surfaces have resulted in increased adhesion and spreading of a variety of cell types [29-37]. There is, however, only one other study performed to date that explored the feasibility of conjugating peptides containing the RGD sequence onto thermoreversible NiPAM copolymers [48].

Stile and Healy were able to covalently graft a large peptide containing the RGD sequence (CGGNGEP**RGD**TYRAY) into NiPAM/AA hydrogels [48]. They were subsequently able to show that the presence of the RGD in the hydrogel resulted in increased cell adhesion and spreading [48]. In this system, rat calvarial osteoblast (RCO) cells were cultured in three dimensional gels made up of NiPAM/AA/RGD polymers. They also acknowledged that there were specific disadvantages associated with their developed system, the major weakness being the undesirable volume change associated with the hydrogel performance in culture. A reported 30% collapse in hydrogel size created an unacceptable uncertainty as to the degree of contact achievable between the

injected matrix and tissue defect. Another significant issue to address was the stability of the hydrogel in culture; Stile and Healy reported that the mechanical integrity of the hydrogel may not be sufficient to support bone tissue regeneration *in vivo*. In addition, while they appeared to have retained the bioactivity of the RGD sequence after modification, the peptide coupling was achieved via a PEG spacer, linked to a bifunctional cross-linker. As discussed in the **INTRODUCTION** section of this report, there are risks associated with the use of crosslinkers; in many cases, the bioactivity of the peptide/protein may be compromised and an additional (in our view, not necessary) step is introduced into a coupling process. We purposed to develop a system whereby the RGD sequence was grafted onto the thermoreversible NiPAM polymers without the use of crosslinkers, resulting in an effective, structurally stable biomaterial for bone tissue regeneration.

There are many factors to consider in ensuring that the proposed biomaterial will enhance osteoinductive activity at the injection site. A major consideration is that the bioactivity of both the BMP and the incorporated RGD sequence is retained after modifications. This project was divided into three separate phases, and took place over the past 18 months. Phase I of the project was carried out to develop and optimize the conjugation reaction between the chosen polymer and peptides containing the RGD sequence. Phase II was carried out to test the bioactivity of the new RGD-containing polymer, using cell adhesion studies, and Phase III was carried out to demonstrate that the BMP was effective in its role to induce osteoblast activity, in conjunction with the RGD-containing polymer.

Phase I: Creating an RGD-containing-polymer

This project uses the NiPAM thermoresponsive polymer as its base biomaterial (Figure 1A). A random copolymer containing NiPAM and the protein-reactive NASI (Figure 1B) monomer units, has been used in this project. This material has been designed so that it may be injected once dissolved in aqueous medium to a specific site, where it will become insoluble at the physiological temperature [5]. This property is desirable for a biomaterial carrier for BMPs, which will ideally create a three-dimensional gel matrix at the injection site and form bone *in situ*.

RGD-containing peptides were conjugated to the copolymer via the succinimide ester groups in the NASI. This method of conjugation eliminates the need for complicated chemistry and additional crosslinking agents. Proton nuclear magnetic resonance (^{1}H-NMR) analysis and reverse phase high pressure liquid chromatography (RP-HPLC) were used to show successful conjugation between the peptide and the polymer. The conjugation reaction was optimized and a correlation was established between the initial concentration of peptide used for the reaction and the final RGD yield in the modified polymer after conjugation.

Phase II: Confirming Bioactivity of Conjugated RGD Sequence

Once an RGD is grafted onto a polymer, it is critical to demonstrate that it retaines its bioactivity. The C2C12 myoblast cell line (ATCC # CRL-1722) was chosen for use in RGD bioactivity assays, primarily because of its documented success in adhesion studies and its response to BMP treatment [40-43]. Although these are muscle-derived cells, BMP treatment differentiates them into the osteoblast lineage.

A protocol for quantifying C2C12 cell adhesion was established and included two simple, but effective techniques. The number of cells adhered to the varying culture surfaces were measured by a Coulter Counter, due to its accuracy and simplicity. As a comparative (and often more reliable) method of quantification, the cell metabolic activity was measured using the 3-(4,5-dimethyl-thiazol-2-yl)-2,5-diphenyl-tetrazolium bromide (MTT) assay [44]. Photographs taken using a phase contrast microscope were also used to assess cell spreading and morphology. RGD-containing surfaces were compared to a variety of control surfaces, including TCPS and unmodified NiPAM/NASI polymers. RGD dose response and non-specific adhesion studies were also carried out to further assess the bioactivity of the incorporated RGD-containing sequences.

Phase III: Cell Response to BMP-2 When Cultured on RGD-containing Polymers

This phase of the project was designed to ensure that biomaterials grafted with RGD had supported cells' ability to respond to BMP. The C2C12 cell response to BMP was examined using an alkaline phosphatase (ALP) assay [45]. By measuring the levels of ALP expressed by C2C12 cells, it was possible to study their biological activity and quantify their differentiation into osteoblasts [25].

In summary, this project was carried out to explore the possibility of employing a thermoresponsive polymer to immobilize adhesion-specific RGD sequences and to serve as a biomaterial carrier for BMP delivery. This thesis was able to demonstrate that the conjugation of RGD to polymers was not only possible, but also created an effective medium for BMP delivery, enhanced cell adhesion and increased osteoinductive activity *in vitro*.

EXPERIMENTAL

A. Materials

NiPAM, methyl methacrylate (MMA), ethyl methacrylate (EMA), acryloyl chloride, N-hydroxysuccinimide (NHS), benzoylperoxide (BPO), 1,4-dioxane, diethyl ether and tetrahydrofuran (THF) were purchased from Aldrich (Milwaukee, WI). NASI was prepared by other members of this group by reacting acryloyl chloride with NHS, as described in [21]. The inhibitors in MMA and EMA were removed by distillation under a high vacuum before polymerization. RGD was obtained from SIGMA (St Louis, MO), while other peptides GRGES and GRGDS were obtained from BACHEM (Torrense, CA). GYRGDS was custom-synthesized by Alberta Peptide Institute (Edmonton, AB) and purified to 95% homogeneity by a reverse-phase high pressure liquid chromatography (RP-HPLC). Molecular weight (MW) of the peptide was confirmed by mass spectroscopy (theoretical: 654.28 amu, experimental: 654.53 ± 0.52 amu). Amino acid analysis was used to confirm the sequence identity of the peptide. The phosphate buffer used for conjugation reactions was prepared by mixing 0.1 M of Na_2HPO_4 and 0.1 M NaH_2PO_4 in H_2O to give a pH of 7.4. The dialysis tubing, with MW cutoff 12-14 kDa (#08-667A), was obtained from Spectrum Laboratories (Rancho Dominguez, CA). The molecular weight standards were polystyrene of 3.7 kDa (M_w/M_n = 1.09), 13.7 kD (M_w/M_n = 1.01), 44.0 kDa (M_w/M_n = 1.07) and 212.4 kDa (M_w/M_n = 1.11), all obtained from Aldrich.

Hanks Balanced Salt Solution (HBSS), Dulbecco's Modified Eagle Medium (DMEM) tissue culture medium, Penicillin/Streptomycin antibiotic solution, cell freezing solution containing dimethyl sulfoxide (DMSO) (#11101-011), and Trypsin/EDTA were

obtained from GIBCO BRL (Grand Island, NY). All tissue culture polystyrene (TCPS) flasks (25 cm^2) and plates (24 and 48 well) were obtained from Corning NY (Corning, NY). Fetal Bovine Serum (FBS) and 3-(4,5-dimethyl-thiazol-2-yl)-2,5-diphenyl-tetrazolium bromide (MTT), as well as ALP assay (Kit # 104-LS, containing #10401 p-Nitrophenol Standard Solution, #221 Alkaline Buffer Solution and #104-40 Phosphatase Substrate 40 mg capsules) reagents were from SIGMA. Myoblastic C2C12 cells were a gift from Dr. Civetilli (University of Washington, St. Louis, MO). The rhBMP-2 was a gift from Dr. W. Sebald (Universitait Wurzburg, Wurzburg, Germany). This BMP was tested in culture, according to methods described by the research group of Dr. Sebald [44] and found to have retained its bioactivity in culture.

B. Polymer Synthesis and Characterization

The preparation of NiPAM, NiPAM/NASI, NiPAM/NASI/MMA and NiPAM/NASI/EMA polymers was described previously [22]. Briefly, desired amounts of NiPAM, NASI, MMA and EMA monomers were dissolved in dioxane, followed by the addition of 0.023 g (0.2 mol%) of BPO. The solution was then purged with nitrogen for 30 minutes while stirring with a magnetic stirrer, after which it was incubated at 70 °C for 22 hours. The polymer was then precipitated by hexane and purified by dissolving the precipitate in THF and precipitating the solution by diethyl ether. The polymers were dried in a vacuum, at 50 °C, for one week.

H^1-NMR spectroscopy (Poruker AM300 spectrometer, retrofitted with MACSPECT 3) was used to determine the compositions of the polymers containing NiPAM, MMA and NASI units. The number of Hs was used to normalize the peak area

integrations corresponding to the characteristic chemical shifts of NiPAM (-C<u>H</u>-: 3.9 ppm), NASI (-C<u>H</u>$_2$-C<u>H</u>$_2$-: 2.8 ppm), and MMA (-C<u>H</u>$_3$: 3.6 ppm). Elemental analysis was used for nitrogen to determine the composition of EMA-containing polymers, due to the overlap of chemical shifts for NiPAM and EMA. As described previously [21], the NASI content of the polymers was also determined via UV-visible spectroscopy. The compositions of all polymers used throughout this project are summarized in Table 3.

Gel permeation chromatography, static light scattering and Precision MW Analysis software were used to determine the polymer molecular weights (MW). A 20 μL sample of each polymer solution (20 mg/mL in THF) was manually injected into a 7.8x300 mm Styragel™ HMW 6E column (Waters Inc.; Milford, MA), eluted with a 1mL/min THF and the elution pattern was detected by refractive index/light scattering detectors (PD2020; Precision Detectors, Andover, MA). The following formulae was used by the Precision software for calculation of MW [46]:

$$MW = K_2 * I_{LS} / K_1 * I_{RI} * (dn / dc), \text{ where}$$

I_{LS} = the light scattering signal intensity,

I_{RI} = refractometer signal intensity,

dn/dc = refractive index increment, and

K_2 and K_1 = calibrations constants, which were obtained by using polystyrene standards from Aldrich.

A spectrophotometer (Ultraspect 2000; Pharmacia) equipped with a water-circulation cell was used to determine the LCST of the polymers, as described in [22]. The polymers were dissolved (5 mg/mL) in 0.1 M phosphate buffer (pH=7.4) and 1 mL sample of each polymer solution was added into a spectrophotometer cuvette. The water

temperature was increased from 10 to 30 °C (in 0.5 °C increments every 10 minutes) using a refrigerated/heated water circulator. The optical density of each sample was measured at 420 nm, while the actual temperature of the sample was measured using a digital thermometer. The data was fitted to a sigmoidal curve and the LCST was taken as the midpoint of the inflection point.

Table 3 – The compositions (mol%) of all NiPAM polymers used throughout this project are given in the table, below. All polymers were synthesized and characterized previously, as described in [22]. D: dioxane, B: benzene. ND: not determined.

Copolymer				Composition (mol %)			
Name	**Solvent**	**MW (kDa)**	**LCST (°C)**	**NiPAM**	**NASI**	**MMA**	**EMA**
D	D	171	26.5	97.29	2.71	-	-
E	D	175	26.2	96.23	3.77	-	-
F	D	183	23.5	94.95	5.05	-	-
L	B	776	ND	92.61	1.39	6.00	-
R	B	416	ND	79.75	3.25	17.00	-
U	B	404	19.9	84.64	-	-	15.36
V	B	637	24.6	77.25	1.25	-	21.50
JY-2*	D	237	27.6	95.00	5.00	-	-

* Prepared separately from other copolymers, as per procedure described in [22].

C. Quantifying RGD-Containing Peptide-Polymer Conjugation

^{1}H-NMR spectroscopy was used initially to investigate RGD peptide conjugation to the NiPAM/NASI copolymer. The reaction was prepared by dissolving NiPAM/NASI (5.1% NASI; 56 mg/mL) in 0.1 M phosphate buffer (pH=7.4) with: (a) no peptide, (b) 2.5 mg/mL RGD, (c) 0.5 mg/mL RGD and (d) 0.5 mg/mL RGD + 0.1 M NH_4OH. The samples were dialyzed extensively against distilled/deionized water (MW cutoff: 12-14 kDa), then lyophilized overnight and finally dissolved in D_2O for analysis with a Bruker AM300 (Billerica, MA). The peak integrations corresponding to the unique chemical shifts of the polymer (-C<u>H</u>- (NiPAM):3.9 ppm) and the peptide (-C<u>H</u>$_2$- (arginine): 3.2

ppm) were normalized for the number of Hs and used to determine the final yield of peptides per polymer chain.

The peptide-polymer conjugation was also quantified using RP-HPLC. Polymers were dissolved in DMF and RGD-containing peptides were dissolved in phosphate buffer. The two solutions were combined in appropriate ratios to give the desired concentrations of peptide and polymer in the resulting conjugate samples. Initially, the reactions were carried out in glass test tubes at 4 °C for 24 hours, after which time the peptide-polymer solution was directly injected onto a C-18 column (VYDAC; Hesperia, CA). Varying solvent gradients were used to determine the optimal environment for quantifying the conjugation reaction (Table 4). The solvent gradients were designated as 'Initial', 'Erin', 'Protein Work' and 'Conjugate'.

Table 4 – Summary of different solvent gradients used to establish optimal conditions for quantifying peptide-polymer conjugation reaction. Solvents used were 0.1% trifluoroacetic acid (TFA) in H_2O (B) and 0.1% TFA in 90/10% Acetonitrile/H_2O (D).

Setup	Time (min)	Solvent Gradient (% D)
Initial	0-20	35-65
	20-22	65-35
Erin	0-20	100-0
	20-22	0-100
Protein Work	0-2	100
	2-12	100-0
	12-15	0
	15-18	0-100
	18-20	100
Conjugate	0-2	0
	2-14	0-100
	14-16	100-0

The 'Initial', 'Erin' and 'Protein Work' gradient setups were used in initial studies (with RGD) to characterize the conjugation reaction. The 'Conjugate' gradient setup was used to measure the extent of all other peptide conjugation to the polymer. In all cases,

the disappearance of the characteristic peptide peak (varied with peptide and gradient used) was used as a measure of successful conjugation to the polymer. Since the polymer typically eluted as a separate peak, a reduction in the peptide peak was used as a quantitative measure of conjugation without interference of the polymer.

In one set of studies, peptide conjugation to polymer films was quantitated by RP-HPLC. For these studies, the GYRGDS, GRGDS and GRGES peptides were reacted with polymer films in 24 well plates at 37 °C for 24 hours. Once the reaction was completed, the supernatant was drained from each well and injected into the C-18 column; the peptide was eluted using the 'Conjugate' linear gradient setup. It was assumed that the conjugation reaction could not occur on the TCPS surfaces without a polymer coating. Therefore, the values obtained from the un-coated TCPS surface were used as a control. The extent of peptide conjugation to each well surface was determined using this control value.

D. Coating Techniques to Obtain RGD-Containing Surfaces

A variety of techniques were evaluated towards the goal of developing a method that allowed a uniform coating of polymer film on the TCPS surface. These polymer coatings were used to test (i) peptide grafting on a surface and (ii) the ability of the peptide-grafted polymers to support cell attachment. Since this was the first study in this lab to look at cell attachment to surfaces, several techniques were attempted to obtain reproducible polymer films for cell attachment. We called these techniques 'Single Coat', 'Bulk Coat', 'Two Coat' and 'Surface Conjugation' techniques (See Table 5).

Table 5 – Coating techniques used to obtain a uniformly distributed polymer film on a TCPS well, while maximizing the number of RGDs present at the cell-surface interface. The 1st Step column describes the composition of the first solution applied to each well. The 2nd Step column describes the composition of the second solution (if any) applied to each well. Peptide-Polymer Conjugate refers to the conjugate created in the lab, which was then used to coat the TCPS surfaces. Unless otherwise indicated, all application volumes were 0.5 mL.

Technique	1st Step	2nd Step
Single Coat	NiPAM Polymer (10 mg/mL) **OR** Peptide-Polymer Conjugate* (10 mg/mL)	N/A
Bulk Coat	NiPAM Polymer (5 mg/mL) **OR** Peptide-Polymer Conjugate** (5 mg/mL)	N/A
Two Coat	0.75 mL Polymer solution (5 mg/mL) **OR** 0.5 mL Polymer solution (5 mg/mL)	N/A **OR** 0.25 mL Peptide-Polymer Conjugate solution** (5 mg/mL)
Surface Conjugation	NiPAM Polymer (10 mg/mL)	0.1M Phosphate Buffer (pH=7.4) **OR** Peptide in Phosphate Buffer (0.1, 0.01 or 0.001 mg/mL)

* : This was prepared by mixing 0.1 mg/mL RGD in 10 mg/mL polymer solution.
**: This was prepared by diluting the conjugate prepared previously (*) with 5 mg/mL polymer solution to give a final concentration of 0.002 mg/mL peptide.

In most cases, to achieve a polymer coating, the polymer was dissolved in methanol in the appropriate quantities to achieve a concentration of 5 or 10 mg/mL. Unless otherwise indicated, 0.5 mL of this polymer solution was added to each well. The plates remained in a fume hood overnight, to allow the methanol to evaporate at room temperature. The second coat (if any) was then added; this was typically 0.5 mL of either 0.1 M phosphate buffer (pH=7.4) or a desired concentration of peptide dissolved in phosphate buffer. The plates were then stored for 24 hours at 37 °C in a 5% CO_2 environment, before seeding with cells.

E. Cell Attachment to Polymer Films

The ability of the various NiPAM copolymers and the peptide-grafted polymers to support cell attachment was typically tested in 24-well TCPS plates (48-well plates, where indicated). C2C12 cells of myoblastic lineage were used for this assay, due to their ability to respond to BMP treatment [41]. The original C2C12 cells were expanded to create a cell bank. This was achieved by culturing cells in 25 cm^2 flasks and DMEM (supplemented with 1% Penicillin/Streptomycin and 10% FBS) until reaching 80-90% confluency, as observed by phase contrast microscopy. Cells were trypsinized (0.25% trypsin/EDTA), and re-suspended in freezing solution to 5.0 x 10^4 cells/mL. The cell solution was then divided into 50 x 1 mL aliquots and transferred into 2 mL cryogenic vials (VWR, Mississauga, ON), which were then returned to - 70 °C in a Controlled Rate Freezing Machine (Planar) at a rate of 1 °C/min. Cells were then stored in liquid nitrogen, in the lab of Dr. McGann (Canadian Blood Services, Edmonton, AB), until required.

At the start of each experiment, a vial of frozen cells was thawed and seeded on 25 cm^2 flasks and cultured until reaching ~80% confluence, as described above. After removing the supernatant, trypsinized C2C12 cells were re-suspended in DMEM (again supplemented with 1% Penicillin/Streptomycin and where indicated, 10% FBS) and added, in known concentrations, to the polymer-coated wells. The seeding density typically used was between 10,000 – 80,000 cells/well (in 1.0 mL of culture medium) but in some cases (indicated in each specific study), this number was as high as 300,000 cells/well. Cells were then incubated at 37 °C in a 5% CO_2 humidified air environment for designated amounts of time, ranging from 3 hours to 6 days (specified in each study).

Culture medium was typically changed one day after seeding and every two days thereafter.

The number of cells adhered to a specific surface was quantified using either a hemacytometer or a Coulter™ Counter (Model ZBI, Beckman Coulter Inc, Hialeah, FL). For either method, at the time of testing, the excess culture media was drained and 0.5 mL of trypsin/EDTA was added to each well. After ~5 minutes, 0.5 mL of fresh culture medium was added and a 0.5 mL sample was taken for quantification. Using a hemacytometer, cells were counted manually from 5 different fields (x2) and averaged, giving the number of cells/mL. Using the Coulter unit, each 0.5 mL sample was diluted with 10 mL of isoton solution (Beckman Coulter) and the number of cells/mL was obtained by averaging the counted number from three runs.

The MTT assay [45] was used to quantify the cell metabolic activity in each particular well. At the desired time point, excess culture media was drained and each well was washed with 0.5mL HBSS and re-supplied with 0.5 mL of fresh culture medium. 0.25 mL of MTT dissolved in HBSS (5 mg/mL) was added to each well to give a final MTT concentration of 1 mg/mL. After incubating at 37 °C for 2 hours, excess medium was removed and pictures were taken at 2.5, 10 and 20 times magnifications using Leica DMIL microscope (Leica Microsystems Wetzlar, Germany) and Cool Snap Digital Camera (Roper Scientific, Tucson, AZ) Rogers Scientific Image and Scion Image software was used to improve picture quality. Each well was dissolved in 2 mL dimethyl sulphoxide (DMSO) and the absorbance of the resulting purple solution was read, using a ELISA reader (Biotech Instruments ELX800, Winooski, VT) at a wavelength of 570 nm.

Washing the wells with HBSS, before dissolving in DMSO resulted in a loss of formazan crystals; this step was therefore eliminated from the typical procedure.

F. Cell Response to BMP-2

The alkaline phosphatase (ALP) assay was used to quantify the C2C12 cell response to the presence of BMP-2 in the culture medium. Cells seeded according to procedures described above (in triplicate samples) were allowed to attach overnight and the medium was replaced with 1.5 mL of fresh medium containing a known concentration of BMP-2. For studies where only the presence of BMP-2 was examined, the concentration typically used was 300 ng/mL; for studies where the BMP-2 dose response was examined, the BMP-2 concentrations in the culture medium were 0, 25, 100 and 250 ng/mL. After 3 or 6 days of incubation, the media was removed and replaced with 0.5 mL of ALP buffer (1.5 mol/L 2-Amino-2-methyl-1-propanol), supplemented with 0.01% Triton X-100. After 1 hour at room temperature, 0.5 mL of phosphatase substrate solution (1 40 mg capsule p-Nitrophenyl phosphate, dissolved in 20 mL distilled H_2O) was added to each well and the absorbances were read at 405 nm by the ELISA reader, at 10 minute intervals for 30 minutes. These values were calibrated using a p-Nitrophenol Standard Solution (SIGMA) and used to determine the BMP-2 induced alkaline phosphate levels in each well. The ALP activity for each well, over 30 minutes was then expressed in units of umol/mL/hr.

G. Experimental Designation

Each separate experiment performed throughout the course of this project was assigned a unique experimental designation, consisting of a roman numeral and an integer. The roman numeral corresponded to the phase of the project the study was performed in, and the integer corresponded to the individual study performed within that particular phase, in chronological order. For example, Study II:4 was the 4th experiment conducted in Phase II of this project. As outlined in the **PROJECT RATIONALE**, experiments performed in Phase I typically involved quantifying conjugation chemistry, while the majority of experiments performed in Phase II were cell adhesion studies, and Phase III typically involved quantifying the cell response to BMP-2. The unique study number is provided for each set of data presented within this report.

RESULTS & DISCUSSION

Phase I: Creating an RGD-containing-polymer

A. Quantifying Peptide-Polymer Conjugation Using NMR

The temperature-dependant-solubility that is characteristic of thermoreversible polymers makes them attractive biomaterial carriers for drug delivery applications because it allows them to be easily manipulated. Many researchers have exploited this characteristic to modulate the release rate of therapeutic proteins [15,18-20,50-52], while others have utilized it to act as a substrate for cell and tissue culture [23-26, 53-55]. Since the phase separation is induced by simply increasing the temperature above the LCST, there is no need for exogenous molecules to be introduced into the system. This reduces the chances of altering the bioactivity of the proteins being released and eliminates the need for harsh enzymes that are normally necessary to discharge cells from an attachment substrate. The retention of protein bioactivity is further ensured by the incorporation of 'protein-reactive' monomer units into the polymer backbone, since they eliminate the need for potentially harmful crosslinking agents.

The NASI units that have been incorporated into the NiPAM copolymer backbones readily react with amines. This is ideal for conjugation with peptides containing the biomimetic RGD sequence, since the N-terminal $-NH_2$ groups are readily available in the peptides. However, the succinimide esters within the NASI groups can undergo hydrolysis in an aqueous environment as well as aminolysis with primary amines. Therefore, the peptide reaction needed to be confirmed to ensure sufficient aminolysis.

The first issue which needed to be explored was whether a peptide containing the RGD sequence could be conjugated to the NiPAM/NASI thermoreversible polymers. The peptide-polymer conjugation reaction performed in hopes of achieving this is illustrated in Figure 3.

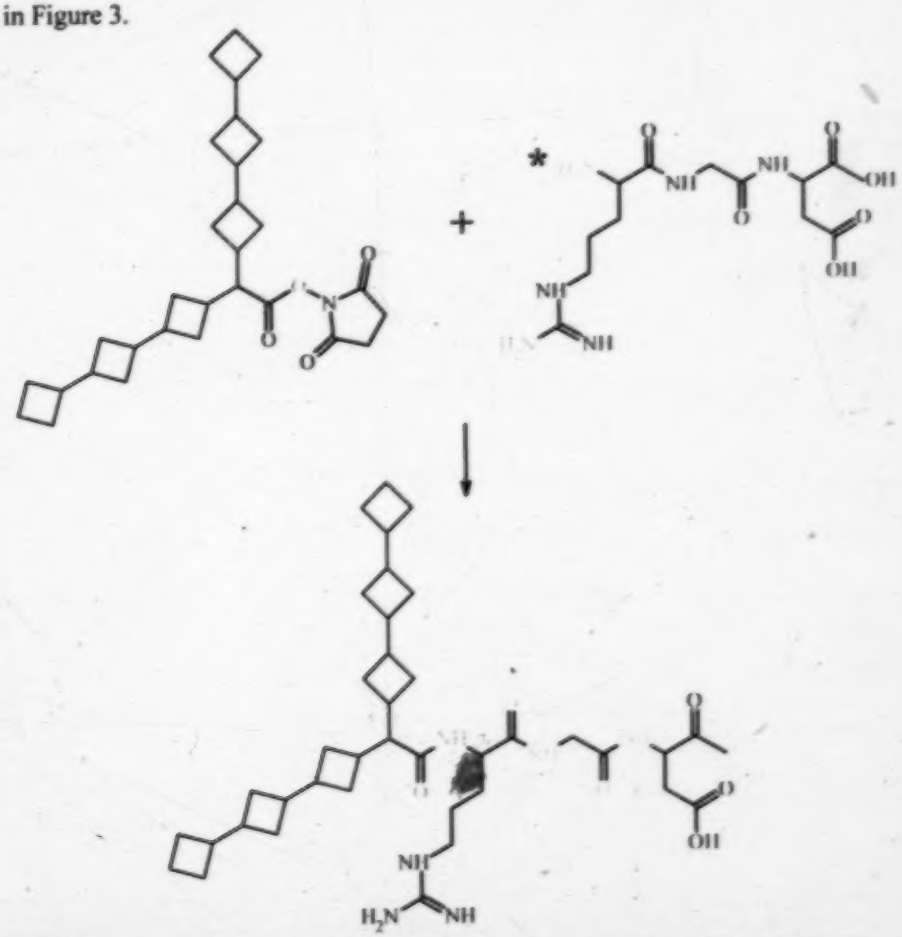

Figure 3 – Schematic of the peptide-polymer conjugation reaction. The alternating NiPAM/NASI copolymer backbone is represented by squares (not to scale). The N-terminus of the peptide (*) reacts with the NASI groups. Note that the resulting bond in the conjugate is identical to the other peptide bonds throughout the peptide structure.

A ^{1}H-NMR spectrum for each of the Arginine, Glycine and Aspartic Acid amino acids was obtained from the Aldrich database and used to guide our efforts in

characterizing the RGD peptide used in these studies. These, as well as the corresponding peaks found in NMR analysis for the RGD peptide are summarized in Table 6. Their respective NMR spectra and chemical structures are in Appendix A.

Table 6 – Proton NMR analysis of Arginine, Glycine, and Aspartic acid (data from Aldrich). The information was used to characterize the RGD ^{1}H-NMR spectrum, run in our lab. The chemical shifts were in D_2O.

Material	Chemical Shift (ppm)	Structure
Arginine (R)	1.6-1.7 3.2-3.3	-C<u>H</u>- and -C<u>H</u>$_2$- -(C<u>H</u>$_2$)$_2$-
Glycine (G)	3.6	-C<u>H</u>$_2$-
Aspartic Acid (D)	2.0-2.8 3.6	-C<u>H</u>$_2$- -C<u>H</u>-
RGD	1.7 1.9 2.5 3.2 3.8 4.0 4.4	R^2 -C<u>H</u>$_2$- R^2 -C<u>H</u>$_2$- D^2 -C<u>H</u>$_2$- R^3 -C<u>H</u>$_2$- R^1 -C<u>H</u>$_2$- D^1 -C<u>H</u>- G^1 -C<u>H</u>-

A ^{1}H-NMR spectrum was also obtained for the unmodified NiPAM/NASI polymer used in the conjugation reaction, also determined in D_2O. The significant peak in the polymer NMR is located at 3.9 ppm; this peak is representative of the –C<u>H</u>- group in the NiPAM monomer (Figure 4). Typically, the NASI monomer exhibits a characteristic peak at 2.8 ppm (-C<u>H</u>$_2$-C<u>H</u>$_2$). Dissolving these samples in D_2O resulted in hydrolysis of the esters in the NASI monomer; therefore the peak at 2.8 ppm was not visible in this particular spectrum. Successful conjugation was confirmed by the presence of an RGD-characteristic peak in the otherwise polymer-resembling NMR spectrum for the conjugate sample (Figure 5). This significant peak is a triplet and has a chemical shift of 3.2 ppm; as shown in Table 6 and further detailed in Appendix A, it is characteristic of the -C<u>H</u>$_2$- group closest to the NH_2 groups in the Arginine of RGD (R^3).

Although an apparent peak was also visible in this region of the polymer spectrum (Figure 4), the peak amplitude was not significantly higher than the corresponding noise level. Another peptide peak was partially visible at 2.6 ppm; this is characteristic of the -C$\underline{H_2}$- group in aspartic acid (D^2). Unfortunately, as is the case for many of the characteristic peptide peaks, this peak occurs at the same approximate chemical shift as another polymer peak and was impossible to use for calculations. Due to the overwhelmingly large polymer:peptide concentration ratio (~400:1), the peptide peaks are considerably smaller in size and in many cases, partially or completely overlapped by the polymer peaks.

The final yield of peptides per polymer in the conjugate sample was calculated using the peak integration from NiPAM, (3.9 ppm) as the only representative polymer peak, and the peak corresponding to Arginine, located at 3.2 ppm (-C$\underline{H_2}$-), as the only representative peptide peak. This value was determined in the following calculations.

Calculating RGD/NiPAM Ratio Using NMR Integrations:

NiPAM ratio = 100/1H = 100 polymer H

RGD ratio = 0.5/2H = 0.25 RGD H $\Rightarrow$ **1 RGD / 400 NiPAM**

Calculating RGD/Copolymer chain Ratio:

NiPAM/NASI Copolymer is 5.05% NASI $\Rightarrow$ 94.95% NiPAM

NiPAM/NASI Molar Mass = 183,000 g/mol

$$\#\ \text{NiPAM/Copolymer Chain} = \frac{(94.95\%) \times (183{,}000\ \text{g/mol})}{113.16\ \text{g/mol}} = 1535$$

$$\#\ \text{RGD/Copolymer Chain} = 1535\ \frac{\text{NiPAM}}{\text{Chain}} / 400\ \frac{\text{NiPAM}}{\text{RGD}}$$

$$= \mathbf{3.8}\ \frac{\mathbf{RGD}}{\mathbf{Chain}}$$

It was determined that the initial reaction yielded 3.8 peptides/polymer chain (Study I:6). In subsequent studies, the final yield of peptide conjugation was found to be directly dependent on the concentration of peptide used in the original reaction solution. This number decreased from 3.8 to 0.7 peptides per polymer as the starting peptide concentration decreased from 2.5 to 0.5 mg/mL. This correlation is consistent with other data obtained by both this author and other members of the group, using a RP-HPLC method. Findings published by Neff et al. also concur with this correlation [30]. They reported that varying the molar ratio of peptide to surface active sites from 1:1 to 10:1 resulted in an increase in the amount of peptide bound [30].

The representative RGD peak was not visible in the spectrum obtained for a sample of the peptide/polymer reaction, which had been repeated to include ammonium hydroxide, NH_4OH (^{1}H-NMR spectrum not shown). It was therefore assumed that the presence of the peptide peak (3.2 ppm, arginine) in the conjugate sample was due to *conjugated* and not free floating peptide. This would have been an artifact if the peptide dialysis was not complete. NH_4OH has a higher reactivity to the succinimide ester groups in the NASI, and was used in excess (100 mM vs. 0.67 mM), therefore competitive inhibition should prevent any reaction from occurring between the NASI and the peptide. Since all reaction samples were dialyzed using fairly large MW dialysis tubing (12-14 kD), any free floating peptide should have diffused out during this time. The presence of a peptide peak in the sample containing NH_4OH would disprove this theory, but its absence confirms that the peptide peak in the conjugate sample was due to successful peptide-polymer conjugation.

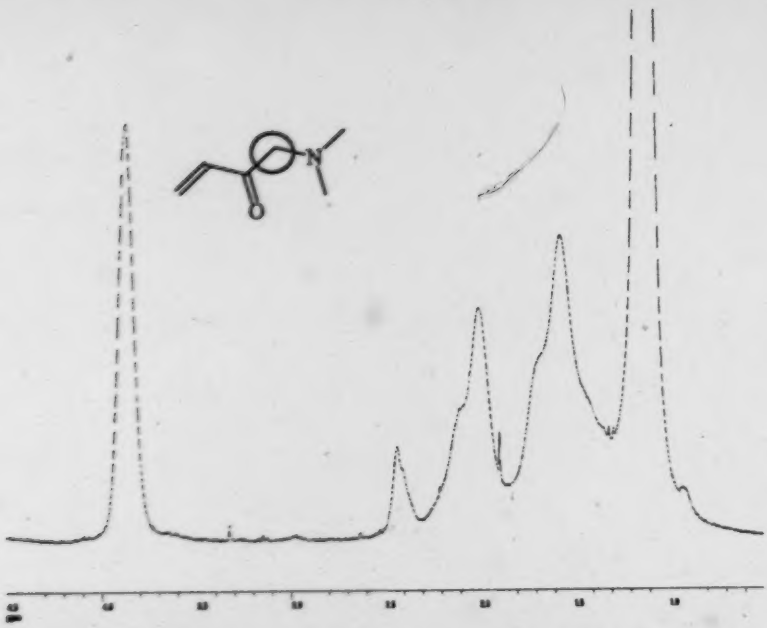

Figure 4 – ^{1}H-NMR spectrum obtained for the NiPAM/NASI copolymer. The characteristic polymer peak for NiPAM is located at 3.9 ppm (-C<u>H</u>-). The small peak at 3.3 ppm is due to the methanol solvent.

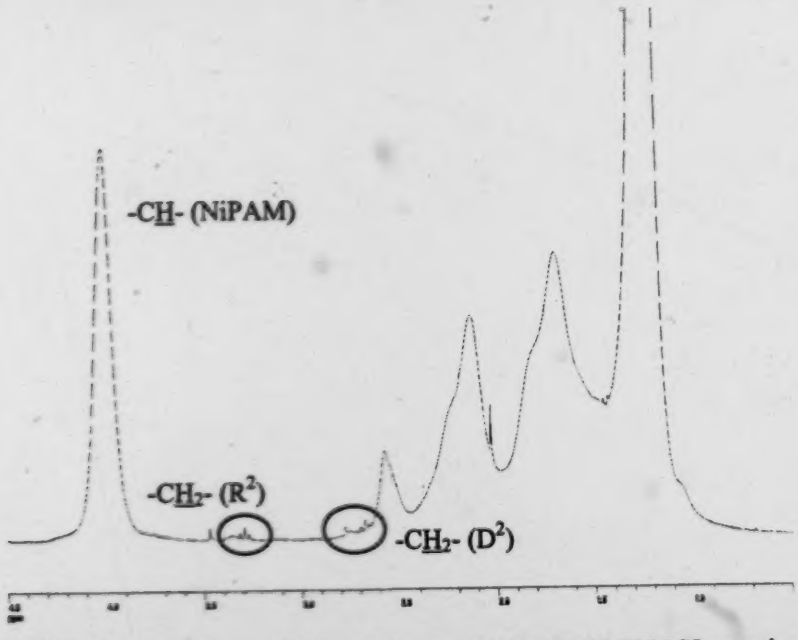

Figure 5 – ^{1}H-NMR spectrum obtained for the RGD-NiPAM/NASI reaction, which confirmed successful conjugation. The NiPAM peak is located at 3.9 ppm (-C<u>H</u>-) and the methanol solvent peak is visible at 3.3 ppm, as expected. The peptide peak used for calculations is located at 3.2 ppm (-C<u>H</u>$_2$- (R^2)).

B. Quantifying Peptide-Polymer Conjugation Using RP-HPLC

While ^{1}H-NMR was effective in quantifying the conjugation efficiency and confirmed the identity of the conjugate, it was thought that RP-HPLC would be a more routine, accessible method of quantification for continued reaction studies. Initial studies characterized the RGD peptide and NiPAM/NASI copolymer in various solvents, using RP-HPLC (λ = 214 nm). This data was displayed in Table 7.

Table 7 – RP-HPLC data obtained from 2 separate studies, when attempting to quantify the conjugation reaction. Solvents were 0.1% trifluoroacetic acid (TFA) in H_2O (B) and 0.1% TFA in 90/10% Acetonitrile/H_2O (D). PB = 0.1 M Phosphate Buffer (pH = 7.4).

Study	Injection Sample	Concentration (mg/mL)	Solvent Gradient	Elution Time (min)	Peak Intensity (Au)
I:2	RGD in PB	0.2	'Initial'	1.1854	0.6560
	RGD in PB	0.4		~ 1	1.1481
	RGD in PB	0.2	'Erin'	1.2432	0.7741
	PB	-		1.1971 ~ 11 ~ 16	0.2212 0.1039 0.1351
I:4	NiPAM/5.1% NASI in Methanol	14.0	'Protein Work'	0.7337 ~14	2.5930 2.5487
	NiPAM/5.1% NASI in Methanol	3.5		0.9400 ~14	1.8698 2.1536
	RGD in PB	0.4		0.6306	1.8145
	Methanol	-		0.6619 8-14	0.2429 0.0182
	PB	pH 7.4		0.7221	0.3100
	NiPAM/5.1% NASI (Methanol) + RGD (PB)	14.0 + 0.4		0.8017 ~14	2.7197 2.5492
	NiPAM/5.1% NASI (Methanol) + RGD (PB)	3.5 + 0.4		0.8499 ~14	2.1695 1.2986

Both the RGD (Study I:2) and the polymer (Study I:4) peak height (in absorbance units) decreased as the concentrations decreased, respectively, showing direct concentration dependant correlation. Although initially, RP-HPLC appeared to show an

isolated peak related to RGD (~1 minute elution time), it was later seen that the peak corresponding to the phosphate buffer interfered with this peak, making RP-HPLC ineffective for analyzing this peptide. Attempts to quantify the peptide-polymer conjugation reaction were inconclusive and, due to its non-retention on the C-4 or C-18 column, the short sequence RGD peptide was deemed unsuitable for the RP-HPLC method. It was decided that RP-HPLC would only be useful to analyze larger RGD-containing peptides, which also contained hydrophobic residues. The hydrophobic residues are more likely to cause the peptide to remain adsorbed to the column longer, thus creating a characteristic peak for the peptide at a later elution point, isolated from the water peak.

The peptide Glycine-Tyrosine-Arginine-Glycine-Aspartic Acid-Serine (GYRGDS) was obtained from Alberta Peptide Institue for these reasons and, as expected, a clear retention peak at 7.5-8.1 min could be obtained using the 'Conjugate' elution conditions outlined in the **EXPERIMENTAL** section. The GYRGDS peptide was used in subsequent conjugation reactions and RP-HPLC was used successfully to reproducibly quantify the amount of peptide reacted. Data obtained in this way for one specific study (II:10) was displayed in Table 8.

Table 8 – RP-HPLC data used to determine the conjugation efficiency for one specific conjugation reaction (Study II:10), using the hydrophobic GYRGDS peptide and 'Conjugate' elution conditions: 0-2min, 0%B; 2-14min, 0-100%B; 14-16min, 100-0%B. Peptide surface density was determined to be 3.4 nmol/cm^2.

	Elution Peak Height (Absorbance units)					
Sample Surface	**1**	**2**	**3**	**4**	**5**	**6**
TCPS	130515	139900	131131	136549	128951	136992
NiPAM/5.1%NASI	117526	123380	122332	127091	119639	125979

The absorbance measured from the TCPS supernatant was assumed to be a result of no reaction, therefore used as the control. The amount of peptide reacted to the NiPAM/NASI surface was calculated, relative to this control. For the data above, the average absorbance for the TCPS was 134006.5 ± 4384.5 Au, while the average NiPAM/NASI absorbance was found to be 122657.8 ± 3654.0 Au. The TCPS value was taken to represent 0.1 mg/mL (i.e. initial coating concentration of the peptide), therefore the amount of peptide reacted on the NiPAM/NASI surface was calculated to be 0.00847 mg/mL (0.1-0.09153 mg/mL). This translates to a conjugation efficiency of ~8.5 %. Based on this value, the peptide concentration on the surface was calculated to be 3.4 nmol/cm^2.

Further studies to optimize this reaction were conducted by other members of this lab group, using varying concentrations of polymer and peptide, as well as varying reaction conditions, solvents, pH and temperature. It was determined that: (i) the conjugation efficiency increased as the polymer concentration was increased; (ii) the conjugation efficiency was directly proportional to the mol% of NASI in the polymers, resulting in no conjugation when the mol% NASI was 0; (iii) the conjugation efficiency was higher at lower temperatures (4 °C), as compared to higher temperatures (~ 37 and 50 °C); and (iv) the optimal pH for the reaction was ~ 8.0. These studies also confirmed that the presence of the peptide in the conjugates did not significantly affect the LCST. These studies were summarized in a manuscript, ready for submission [49].

RP-HPLC was effective in showing that ~10% conjugation was consistently achieved with the larger peptides containing hydrophobic residues. Our conjugation efficiency appeared to be relatively low, when compared to results obtained by other

researchers who also used the NASI chemistry to couple RGD-containing peptides to various polymers. As an example, Hern and Hubbell were able to achieve ~ 75% incorporation of acrylated YRGDS into PEG diacrylate hydrogels [32]. This significantly higher conjugation efficiency can be attributed to the difference in reactivity of NASI units used in the reaction. Studies performed by Uludag et al [21] show that the aminolysis rate for a NASI monomer is significantly higher than that exhibited by a polymerized NASI, due to the considerable hindrance provided by the polymer attached to the succinimide. The difference between the NASI reactivity in monomeric and polymeric forms was 120-fold. Hern and Hubbell coupled the peptides to NASI monomers and then polymerized them with PEG diacrylate to create the RGD-containing hydrogels. In our hands, the peptides were coupled to polymerized NASI units within the NiPAM/NASI copolymer backbone. It is therefore to be expected that our conjugation efficiency should be significantly lower than that obtained by Hern and Hubbell. Furthermore, it is thought that the degree of coupling achieved in our studies (i.e. the peptide surface density, ~ nmol/cm^2) is within a physiologically relevant range of ligand densities for affecting cell behavior, as suggested by Hern and Hubbell [30].

In a related study, Chen et al. explored the effectiveness of coupling insulin to NiPAM/AA copolymers, for use in cell culture [56]. The coupling was performed by using water-soluble carbodiimide (WSC) and acrylic acid moieties as the coupling reagent. This gives N-hydroxysuccinimide esters as the reactive species, which is identical to the NASI groups in our study. Chen et al. were able to achieve 1.0 mol of coupled insulin for every mol of polymer in the conjugates. This was lower than the peptide yield in our conjugates (3.8 peptides/polymer), which is to be expected, given the

relatively larger size of insulin, compared to our peptide (~ 6.1 kDa vs. 350-600 Da). The conjugates gave a maximum surface concentration of insulin of about 0.4 $\mu g/cm^2$, which was 1-10% of the amount of free insulin required to produce the same stimulatory effects on cell growth. In our hands, the maximum surface density of conjugated peptide was determined to be 2.2 $\mu g/cm^2$. While insulin is a much larger protein than any of the RGD-containing peptides used in our studies, we feel that the 8.5 % peptide conjugation efficiency achieved in our hands, with a similar NiPAM copolymer, is more than acceptable. The effectiveness of these conjugates was assessed in Phase II of the project, using C2C12 cell culture and is discussed in detail in the later pages of this report.

C. Hydrolysis and Stability of the Peptide-Polymer Conjugation Reaction

Hydrolysis of succinimide esters in an aqueous environment will compete with peptide conjugation, resulting in a decrease in the effectiveness of peptide coupling. Studies conducted by other members of this group found that the relative aminolysis:hydrolysis rate for most proteins was typically less than 2 for $-NH_2$ concentrations up to 3 mM, and this relationship was not dependant upon either the protein pI or MW [54]. It is known that lysine and arginine $-NH_2$ groups (pK_a of 10.8 and 12.5 respectively) are very reactive towards the succinimide ester and the possibility of enhancing the conjugation by the presence of an additional $-NH_2$ group was explored by others in this lab (unpublished data). A lysine containing peptide, GRGDSPK, was reacted with NiPAM/NASI and its conjugation efficiency was compared to that obtained using the GYRGDS peptide. No significant difference was observed in conjugation

efficiency between the two peptides. Therefore, it was assumed that the majority of the conjugation between the NiPAM/NASI polymers and the peptides containing the RGD sequence took place at the N-terminal $-NH_2$ sites.

Other studies indicated that the aminolysis:hydrolysis rate can be improved by controlling two variables, the pH of the reaction medium and the NASI concentration in the NiPAM/NASI copolymer. There was a tendency for lower hydrolysis rate at a higher NASI mole ratio [21], and that conjugation efficiency was directly proportional to the NASI concentration in the polymer (unpublished data). Therefore, NiPAM/NASI copolymers with a minimum of 2.71 % NASI (polymer D) were used in this project, the highest possible concentration being preferred (polymer F, 5.05% NASI). It was shown that the NiPAM/NASI polymer underwent an increased aminolysis rate at higher pHs, the relative reactivity of the polymer being highest at pH 7.4; the protein reactivity was also better at this pH [21]. All conjugation reactions reported in these pages were carried out in 0.1 M phosphate buffer (pH 7.4) for this reason.

Minimizing hydrolysis also minimizes the number of –COOH groups generated, which are capable of altering the polymer LCST. It is known that charged groups, such as $-COO^-$ and $-NH_3^+$, increase the LCST while hydrophobic groups, such as $-CH_3$ and $-CH_2CH_3$ lower the LCST. Conjugating RGD-containing peptides to NiPAM copolymers will introduce at least one more positively charged group (due to arginine) and possibly other charged or hydrophobic groups, depending on the other amino acids that are present in the peptide. To ensure that the polymer is still an effective biomaterial carrier for BMPs *in vivo*, it is critical to maintain an LCST lower than the physiological temperature. While it is desirable to maximize the yield of peptide conjugated to the polymer, there

does exist an upper limit. Typically, with polymers containing acrylic acid and other positively-charged groups, > 1 mol% is needed to observe an increase in LCST. The maximum number of peptides per polymer obtained in this project was ~4 (~0.25 mol%), which suggested that peptide conjugation did not affect the polymer LCST, or its probable effectiveness *in vivo*.

As well as maintaining an effective LCST, stability is also an important issue to consider, when developing a biomaterial for use *in* vivo. The peptide-polymer conjugation reaction results in the formation of bonds resembling those present throughout typical peptide sequences, i.e. -O=C-NH, which are typically very stable. Chen et al. reported that no significant release of immobilized insulin from NiPAM/AA films was detected in culture [56], indicating that their conjugates were fairly stable. The bonds formed between the insulin and polymer as a result of their coupling procedure were similar to those obtained in our peptide-polymer conjugates. Although no studies have been performed to assess the stability of our newly formed peptide-polymer bonds, it is likely that they would behave similarly to those obtained by Chen et al. and other typical peptide bonds, allowing for a stable conjugate.

Phase II: Confirming Bioactivity of Conjugated RGD

A. C2C12 Cell Attachment to NiPAM/NASI Copolymer Using Hemacytometer

The compatibility of the NiPAM/NASI copolymer with cells was examined by assessing the cellular adhesion to the surfaces of TCPS wells, which had been previously coated with the polymer. The muscle-derived C2C12 cell line was chosen for use in this work because of its versatility, which allowed them to be employed in both Phase II and Phase III of this project. Others had shown that when cultured in serum, these cells express typical fibroblast morphology. Once confluent, they differentiate into myoblastic cells and when cultured in the presence of BMP-2, these cells de-differentiated from the myoblastic phenotype and expressed typical osteoblast features. Therefore, the C2C12 cells were effective in testing the ability of RGD-containing surface to enhance anchorage-dependent cell adhesion (Phase II) while also being able to investigate osteoinductive activity due to the presence of BMP (Phase III).

Adhesion was quantified first by using a hemacytometer (II:2), to count the number of cells adhered at different incubation time points. The ability of cells to adhere to the polymer surface in medium with and without FBS was examined. The initial data was summarized in Table 9.

Table 9 – C2C12 cell adhesion to TCPS and NiPAM/NASI surfaces in medium both with and without FBS (Study II:2). All numbers are expressed in percentages of the original number of cells seeded in each well (~1.5 x 10^4 cells/cm^2).

Incubation Time (hours)	Medium Without Serum		Medium with Serum	
	TCPS	NiPAM/NASI	TCPS	NiPAM/NASI
3	34 ± 19	33 ± 18	49 ± 26	93 ± 46*
24	38 ± 15	100 ± 41*	102 ± 39	120 ± 45*

* These values are not representative of the observed cell growth in the respective wells; they are assumed to be inaccurate, due to the significant error associated with the hemacytometer.

After 3 hours of incubation, 34 ± 19% of cells originally seeded in medium without FBS on the TCPS surface adhered; 49 ± 26% of cells in medium containing FBS also adhered to the TCPS surface during that time. After 24 hours, 102 ± 39% of cells in medium containing FBS adhered to the TCPS surface, whereas only 38 ± 15% of those in medium without FBS remained. The presence of FBS in the medium did not appear to affect initial cell attachment to the TCPS surface, but caused a significant increase in attachment after 24 hours.

Cells seeded onto the control TCPS wells adhered quickly (within 3 hours) and began to spread and proliferate rapidly, reaching near confluence after 24 hours. They exhibited a long, thin shape once adhered, characteristic of typical myoblastic (muscle cell) morphology. In contrast, once an effective coating technique had been developed, very few cells adhered to the NiPAM/NASI polymer surfaces, and those that did remained round, suspended in medium and did not exhibit typical muscle cell morphology. Their growth was sparse and markedly less than that of cells on TCPS; cells remaining after washing grew in clumps, forming spheroids. This significant observed difference is illustrated in Figure 6. Unfortunately, the cell numbers obtained using the hemacytometer did not accurately reflect the observed difference in cell growth on the two surfaces, since there was a significant error associated with the majority of these values (see SD values in Table 9). This error might be due to the fact that the cell numbers are low to begin with; a small variation between fields results in significant standard deviation values for the average. Also, cells growing in spheroids were difficult to count in the hemacytometer, which was designed for singe cell suspensions. For these reasons, the Coulter Counter was employed for subsequent studies.

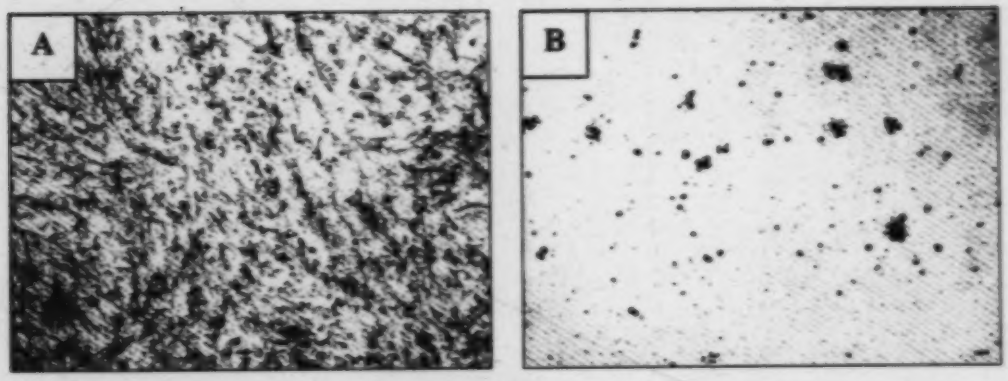

Figure 6 – Cell growth observed on both TCPS and NiPAM/NASI-coated surfaces, after 24 hours of incubation. A – C2C12 cells adhered and spread quickly on the TCPS surface, retaining myoblastic morphology. B - NiPAM/NASI-coated surfaces supported little or no C2C12 cell attachment; cells grew in spheroids or remained round and suspended in medium. Photos were taken at 10x magnification.

B. C2C12 Cell Attachment to NiPAM/NASI Copolymer Using Coulter Counter

Studies were conducted to further assess the cell compatibility of the NiPAM/NASI-coated surface; TCPS was again used as a control. The Coulter Counter was used to measure the number of cells adhered to both surfaces. This is an automated technique that does not rely on operator variation. The results of one study (II:4) were displayed in Figure 7.

In the absence of FBS, the number of cells on the NiPAM/NASI surface after 3 hours was similar to the number of cells on TCPS (18 ± 3 vs 18 ± 4 %, respectively). A significant increase in attachment on the TCPS surface was seen for cells cultured in medium containing FBS after 3 hours. Cell attachment on TCPS was 69 ± 4% while only 16 ± 2% of cells remained on the NiPAM/NASI surface, illustrating the importance of FBS to obtain an accurate control response for TCPS surfaces, especially for initial adhesion measurements.

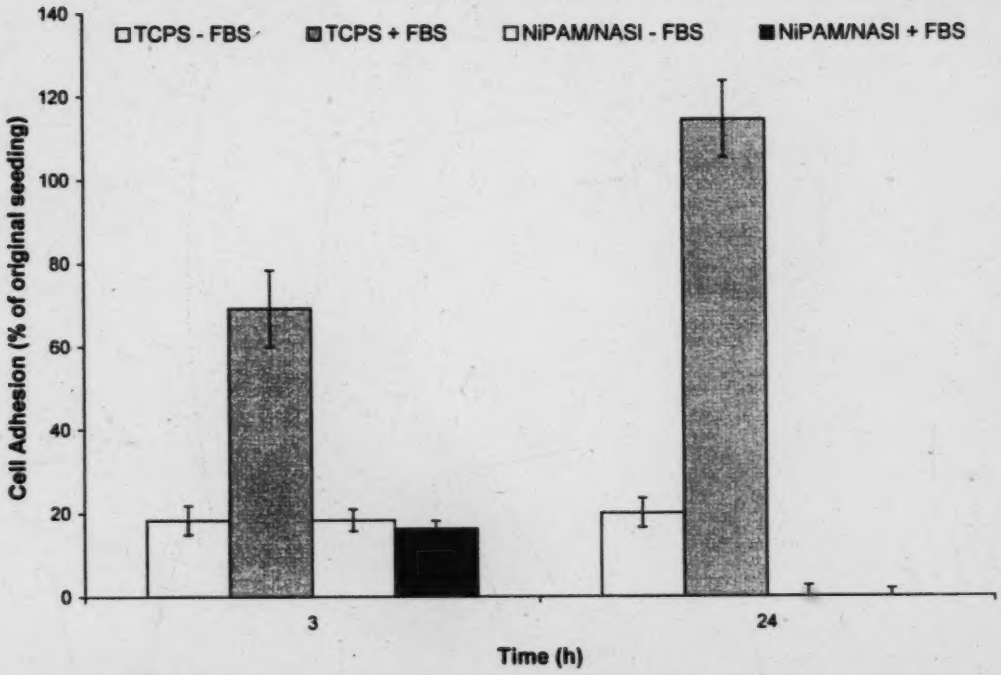

Figure 7 – C2C12 cell adhesion to NiPAM/2.7%NASI and TCPS surfaces, as measured after 3 and 24 hours of incubation time, using a Coulter Counter (Study II:4). The number of cells adhered are expressed as a percentage of the original seeding density (1.5×10^4 cells/cm^2). These values are the mean ± SD of three counts. The effects of supplementing culture medium with FBS are also displayed.

The significant difference between the cell compatibility of the two surfaces was clear after 24 hours. In medium containing FBS, the TCPS surface supported 114 ± 9% of the original number of cells seeded; NiPAM/NASI-coated surfaces did not support any cell attachment in the absence or presence of FBS (<1% with and without FBS). The majority of these values were consistent with the growth (or lack of it) observed visually, on the different surfaces. The error associated with these values was also considerably less than those obtained using a hemacytometer in the previous experiments, making the Coulter Counter a more reliable device for use in these studies.

This difference in the cell compatibility of the two surfaces was consistently evident, both qualitatively and quantitatively, after 24 hours of incubation (other data not shown). The number of cells adhered to the NiPAM/NASI surface was always significantly less than that measured for the TCPS surface, regardless of the quantification method or composition of the culture medium used. This decrease in cell number was typically more pronounced in medium containing FBS (ranging from 3-57 times less, typically ~ 10) than in medium that was not supplemented with FBS (ranging from 2-8 times less, typically ~ 5). The cells adhered to either surface were generally much lower when cells had been cultured in medium without FBS. This was assumed to be due to the absence of important ligands and growth factors contained in the serum, which are normally responsible for mediating adhesion and differentiation.

It is a well-known fact that cells generally do not adhere to hydrophilic surfaces [27]. NiPAM/NASI surfaces described in our studies were incubated with 0.5 mL of 0.1 M phosphate buffer (pH 7.4) overnight; the incorporated NASI units were therefore assumed to undergo hydrolysis, as oppose to aminolysis, when incubated with peptide in phosphate buffer. The hydrophilicity of the surface is expected to have increased, due to this hydrolysis; this may be a contributing factor to the poor compatibility of our NiPAM/NASI surfaces with cells. It is likely, however, that the major factor was the polymer surface density used in our studies.

Many other researchers have studied the compatibility of various NiPAM copolymers and found, in most cases, that these polymer surfaces do in fact support some degree of cell attachment. These studies were summarized in Table 1, in the **INTRODUCTION** section. A variety of cell types were used, including mouse

fibroblast STO cells (MF-STO), human retinal pigmented epithelium (HRPE), and bovine aortic endothelium (BAE); it was fairly consistent throughout all of these studies that while cells did attach to the NiPAM copolymer surfaces, it was to a lesser degree than that observed on the TCPS control surfaces and regardless of the phenotype, cells remained fairly round and did not display typical morphology [23-26].

While the morphology seen in these studies is consistent with that observed in our hands on the NiPAM/NASI copolymers, the adhesion numbers are very different. von Recum et al. [25] reported that both BAE and HRPE cells grew to confluence on TCPS wells that had been coated with P(IPAAm-co-CCMS) at a surface density of 4.0 $\mu g/cm^2$. Kwon et al. reported that more than 90 % of BAE cells (30,000 cells/cm^2) seeded onto NiPAM-grafted TCPS dishes (1.6 $\mu g/cm^2$) had attached and spread, after one hour of incubation at 37 °C [57]. These results are not unexpected, given the polymer surface densities that were used. The aim of the majority of these studies [23-26, 57] was to show that cells cultured on thermoreversible NiPAM copolymer surfaces could be detached in sheets, with their morphology intact, upon cooling below the particular polymer LCST. This is a very attractive technique for cell harvesting because it eliminates the need for harmful enzymes, such as trypsin/EDTA, which are typically used to detach cells from adhesion substrates. In order for the effectiveness of this technique to be explored, cells needed to adhere and grow on the NiPAM copolymer surfaces first, hence the low surface densities.

Within this thesis, studies were done on the coating techniques, to ensure a complete and uniform polymer coating was achieved on the TCPS surfaces (further detailed in the later sections of this report). It is believed that the lower surface densities

used in other studies (~4.0 μg/cm^2) were not enough to achieve a similarly uniform polymer coating. As a result, the cell growth observed in aforementioned studies was most likely due to cells growing, in part, on exposed TCPS sections of the wells, rather than on the actual polymer surfaces. It is possible that serum proteins could still adsorb to the NiPAM layer, hence cells could attach. In comparison, the absence of cell growth on NiPAM/NASI surfaces seen in our lab was obtained using polymer surface densities of ~ 1300 μg/cm^2, which is ~ 850 times that used by others discussed here. The protocol performed by von Recum et al. [25] does not appear to include the overnight incubation with phosphate buffer, used in our studies. This would affect the hydrophilicity of their polymer surfaces and may account for some of the large discrepancy in the comparison with our results. Kwon et al. [57] reported to have washed the NiPAM-grafted surfaces 'extensively with cold water', to remove all unreacted and/or ungrafted polymer, then allowed the surfaces to dry overnight at room temperature, as we did in our studies. Regardless of the exact protocol used, we are confident that complete NiPAM/NASI-coated surfaces, in general, support little or no cell attachment. Most importantly, the NiPAM/NASI surface appeared to be suitable to use as a negative control for assessing the bioactivity of the RGD-containing polymer (created in Phase I of this project) in subsequent studies.

C. Effects of Cell Density on Cell Attachment to NiPAM/NASI Copolymer

In our hands, the effect of cell seeding density on adhesion to the NiPAM/NASI surfaces was also explored. The seeding density typically used in our experiments was 0.5 to 2.1 x 10^4 cells/cm^2. One study was conducted using densities ranging from 1.5 x

10^4 to 1.9 x 10^5 cells/cm^2 (~5, 10 and 15 times that which had been used previously). These values were compared to TCPS and NiPAM/EMA surfaces, which had been seeded with the cell density previously used. All cells were cultured in medium which had been supplemented with FBS and this study (II:13) was conducted over a 6 day period, with adhesion being quantified after 1, 3 and 6 days of incubation (Table 10).

Table 10 – Cell adhesion data for cells seeded at 1.5 x 10^4, 8.5 x 10^4, 1.5 x 10^5 and 1.9 x 10^5 cells/cm^2 (x1, x5, x10 and x15 the cell density used in Table 9) onto NiPAM/5.1%NASI (Polymer F) surfaces, compared to 1.5 x 10^4 cells/cm^2 seeded on TCPS and NiPAM/EMA (15.4% EMA, Polymer U) surfaces. Values are expressed as % of original number of cells adhered, mean ± SD from 3 counts obtained for each polymer film, of which there were duplicates.

Time (days)	TCPS x1	Polymer U x1	Polymer F x1	Polymer F x5	Polymer F x10	Polymer F x15
1	226 ± 9	81 ± 16	4 ± 1	12 ± 8	13 ± 2	20 ± 5
3	121 ± 13	69 ± 8	4 ± 2	4 ± 2	9 ± 0	1 ± 1
6	185 ± 5	60 ± 11	13 ± 5	7 ± 1	7 ± 5	8 ± 2

After 1 day, the percentage of cells adhered to each surface increased as the cell seeding density increased. However, this increased adhesion due to increased cell density was not seen in long-term culture; by the 3rd and 6th day after seeding, there were very few cells remaining. As described in the **EXPERIMENTAL** section, all surfaces were washed at regular intervals; it is then to be expected that any and all cells that had not adhered to the surface would be washed away. For all NiPAM/NASI coated surfaces, regardless of the cell seeding density or incubation time, cells remained round, clumped and suspended. It was concluded from this study that increasing the cell density did not improve the relatively low compatibility of the NiPAM/NASI surface with the C2C12 cells. Furthermore, the NiPAM/NASI surfaces were deemed suitable for use as negative

control surfaces for assessing the ability of polymers incorporated with polymers containing the RGD sequence to increase cell adhesion.

D. C2C12 Cell Attachment to RGD-Containing Polymers

As mentioned above, extensive studies were conducted to develop a technique that would achieve two goals: (i) to apply a complete and uniform NiPAM/NASI polymer coating to the TCPS wells, and (ii) to maximize the surface density of RGD moieties available at the surface to interact with the cells. As in the case where the cell compatibility of the NiPAM/NASI surfaces was being explored, it was essential to completely coat the TCPS wells with polymer, to ensure that TCPS-mediated attachment was eliminated. We have shown that NiPAM/NASI surfaces supported little cell attachment. The challenge here was to develop a technique that localized RGD moieties at the surface, while ensuring that the NiPAM/NASI polymer film remained intact to prevent non-specific adhesion. The recurring problem was that, due to the small concentrations of peptide used and low peptide/polymer yield obtained in the conjugates, it was difficult to ensure that the incorporated RGD sequences were in fact at the cell-surface interface. A variety of different techniques were evaluated during the initial phase of this project: Single Coat, Bulk Coat, Two-Coat, and Surface Conjugation. A complete account of the steps involved in each of these trial techniques was given in the **EXPERIMENTAL** section.

I: Single Coat

The first coating technique attempted was the 'Single Coat' technique; this involved a one-time coat of the RGD-containing polymer, which was created using the RGD peptide and previously analyzed using ^{1}H-NMR (3.8 peptides per polymer), as described in the **EXPERIMENTAL** section. Briefly, the peptide was reacted with the polymer, dialyzed, dried, dissolved in methanol and coated on the TCPS well. Uncoated TCPS surfaces were used as a positive control and the unmodified NiPAM/NASI discussed above, were used as the negative control surface. The cell attachment in medium containing FBS was observed and quantified using a Coulter Counter after 24 hours of exposure (Study II:12). These values are expressed as the percentage of cells remaining (after washing) from the original number of cells seeded.

As expected, the number of cells adhered to the TCPS surface (94 ± 54%) was significantly higher than the NiPAM/NASI and RGD/Polymer conjugate coated surfaces, which yielded 3 ± 1% and 7 ± 1% adhesion, respectively. It is apparent from these results that the conjugate-coated surfaces did not show increased cell adhesion or spreading. There are two possible explanations for these results: (i) the conjugated RGD was not effective for cell adhesion (this was considered unlikely), or (ii) the RGD surface density was not sufficient to induce increased adhesion. If indeed the problem was the low RGD surface density, it may have been due simply to the absence of RGD moieties on the surface, i.e., the RGD moieties were buried inside the polymer layer. Alternatively, poor conjugate stability might have resulted in peptide detachment from the surface. As previously discussed, the peptide bonds formed in the conjugation reaction are typically very strong and as such, it is unlikely that these bonds would break.

The problem might have been that the conjugate was water-soluble and therefore might also have been soluble in the tissue culture medium and washed away during the washing steps.

II: Bulk Coat

The second technique, 'Bulk Coating', involved diluting the RGD-containing polymer (created in Phase I of this project) with a higher concentration of NiPAM/NASI polymer solution. This 'bulk' mixture was then used to add a single surface coating to selected wells in the TCPS plates and the observed cell response was recorded after 3 and 24 hours and is summarized in Table 11. Once again, un-coated TCPS and unmodified NiPAM/NASI surfaces were used as positive and negative controls, respectively.

Table 11 – Observed cell response to TCPS, NiPAM/NASI and RGD/Polymer Conjugate when assessing effectiveness of 'Bulk Coating' technique (Study II:5, 3 hours). All values are expressed in percent adhesion (mean ± SD of three counts), when compared to number of cells originally seeded (~0.8×10^4 cells/cm^2).

Medium	TCPS	NiPAM/NASI	RGD/Polymer Bulk Coat
- FBS	63 ± 27	128 ± 11	49 ± 8
+ FBS	348 ± 25	123 ± 4	109 ± 2

The inability of cells to adhere and proliferate in medium not containing FBS, after only 3 hours, is again illustrated here, for all surfaces. It was decided from this data that 3 hours was not enough time to show significant differences in the cell adhesion to the varying surfaces; the minimum incubation time for all subsequent studies is 24 hours.

The number of cells adhered to the RGD/Polymer Conjugate 'Bulk Coat' surfaces was not higher than either the positive or negative control surfaces. It was assumed that this was due to similar problems as were discussed in the case of the 'Single Coat'

Technique; as such, the 'Bulk Coat' Technique was deemed ineffective for assessing RGD/Polymer conjugate bioactivity. It was once again clear that another technique needed to be evaluated; one which ensured that RGD was available on surface to interact with cells appeared to be necessary, in order to effectively evaluate bioactivity.

III: Two-Coat

A new technique was developed in hopes of achieving this; it involved a two-step process where the TCPS well surfaces were coated twice, over a two day period. Since we had already shown that, if coated properly, the NiPAM/NASI surfaces supported very little cell attachment, the first application was of NiPAM/NASI only, ensuring that the well was completely coated, in order to eliminate any and all non-RGD-mediated adhesion. This 'Two-Coat' technique was found to give satisfactory results in showing that the RGD-containing polymer surfaces increased cell adhesion. These results are displayed in Figure 8.

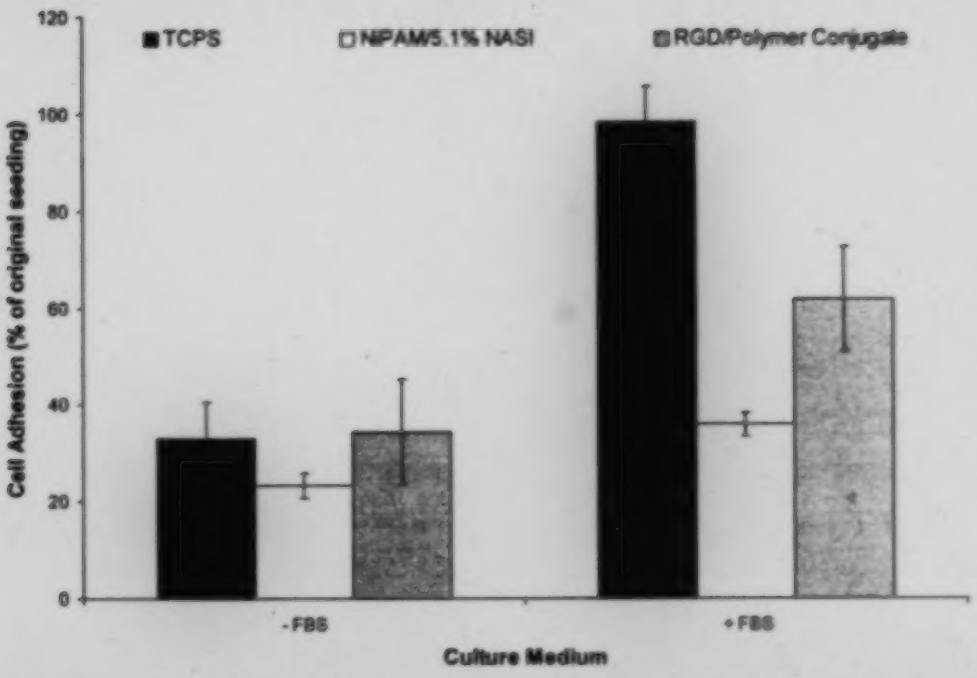

Figure 8 – Cell adhesion to TCPS (positive control), unmodified NiPAM/NASI (negative control), and the 'Two-Coat' RGD/Polymer conjugate surfaces, in medium containing (+) and not containing (-) FBS. Values are expressed as the percentage of cells adhered, as compared to the original seeding density ~ 4.8×10^4 cells/cm^2 (mean ± SD, from three counts each of duplicate samples) after 24 hours (Coulter Counter , Study II:7).

Although the numbers obtained from this study do show an increase in adhesion on the RGD/NiPAM/NASI surfaces, when compared to the NiPAM/NASI surfaces, the visual observations were still somewhat unsatisfactory. The cell growth was not uniform throughout each individual well; cells were adhering and spreading much better in a ring around the outside of each well (photo not available). This was an indication that this technique was not uniformly coating each well and the TCPS surface was being exposed around the outside.

It was thought that the non-uniform coating seen with this technique was due to the methanol used as a solvent for the second coating on the NiPAM/NASI wells; that the

methanol was disturbing and/or dissolving the initial polymer coating. To remedy this, the 'Two-Coat' technique was repeated, using HBSS as the solvent instead (i.e. RGD-conjugated polymer dissolved in HBSS), for the second application. Ideally, the HBSS would not have dissolved the NiPAM/NASI coat and this polymer coating would remain uniform, thereby disallowing normal cell growth throughout the entire surface. Unfortunately, due to the large water content of the HBSS, it did not evaporate as quickly as the methanol and was deemed not practical for these applications. Consequently, the plate was left to dry for ~ 3 weeks, after which the cells were seeded, as per the procedure outlined in the **EXPERIMENTAL** section. The results of this study are summarized in Table 12. There was no obvious benefit of the RGD/NiPAM/NASI polymer in this study.

Table 12 – The observed cell attachment to TCPS, NiPAM/NASI and RGD/Polymer conjugate surfaces created using the Two-Coat' technique (modified to use HBSS as the solvent for the second coat, Study II:9). Cell adhesion in culture medium with/out FBS was measured for each surface, using a Coulter Counter, after 24 hours. All values are expressed as percent adhesion (mean ± SD) of the number of cells originally seeded (~ 2.1×10^4 cells/cm^2).

Medium	TCPS	NiPAM/NASI	RGD/Polymer Conjugate
- FBS	85 ± 4	54 ± 21	37 ± 13
+ FBS	103 ± 12	28 ± 6	25 ± 3

IV: Surface Conjugation

The 'Surface Conjugation' technique, which again involved a two step process, proved to most effectively achieve the original two goals – to eliminate all non-RGD-mediated adhesion and maximize the RGD surface density. This first application was again, the NiPAM/NASI polymer in methanol, which evaporated overnight, and the second application this time was dissolved in phosphate buffer. The second coating was

performed at 37 °C, a temperature higher than the LCST, which makes the polymer layer insoluble in this medium. It was thought that, due to its hydrophilicity, the phosphate buffer would not disturb the initial polymer coating; this proved to be a correct assumption. The negative control for these experiments became wells coated with NiPAM/NASI in methanol, which was subsequently treated with the 0.1 M phosphate buffer. The RGD conjugate wells received an initial application of NiPAM/NASI as well, followed by an application of *unconjugated* peptide containing the RGD sequence, also dissolved in 0.1 M phosphate buffer, as per the original reaction conditions. In this technique, the peptide/polymer conjugation reaction took place on the surface within each individual well, ensuring that the RGD moieties were indeed exposed to interact with cells, upon seeding. Because the conjugation reaction was taking place on the surface of each well, it was possible to measure and maximize the RGD surface density with a fair degree of certainty, using RP-HPLC, as outline in the **EXPERIMENTAL** section. An example of this reaction data, obtained using the RP-HPLC, was displayed previously in Table 8 of this section. While this is not the ideal way[1] to reproduce the peptide-polymer reaction and test the bioactivity of the modified RGD, it was the first time that we were able to undoubtedly attribute increased adhesion to the presence of the RGD moiety.

The visual observations alone were enough to set this technique apart from the others. The ring of cell growth around the outside of the wells was no longer present and the surface coatings appeared to be fairly uniform. As well, a distinct difference was noted in the morphology of the cells in the wells where the RGD-containing peptide had been

[1] Ideally, one would perform the conjugation reaction not in tissue culture well, but as a separate reaction, characterize the conjugation efficiency (number of peptides per polymer) and coat the wells with the characterized conjugate. In addition to not being practical, this method may contribute to batch variability.

immobilized; the cells were adhering and spreading quickly on NiPAM/NASI surfaces treated with GYRGDS, resembling the growth seen on the TCPS surfaces (Figure 9). The cell attachment data corresponding to these observations are summarized in Table 13. Due to its success, this technique was used for all subsequent experiments.

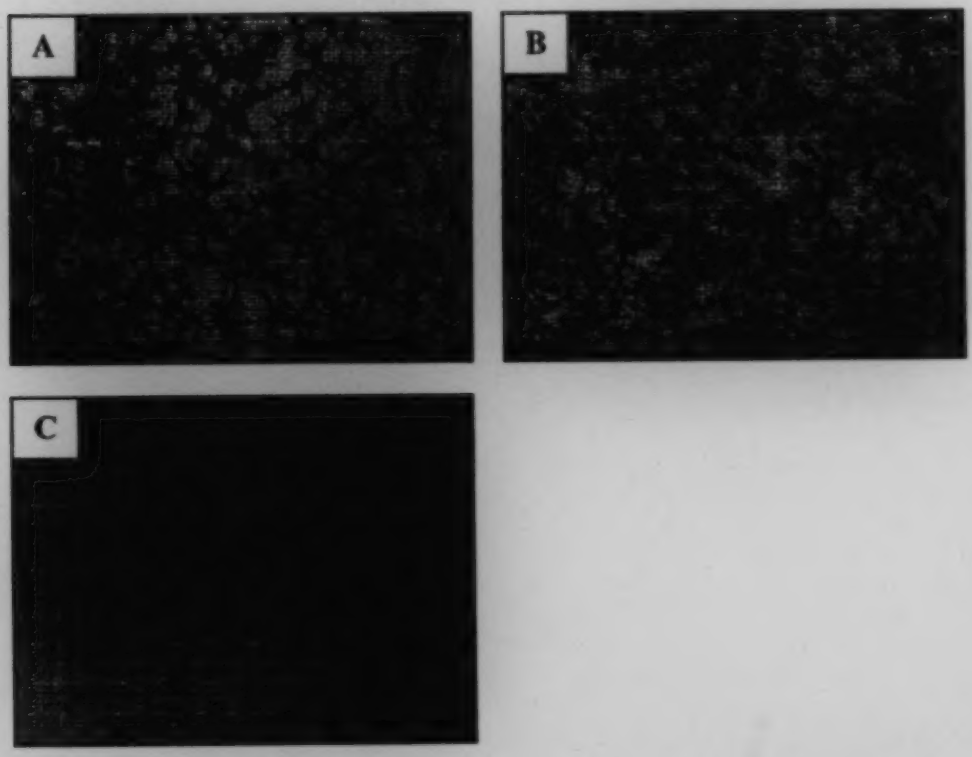

Figure 9 – C2C12 cells adhered and spread to the RGD-conjugated polymer surface (A), created using the Surface Conjugation technique, in a manner comparable to that observed on the TCPS control surfaces (B), and the NiPAM/5.1% NASI surface (C). GYRGDS Peptide surface density in conjugate ~ 3.4 nmol/cm^2. (10x magnification)

Table 13 – Cell adhesion to the RGD-conjugated polymer surface, compared to the TCPS and NiPAM/NASI controls (positive and negative, respectively). All values are expressed as percentage of cells (mean ± SD) remaining from the original number seeded (~ 2.1 x 10^4 cells/cm^2). (Coulter data, Study II:8)

Medium	TCPS	NiPAM/NASI	RGD/Polymer Conjugate
- FBS	37 ± 5	8 ± 2	24 ± 5
+ FBS	126 ± 8	17 ± 8	88 ± 16

Cell adhesion and spreading was consistently higher on RGD-containing polymer surfaces, as compared to that observed and measured on NiPAM/NASI surfaces. For cells cultured in medium not containing FBS, the measured increase ranged from 1.4 to 2.9, typically showing ~2.5 times the number of cells adhered to RGD conjugate surfaces. Cells cultured in medium supplemented with FBS showed an increased adhesion on RGD surfaces ranging from 1.4 to 10.6, with a typical value of ~5 times that seen on the NiPAM/NASI surfaces. In all of our studies, except where the effects of varying concentrations of peptide were explored, the RGD surface density used was assumed to be in the order of 3.4 nmol/cm^2 when 0.1 mg/mL peptide concentration was used for the immobilization reaction. This significant increase in adhesion was also reported by other researchers, who have also incorporated the RGD sequence into various materials and studied the effects on adhesion, for a range of peptide surface densities and a variety of different cell types (summarized in Table 14). It is possible to compare our results to some of the results presented in Table 14, where peptide grafting densities were provided in the same units as calculated in this thesis (nmol/cm^2).

Table 14 – Cell response to RGD incorporation into biomaterials at varying peptide surface densities.

Study	Surface	Peptide	Cell Type	Peptide Surface Density	Critical Observation (incubation time)
[30]	PS/PEO	GYRGDSY	NIH 3T3	1.4×10^4 molecules/μm^2	**Adhesion (24 hr):** 17.5 times greater on RGD surface vs. no peptide
[32]	PEG (with spacer)	YRGDS	HFF	0.01, 0.1 and 1.0 pmol/cm^2	**Spreading (24 hr):** 3 (a), 6 (b) and 13 (c) times greater on RGD surfaces vs. no peptide
[34]	Glass	RGDS	SHR	2.0 nmol/cm^2	**Adhesion (4 hr):** 2.5 times greater on RGD surface vs no peptide glass
[58]	PLAL	RGD	BAE	0.4 nmol/cm^2	**Spread Cell Area (4 hr):** 5 times greater on RGD suface vs. no peptide PLAL
[59]	PU	GRGDSY/ GRGDVY	EC	100 and 250 μmol/g	**Adhesion (24 hr):** Increased significantly as peptide concentration increased vs. no peptide. Greater difference with GRGDVY vs. GRGDSY.
[60]	Quartz	RGD	RCO	~4 nmol/cm^2	**Spread Cell Area (4 hr):** 3.1 times greater on RGD surface vs. no peptide quartz
[61]	Glass	RGD	HFF	0.1, 1.0 and 10 fmol/cm^2	**Morphology (24hr):** Cells adhered to 0.1 fmol/cm^2 surface, but did not spread. Spreading occurred at 1.0 fmol/cm^2, but focal contacts were not present. Minimum density of 10 fmol/cm^2 was required for both spreading and focal contact.

Polymers: PS – polystyrene; PEO – polyethylene oxide; PEG – polyethylene glycol; PLAL – poly(lactic acid-co-lysine); PU – polyurethane;
Cells: NIH 3T3 – Swiss albino fibroblasts; HFF – human foreskin fibroblasts; SHR – spontaneously hypertensive rat smooth muscle cells; BAE – bovine aortic enthothelial cells; EC – endothelial cells; RCO – primary rat calvaria osteoblast-like cells;

Mann et al. were able to increase smooth muscle cell (cultured in media supplemented with FBS) adhesion to aminophase glass with covalently bound RGDS (peptide surface density 2.0 nmol/cm^2) by a factor of 2.5, when compared to clean glass

[34]. This increase was measured after only 4 hours in incubation; they also reported that after 24 hours, there were no differences between the amount of adhesion on the control surfaces and the adhesive peptide-grafted surfaces, likely due to the presence of serum proteins in the media. Hern and Hubbell immobilized YRGDS to PEG diacrylate hydrogels via a PEG spacer [32] and were able to show that the presence of the peptide (1.0 pmol/cm^2) significantly increased human foreskin fibroblast cell adhesion. These studies were also performed in medium with and without FBS. Similar to the results seen in our experiments, they reported that cell adhesion and spreading of cells in serum-free medium was only slightly less than that seen in serum-containing medium (~20% less after 24 hours). FBS and other similar serums contain many proteins, growth factors, etc. that may indirectly influence cell adhesion and spreading. However, the results obtained for cells cultured in medium without FBS confirms that adhesion and spreading were at least partially mediated by the presence of the RGD sequence on the surface.

E. Cell Attachment by MTT Assay

The majority of the previous studies have used the Coulter Counter because it had proven to be a more accurate method of measuring the number of cells adhered to a particular surface, when compared to the hemacytometer. The data obtained using the hemacytometer was inconsistent and generally did not reflect the amount of cells adhered to the polymer surfaces, as observed visually. This error may have been due to the fact that the number of cells re-suspended from the polymer surfaces was quite low to begin with (i.e. relatively large variation in hemacytometer counts). The hemacytometer method was more effective when used to make a comparison between the number of cells

ahered to the TCPS surfaces and the RGD-containing polymer surfaces, because the numbers were generally much higher to begin with.

The Coulter Counter was generally a more accurate method of counting the number of cells adhered to the NiPAM/NASI surfaces, when compared to the hemacytometer. This was because a 0.5 mL sample from each well was taken and diluted with isoton for counting; this is 50 times the volume used for the hemacytometer method (10 μL). It is assumed that there would then be 50 times the number of cells in the larger volume and small variations between each count would not result in such a significant error. Unfortunately, while the Coulter method eliminated the large error due to field variation, it incurred another source of discrepancy. Cells added to the NiPAM/NASI copolymer surfaces were growing in spheroids, which were technically difficult for a Coulter unit to count accurately. The Coulter counter was designed for cell suspensions, not aggregates of cells. On a number of occasions, the spheroids in the NiPAM/NASI surface samples appeared to have clogged the Coulter unit, resulting in abnormal behavior and very inaccurate numbers until the blockages were cleared. It appeared that while both the hemacytometer and the Coulter methods were able to effectively quantify the number of cells adhered to the TCPS and RGD-containing polymer surfaces, they were not very accurate when used to count the cells on the NiPAM/NASI surfaces, where the cells were growing in aggregates. This led to the idea of using the MTT assay as a more effective means of quantifying cell adhesion to any given surface.

The MTT assay (as described in the **EXPERIMENTAL** section) is used to measure cell metabolic activity, rather than literally counting cell numbers. It was

thought that this assay would be equally as effective as the Coulter Counter, without the complications involving the spheroids, since its effectiveness did not depend on the type of cell growth seen in the different surface samples. This assay is based on the transformation and colorimetric quantification of MTT, which has been reduced by the respiratory chain and other electron transport systems within the cell. As a result, the reduced MTT (and other tetrazolium salts) form non-water-soluble violet formazan crystals within the cells, the amount of which can be determined by reading the absorbance with a spectrophotometer [62]. This number serves as an estimate for the number of mitochondria present in the sample, thereby providing an estimate of the number of living cells in the sample.

The MTT assay proved to be an effective way of quantifying cell adhesion to a particular surface; this and the Coulter method appeared to compliment each other, giving fairly consistent data. The results of one such study, used to assess the correlation of values obtained with the two methods are displayed in Figure 10.

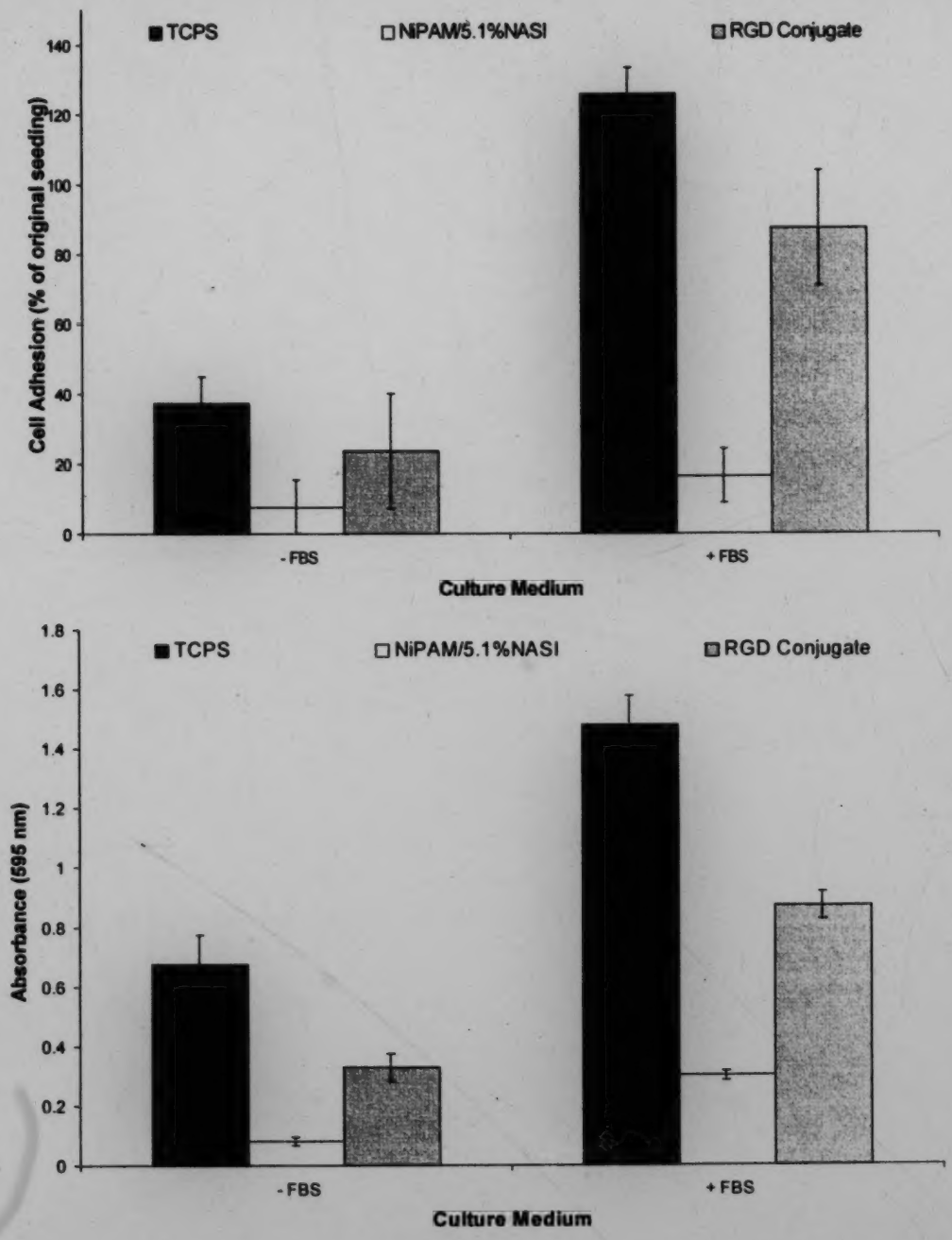

Figure 10 – Cell adhesion data obtained using the Coulter Coulter (top) and the MTT Assay (bottom). TCPS and NiPAM/NASI are the positive and negative controls, respectively. 'RGD Conjugate' refers to the NiPAM/NASI surface, to which 0.1 mg/mL GYRGDS had been immobilized. Surfaces were studied in culture medium both with and without FBS. Cells were seeded at a density of ~1.6×10^4 cells/cm^2 (Study II:8).

For this specific study, the Coulter data showed that the RGD-containing polymer surface increased cell adhesion by a factor of 5.3 in medium containing FBS and 3.1 in medium without FBS, when compared to the unmodified NiPAM/NASI surface. The MTT data showed that cell adhesion on the RGD-containing surface is increased 4.1 fold in medium containing FBS and by a factor of 2.9 in medium without FBS, when compared to NiPAM/NASI. These results show that values obtained from counting cell numbers and measuring cell metabolic activity are comparable and that the RGD-conjugated polymer undoubtedly increased cell adhesion, when compared to the unmodified NiPAM/NASI surface, regardless of the culture medium.

The surface conjugation study done to compare the MTT Assay to the Coulter method was repeated and the results were duplicated (Study II:9), confirming the effectiveness of the MTT method. The data for the repeated study was summarized in Table 15.

Table 15 – Cell adhesion to TCPS, NiPAM/NASI and the RGD/Polymer Conjugate (NiPAM/NASI + 0.1 mg/mL GYRGDS) surfaces in medium with/out FBS. (Study II:9). Values were obtained using the MTT Assay and are expressed as absorbances (mean ± SD) read at 595 nm. Cells were seeded at a density of ~2.0×10^4 cells/cm^2.

Medium	TCPS	NiPAM/NASI	RGD/Polymer Conjugate
- FBS	0.703 ± 0.019	0.380 ± 0.146	0.946 ± 0.614
+ FBS	1.971 ± 0.029	0.466 ± 0.090	1.832 ± 0.412

The MTT Assay also showed that cells cultured in medium without FBS consistently exhibited slower growth, if any, and did not spread as well, to any surface. There was a slightly larger increase in adhesion to the RGD-containing polymer surface, over a 24 hour period, when cells were cultured in medium containing FBS. In medium not containing FBS, the RGD-containing surface increased adhesion by a factor of 2.4. In medium supplemented with FBS, the increase in adhesion was nearly 4 fold.

With the addition of running duplicates of all samples for both Coulter and MTT testing, the experiments had become rather large and the issue of conserving materials and time became prominent. It was thought that using duplicates to compare MTT and Coulter results was more effective than comparing adhesion with and without the presence of FBS. Therefore, the experiments involving medium not containing FBS were eliminated from subsequent studies.

F. Effects of Different Polymer Surfaces on C2C12 Cell Attachment

Many of the polymers used in this thesis varied only slightly in composition, e.g., 5.1% vs. 3.8% NASI, and it was assumed that they would have the same conjugation reaction to RGD-containing peptides, as well as maintain a similar compatibility with the C2C12 cells. This was not true in all cases, however. Regardless of the care and caution taken when preparing different materials, some degree of batch variation was inevitable. Since some of the polymers used in these studies were prepared by different people, there was some batch variation and some materials elicited a cell response very different to that which was expected.

All initial experiments in this project were performed using a NiPAM/NASI copolymer containing 5.1 % NASI, which was synthesized by X.J. Fan [22]. When all of this polymer had been used up, a new batch of polymer was synthesized by J. Yang, using a procedure similar to Uludag and Fan [22]. This polymer was designated JY-2. When used for the RGD conjugation reaction, JY-2 (containing 5.0% NASI) elicited a very different response *in vitro*. The results from one particular study, where cell response to different RGD concentrations were evaluated, were displayed graphically in Figure 11.

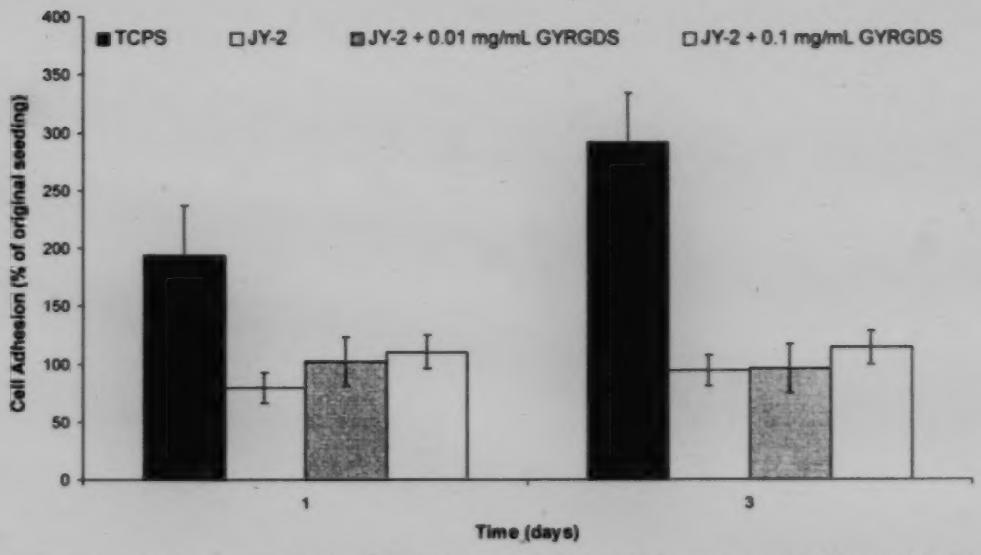

Figure 11 – Cell adhesion to the TCPS, JY-2 and RGD/JY-2 conjugate surfaces, after 24 hours. These values are reported as mean ± SD percentages of the original number of cells seeded. The original seeding density was ~ 1.3 x 10^4 cells/cm^2. (Coulter Counter, Study II:10).

Results from both the Coulter Counter and the MTT assay were abnormal when using the JY-2 polymer. While no difference was seen between the polymer surfaces that did or did not contain the RGD sequence, all of these numbers (from both methods) were

consistently higher than previously reported. Since the only parameter to change in this study vs. previous studies was the polymer, it was thought that the JY-2 polymer caused substantial 'background' interference (the data from the MTT assay was inconclusive and was not presented here). With the Coulter counter, it's possible that the polymer particles gave erronious readings, resulting in their recognition as cells. With the MTT assay, we have visibly seen formazan formation in polymer coated wells that had no cells remaining.

The visual observations, more than the numerical results, illustrated the differences seen with the JY-2 polymer. Both the unmodified polymer and RGD/JY-2 conjugate were not as stable in culture as the previous material; the polymer coatings began to lift up from the TCPS well surfaces after 1 day. As well, the increased cell adhesion previously seen on the RGD-containing polymer surfaces was not reported here, even after 3 days. The morphology of the cells was also different on the RGD/ JY-2 conjugate surfaces; cells did not adhere or spread nearly as well as the previous conjugates. There was very little difference seen between the unmodified JY-2 and RGD/JY-2 conjugate surfaces. In both cases, the majority of cells remained round, clumped and suspended in medium. There was a significant amount of debris (whether this was the polymer degrading or cellular debris is uncertain) observed in nearly all coated wells and it was thought that this debris interfered with the testing methods. These results indicated that caution was necessary in the use of different batches of polymer, even though the composition of the polymers might be relatively similar.

A 'polymer screen' was designed to assess the cell compatibility of a number of different available polymers, including the JY-2. The composition of the polymers used

in this study (II:11) were as follows: JY-2: NiPAM/5.0%NASI; F: NiPAM/5.1% NASI; L: NiPAM/1.4%NASI/6.0% MMA; R: NiPAM/3.3%NASI/17.0%MMA; V: NiPAM/1.3%NASI/21.5%EMA; U: NiPAM/15.4%EMA. Polymer U was included in this study because of its previous use in *in vivo* studies: this polymer was effective in retaining BMP-2 when injected into a muscle site [54]. The results of this study were summarized in Figure 12.

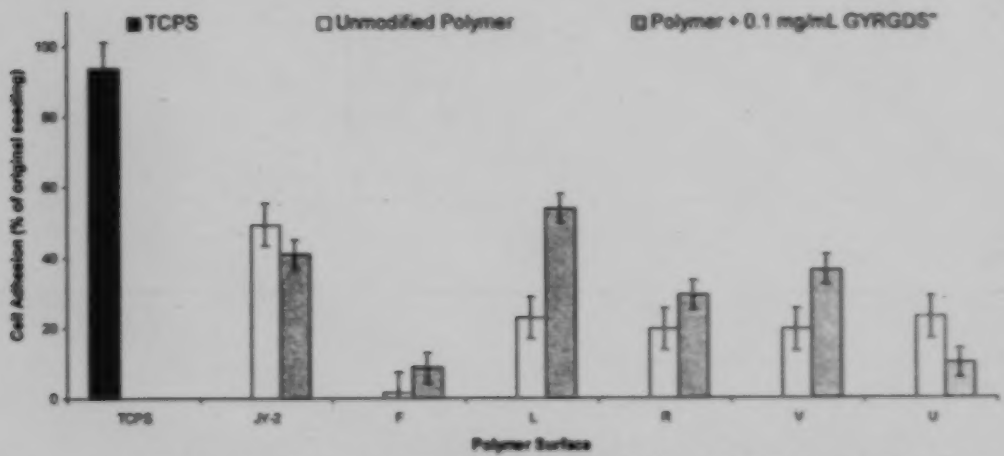

Figure 12 – Cell adhesion on a selection of unmodified and RGD modified polymer surfaces, as compared to a TCPS control surface (Coulter Counter, Study II:11). These values are expressed as the mean ± SD percentage of cells remaining from the original seeding number after 24 hours. The cells were seeded at a density of ~0.5 x 10^4 cells/cm^2.

The Coulter numbers showed that none of the polymers supported cell attachment comparable to that of the TCPS control. Polymer F appeared to be least supportive of cell attachment, both unmodified and modified to contain the immobilized RGD moieties. Visually, however, Polymer F yielded the best results; the unmodified surface supported very little growth, and cells remained clumped and suspended, as seen before. The RGD-containing surface supported growth similar to that of the TCPS surface.

though to a lesser extent, in quantity; cells on this surface were well spread and morphologically intact. These visual observations were the most important result from this study; none of the surfaces, except polymers F and U, were appealing to the cells. Polymer U supported some cell attachment and the cells appeared to have retained their round morphology; they remained in a pluripotent state, not differentiated and spread, as on TCPS (Figure 13). Polymers L, R and V looked identical to JY-2, whose compatibility with cells remained similar to the previous studies with polymer F, where cells remained round and suspended, clumped. In the cases of polymer L, R, V and JY-2, the wells also contained a large amount of cellular/polymeric debris. As a result of this study, polymer F was used for subsequent studies, while quantities lasted, and polymer U was also used, as a positive control for *in vivo* studies.

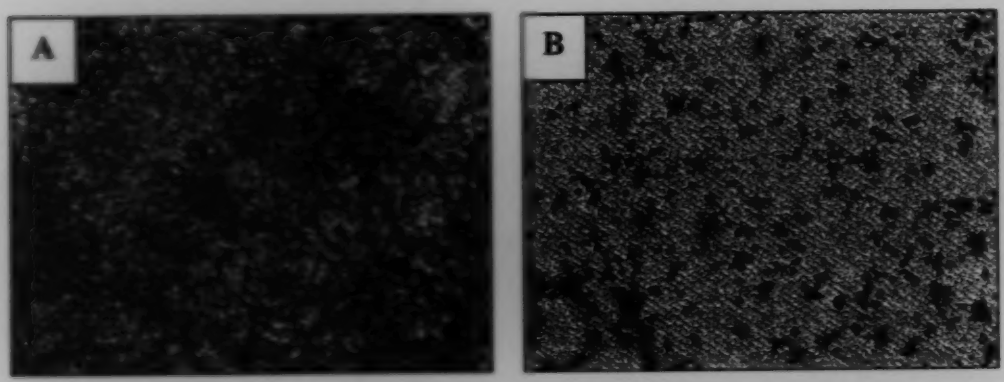

Figure 13 – C2C12 cells adhered and expressed typical fibroblast morphology on TCPS surfaces (A), while remaining round and in an undifferentiated, pluripotent state on Polymer U (NiPAM/EMA) surfaces (B). Photos taken using phase-contrast microscopy at 10x magnification.

G. Effectiveness of Techniques to Quantify Cell Adhesion

The closest correlation between the cell growth observed visually and by quantitative methods was obtained using the Coulter Counter to measure the number of

cells adhered to the NiPAM/NASI surfaces. The MTT assay worked for most surfaces, providing an accurate measure of the number of cells present in each well. As mentioned above, in the study done to compare the different polymer surfaces (II:13), we observed an unexpected MTT signal for some of the polymers. The absorbance values obtained for some of the polymer coatings were generally higher than the background value, i.e. there was an MTT absorbance signal without cells. It appeared that the polymer coatings were possibly a source of 'background' absorbance, resulting in higher readings for all coated surfaces (Figures 11 and 12). Therefore, caution was necessary to ensure that there was no excess MTT transformation, due to the polymer films (and not cells).

Polymers L (NiPAM/1.3%NASI/6.0%MMA), R (NiPAM/3.3%NASI/17.0%MMA) and V (NiPAM/1.3%NASI/21.5%EMA), as well as JY-2 (NiPAM/5.0%NASI) appeared to degrade in the TCPS wells, resulting in a large amount of cellular/polymeric debris. The cells rejected these surfaces, remaining round and suspended; after washing, there were virtually no cells left on any surface. If the MTT assay was accurately reading cell metabolic activity (i.e. cell number), the absorbance values for these wells would have been very low, simply due to the absence of cells. MMA and EMA contain hydrophobic groups; typically, polymers containing these monomers become more hydrophobic, thus lowering the LCST [21,22]. Since anchorage-dependent cells tend to prefer to adhere to hydrophobic surfaces, it was expected that polymers L, R and V would support some degree of cell attachment, as in the case of polymer U. This was strangely not the case.

The cell response to the JY-2 polymer was the most peculiar. Having a similar NASI content (5.0%) to the other polymers used throughout this project, it was expected that JY-2 would yield comparable results to polymers E and F (3.8 and 5.1% NASI, respectively). However, JY-2 behaved very differently than expected. As mentioned, the JY-2 polymer was synthesized by a different individual than the person who synthesized polymers E and F, although both used a similar procedure [22]. It was assumed that some degree of batch variation between the two polymers resulted in the rejection of the JY-2 polymer by the cells. Possibly, JY-2 was slightly more hydrophilic; perhaps a residual solvent, such as ether, was the reason for the cells rejecting the JY-2 polymer and the 'background' absorbance levels measured by the MTT assay.

The 'background' absorbance complications associated with some of the polymers made it difficult to compare the absorbance values generated for the RGD-conjugated surfaces to the TCPS controls. Two other factors which may have contributed to some of the variability in MTT results were (i) suspended microbial growth and (ii) extended incubation time after dissolving samples in DMSO. Both of these increased the absorbance values beyond the detection limit of the plate reader (data not shown). We were therefore, forced to exclude these studies from the overall approach. For the majority of all other studies described within this report, the data obtained using the MTT assay was accurate; this assay was effective in showing the increased adhesion due to the presence of the RGD sequence. Whenever possible, duplicate plates were prepared and the cell adhesion to the various surfaces was quantified using both the Coulter Counter and the MTT assay, as they appeared to compliment each other.

While many other researchers also use MTT [62-66], and have found it to be accurate and effective, there are other methods available, for quantifying the number of cells in a particular sample. A recent improvement to the MTT assay uses the substrate 5-(3-carboxy-methoxyphenyl)-2-(4,5-dimethylthiazolyl)-3-(4-sulfophenyl) tetrazolium (MTS) [66]. This method has been found to be better for use in cell proliferation assays because the formazan product is soluble and released into the culture medium. Conversely, the drawbacks are that the MTS substrate is not as stable as MTT, it degrades spontaneously to generate high background levels, and it cannot be used for some human cell lines, due to inefficient metabolism of the substrate, as well as toxicity of MTS to such cells [66].

Two other methods, the hexosaminidase assay and the acid phosphatase assay, also employ enzyme-substrate reactions to quantify cell number, and are used by many researchers [66-68]. The hexosaminidase assay uses p-nitrophenol-N-acetyl-B-D-glucosaminide as a synthetic substrate for the cytoplasmic enzyme hexosaminidase. A standard curve is typically prepared, relating hexosaminidase activity measured by the colorimetric assay to the number of cells. The absorbance of each sample is read at 405 nm on a microplate reader and, using the standard curve, this value is converted to cell number [67]. This method has been used to accurately quantify very low numbers of cells (~ 60-12,000 cells/75 μL); the hexosaminidase assay is more sensitive than the MTT assay, and as such is the preferred method to quantify very low cell numbers [67]. The acid phosphatase assay is based on the conversion of p-nitrophenyl phosphate (pNPP) to p-nitrophenol by cytosolic acid phosphatase (similar to ALP assay). As in the case of the ALP assay, the p-nitrophenol product absorbs light at 405 nm, and absorbance at this

wavelength is an estimate of cell number. The sensitivity of this method is similar to the MTT assay, and it is also applicable for counting nonadherent as well as adherent cells in culture, [66].

Protein assays are also very effective for quantifying nonadherent as well as adherent cells, as this method is a measure of the total protein present in a sample. Typically, aliquots of cell suspension are taken and their adsorbance read at 570 nm on a microplate reader. These values are compared to a standard curve prepared with such proteins as bovine serum albumin and a value for the total protein present in the sample is obtained. This type of assay is not only used to quantify cell number, but also (i) protein adsorbed to a surface [67], and (ii) as a way to normalize other measured activity to a per mg of protein basis (e.g. Bradford's method), such as that obtained using the ALP assay [69]. This last method was attempted in our lab, but not found to be sensitive enough for our purposes (data not shown).

All of the methods described here have been found to be effective for quantifying cell number. While we feel that MTT is equally as effective, these other methods would provide complimentary results. The ability to record visual observations, using a digital camera unit attached to the microscope was the most valuable complimentary technique. It was not only a means to observe cell morphology, but also to confirm the cell number data and the effectiveness of the various methods used in our studies. The pictures taken with this unit became the only 100% effective method of consistently documenting the decreased and increased cell adhesion seen on the NiPAM/NASI and RGD-containing polymer surfaces, respectively. The phrase 'a picture is worth a thousand words' definitely applies in this case. The pictures included in this report not only confirm the

numbers obtained with the various quantitative methods, but they also provide qualitative measurements of cell growth. They show that the RGD-containing polymer surface not only increased adhesion, but also mediated growth and differentiation. The cells cultured on the RGD-containing polymer surfaces *looked* like the cells cultured on the TCPS control surfaces, indicating that their morphology was intact, and that is perhaps the most significant result to be reported in this project thus far.

H. GRGDS-Dose Dependent Cell Attachment

Studies were conducted to determine if the concentration of immobilized GRGDS influenced cell adhesion. Both the Coulter and MTT methods were used to quantify adhesion to these RGD/Polymer conjugate surfaces, as compared to TCPS, unmodified NiPAM/NASI and NiPAM/EMA (Polymer U) control surfaces, over a 6 day period. The values obtained for two different NiPAM/NASI polymers, containing 5.1% and 3.8 % NASI, respectively (polymers F and E, both synthesized by X.J. Fan), after 24 hours of incubation were displayed in Figure 14.

Compared to buffer treated surfaces, the GRGDS-treated surfaces increased cell adhesion by a factor of 3, 6, and 23, for concentrations of 0.001, 0.01 and 0.1 mg/mL GRGDS, (RGD concentration: x.01, x .1 and x 1) respectively, using Polymer F (Study II:14). Results from Polymer E (Study II:15) yielded similar results, increasing cell adhesion on the 0.001, 0.01 and 0.1 mg/mL GRGDS surfaces by factors of 6, 17 and 25, respectively. In this case, even the 0.001 mg/mL GRGDS conjugate surface appeared to yield better cell adhesion than the unmodified NiPAM/3.8%NASI surface.

The RGD Dose Response was also evident in the data from the MTT assay, for both NiPAM/NASI polymers used. Cell adhesion to the RGD conjugate, created using

the 5.1% NASI polymer, was increased by factors of 1.5, 2, and 6, for the increasing GRGDS concentrations, respectively. In this case, the cell adhesion to the 0.1 mg/mL GRGDS conjugate (highest concentration) value was very close to both the NiPAM/EMA and TCPS surfaces, reflecting the visual observations. The values obtained for the 3.8% NASI polymer conjugates were lower than expected, but the RGD dose response was still visible. RGD conjugates created using this polymer increased cell adhesion by factors of 2, 2 and 3, for the increasing GRGDS concentrations, respectively. An important point to note here is that the 0.1 mg/mL GRGDS conjugate in this case yielded similar results than both the NiPAM/EMA and TCPS control surfaces.

Visual observations concurred with the numbers for this particular study. The unmodified (i.e. buffer treated) NiPAM/NASI polymers, as expected, supported little or no cell attachment. The NiPAM/EMA control surface (Polymer U) supported some cell attachment, but again, the cells remained rounded and did not spread, as seen on the TCPS surface. After 24 hours, all of the surfaces containing the immobilized RGD sequence clearly showed increased cell adhesion, compared to non-RGD treated surfaces, in a dose dependant manner, both visually and numerically. The cell growth and morphology on these surfaces also resembled that seen on the TCPS surfaces (Figure 6).

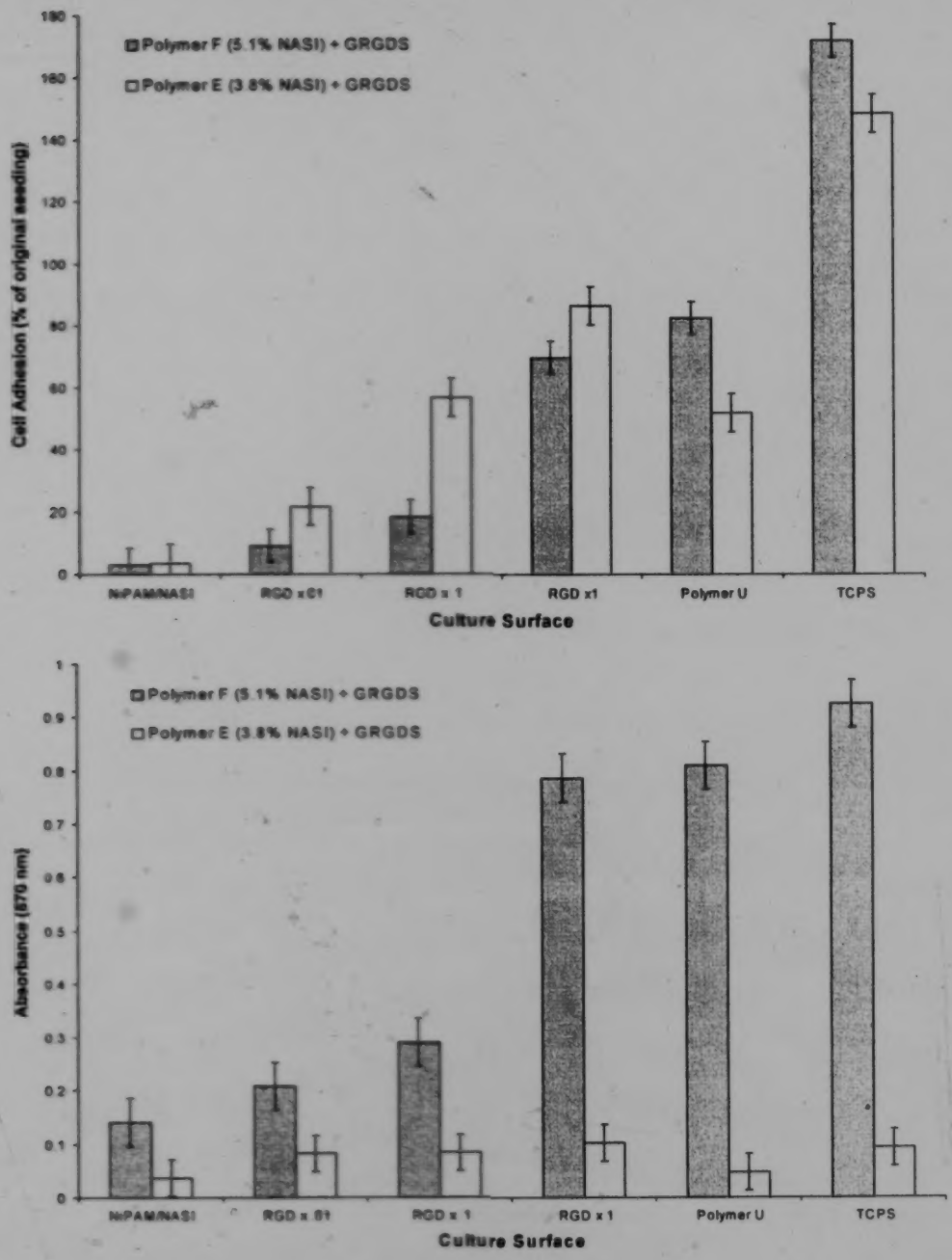

Figure 14 – Cell adhesion to two different NiPAM/NASI polymers (F and E, containing 5.1% and 3.8% NASI, respectively) which have been modified with varying concentrations of GRGDS, as compared to TCPS, Polymer U and unmodified NiPAM/NASI control surfaces. This data was from a Coulter Counter (top) or MTT assay (bottom), after 24 hours, and is expressed as the mean ± SD.

In general, these studies showed that the increased adhesion on the GRGDS surfaces was indeed dose responsive. In virtually all cases, there was a direct correlation between the GRGDS peptide concentration and the number of cells adhered to that surface. While some variation in the dose response was noted, the highest peptide concentration (3.4 nmol/cm^2) consistently resulted in significantly more cells adhered (~15 times more), when compared to the NiPAM/NASI surface. In some studies, even the lowest concentration of conjugated GRGDS (0.034 nmol/cm^2) resulted in ~3 times the number of cells adhered to its surface, when compared to the NiPAM/NASI surface (Figure 14).

The morphology of the cells was also GRGDS dose dependent; cells adhered to the lowest concentration spread slightly more than the round cells seen on the NiPAM/NASI surfaces, while cells adhered to the highest concentration of conjugated GRGDS spread in a manner similar to those cells observed on the TCPS control surfaces. Again, this spreading further confirmed that adhesion to the peptide-conjugated surfaces was mediated by cell-surface receptor interaction with the incorporated RGD sequence.

An important conclusion from the dose response studies was the determination of the minimum surface density required to induce increased cell adhesion and spreading. In our experiments, the lowest surface density was expected to be 0.034 nmol/cm^2 (assuming that peptide conjugation is concentration independent); as described above, in some studies, this density was effective at increasing the adhesion ~3 fold, from the unmodified NiPAM/NASI surfaces. Our results correlate well with the findings of Massia and Hubbell, who explored the morphology of human foreskin fibroblast cell spreading on a polymer-modified glass substrate containing immobilized RGD peptides

at varying peptide concentrations [61]. It was determined that the minimum RGD concentration required to support cell adhesion (but not spreading) was 0.1 fmol/cm^2, while maximal spreading and focal contact formation was seen at an RGD concentration of 10 fmol/cm^2 [61]. In our studies, a GRGDS concentration of 3.4 nmol/cm^2 was required for a similar biological response. Based on these results, it is expected that our materials (i.e. peptide surface densities) should be suitable for significantly increased cell attachment.

In a related study, Hern and Hubbell and the activity of their PEG-immobilized YRGDS [32]. They tested fibroblast spreading on 4 different concentrations of peptide immobilized via a PEG spacer: 0.001, 0.01, 0.1 and 1.0 pmol/cm^2, and found that 0.01 pmol/cm^2 was the lowest concentration which specifically promoted spreading. They also reported that surfaces containing peptide conjugated without the PEG spacer arm did not promote specific adhesion and spreading, even at the highest concentration of 1.0 pmol/cm^2. Hern and Hubbell's results were significant to our own studies in two ways. First, our GRGDS-conjugated polymer surfaces promoted biospecific C2C12 cell adhesion and spreading to a similar extent as seen on Hern and Hubbell's YRGDS-conjugated hydrogels (via PEG spacer), at comparable peptide surface densities. Second, without the use of the PEG spacer, the YRGDS-conjugated hydrogels did not promote biospecific adhesion and spreading, regardless of the peptide concentration used. Therefore, our GRGDS-conjugated surfaces appeared to be inherently different from the surfaces of Hern and Hubbell [32]: an RGD effect was observed without the need for a PEG spacer arm. These results indicate that the PEG chains in the hydrogel could have possibly sterically inhibited the cell-surface receptor recognition of the adhesion peptide.

This might have been the case when a PEG spacer arm was not used for peptide conjugation. Our studies indicated that the GRGDS adhesion peptide is successfully interacting with cell-surface receptors. Perhaps, not having the hydrophilic PEG spacer and having a relatively hydrophilic polymer was beneficial in our system.

I. Cell Density Effects on Cell Growth on Polymer Films

The C2C12 cell seeding density varied from experiment to experiment, for a number of studies performed throughout this project. It was hypothesized that some of the variability in MTT, Coulter and photographic results were due to the cell seeding density used, because it affected the proliferation state of the cells at the different time points when cell number and activity were measured.

Studies were done to assess the effects of the cell seeding density on the cell proliferation on the polymer films, over a period of 6 days in culture. The cell adhesion observed on the various surfaces at two different cell seeding densities (~2.1 and 0.6 x 10^4 cells/cm^2, respectively) are displayed in Figures 15A and 15B.

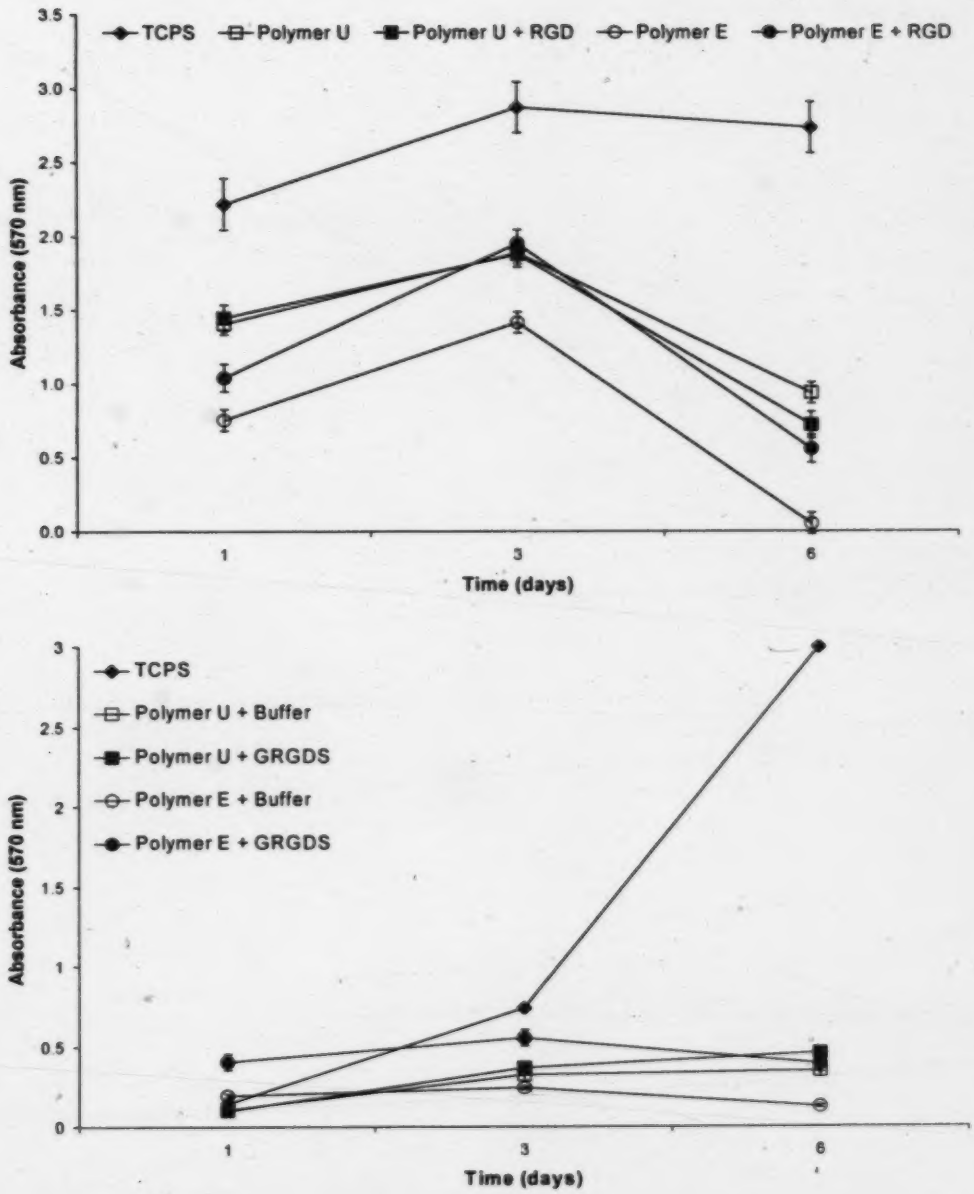

Figure 15 – Cell proliferation on polymer films at high (A) and low (B) seeding densities (~2.1 and 0.6 x 10^4 cells/cm^2, respectively), over a 6 day time period. Values are mean ± SD absorbances measured with MTT assay. Cells were cultured in 48-well plates.

In this specific study, at the higher cell seeding density, the number of cells adhered to the TCPS control surfaces increased from day 1 to day 3, but decreased slightly by day 6. It appeared that once the cells had become confluent, their metabolic activity had stabilized. This was the typical response for many other studies performed (data not shown), and was confirmed by visual observations. At all time points measured, the cell adhesion to the GRGDS-conjugated surface was higher than the NiPAM/NASI surface. However, the number of cells adhered to the TCPS control surfaces was consistently higher than the GRGDS-conjugated surfaces. Again, this was confirmed by visual observations; cells adhered to the GRGDS-conjugated surfaces exhibited similar morphology to the cells cultured on the TCPS surfaces. The presence of RGD did not alter the cell adhesion to the Polymer U surfaces; adhesion to Polymer U surfaces was higher than both the NiPAM/NASI and the GRGDS-conjugated NiPAM/NASI surfaces.

Cells seeded at the lower density in this study which were then cultured on TCPS surfaces continued to proliferate throughout the 6 day study period, while the cell numbers on the other surfaces were considerably lower. Consistent with previous results, there were more cells on the GRGDS-conjugated surfaces than the NiPAM/NASI surface. After 3 days in culture, the number of cells adhered when the low seeding density was used did not reach the same levels as when the high seeding density was used. There was no significant change in cell number between day 3 and day 6. This was one of the only incidents were the GRGDS-conjugated surfaces did not have a significant affect on cell attachment, when compared to the NiPAM/NASI surfaces. It was assumed that it was not simply coincidence that these unique results occurred in a

particular study when the cell seeding density used (0.3 x 10^4 cells/cm^2) was much lower than all other studies.

In general, for cells cultured on TCPS surfaces, the MTT values (i.e. cell numbers) increased from 1 to 3 days, as expected, followed by a decrease from the 3rd to the 6th day, in all experiments but one (Figure 15B), in which a very low seeding density was used (~ 0.6 x 10^4 cells/cm^2). It became apparent that after 6 days incubation, cells had reduced their metabolic activity and/or lost viability; as noted, this MTT data was consistent with visual observations. While this was unexpected initially, evaluation of the seeding density used for the different experiments accounts for the decreased activity. In general, at higher seeding densities, the cells had reached confluence by 3 or 4 days in culture, and, as reported by Winn. et al [40], a decrease in the cell proliferation rate is to be expected, once the cells have become confluent. At the lower seeding density, the cells on the TCPS control surface typically did not reach confluence until near the 6th day, thereby accounting for the continued increase in cell metabolic activity on that surface.

J. Non-Specific Adhesion Studies

To further confirm that the increased adhesion and spreading was RGD biospecific, the inactive peptide GRGES was used as a negative control in some of our experiments. GRGES was conjugated to the NiPAM/NASI polymer-coated surfaces also at a surface density of 3.4 nmol/cm^2 (assuming a similar level of reaction to that of the GRGDS peptide) and adhesion to these surfaces was quantified using the MTT assay. The results of one specific study were displayed in Figure 16. Note that this data is a

reproduction of Day 1 numbers from Figure 15B, with the addition of the GRGES-conjugated surfaces. The number of cells adhered to the GRGES-conjugated surface was consistently less than the TCPS control and GRGDS-conjugated surfaces.

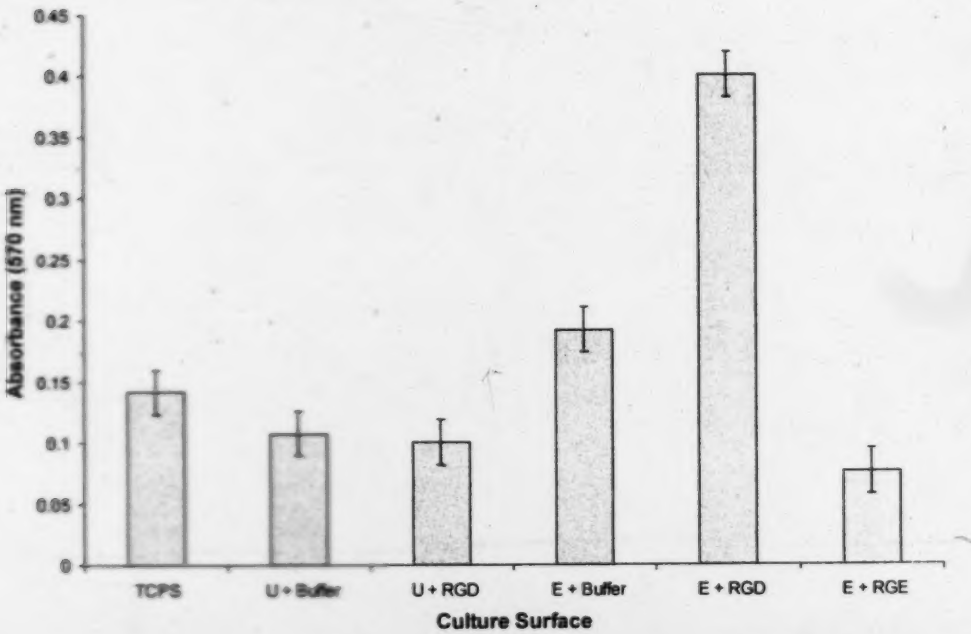

Figure 16 – Biospecific cell adhesion on GRGDS-conjugated surface, after 24 hours, as compared to TCPS control, NiPAM/15.4%EMA (Polymer U), NiPAM/3.8%NASI (Polymer E) and GRGES-conjugated surfaces (48-well plates, ~0.6 x 10^4 cells/cm^2). Surfaces not reacted with peptide were coated with 0.1 M phosphate buffer (pH 7.4).

After 24 hours, the GRGES-conjugated surfaces supported little attachment and the quantitative measurements shown above (MTT) indicated that there was signficantly less metabolic activity in wells where GRGES had been conjugated to the NiPAM/NASI surface. This confirmed that adhesion to the GRGDS-conjugated surfaces is indeed specifically mediated by the RGD moiety. Visual observations confirmed these results: cells cultured on the GRGES-conjugated surfaces, generally less remained and those that

did were round and suspended in medium, closely resembling those observed on the unmodified NiPAM/NASI surfaces. In contrast, cells seeded onto the GRGDS-conjugate surfaces adhered and spread, retaining myoblastic morphology. These observations were illustrated in Figure 17, below.

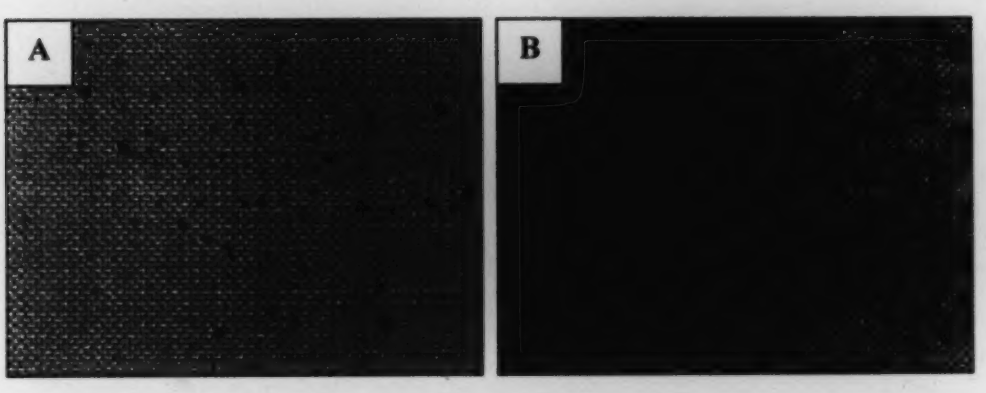

Figure 17 – Observed C2C12 cell response to GRGES-conjugated surfaces (A) confirms that adhesion and spreading on the GRGDS-conjugated surfaces (B) is biospecific. Photographs were taken using Phase Contrast Microscope at 10x magnification.

Hern and Hubbell reported findings similar to our own, when the inactive YRGDS peptide was immobilized on the PEG surfaces [32], as did Mann et al., who measured adhesion and ECM deposition on glass surfaces grafted with the RGES peptide, as a negative control [34]. The fact that the GRGES peptide did not support cell spreading, when conjugated at similar surface concentrations as the GRGDS peptide provides strong evidence that the adhesion and spreading seen on the RGD conjugate surfaces was biospecific. Therefore its bioactivity was retained through modification, and the RGD-containing polymers developed in our hands are able to effectively increase adhesion and spreading on an otherwise unsupportive surface.

Phase III: BMP-2 Responsiveness of Cells Grown on RGD-containing Polymers

A. C2C12 Cell Response to BMP-2

BMPs were chosen for their well-known and well-documented ability to induce osteoblast activity. Since their abilities were discovered, many different types of BMP have been synthesized and studied. BMPs belong to the transforming growth factor-β (TGFβ) gene superfamily, of which there are forty-three members [70]. Other members of this family include growth and differentiation factors (GDFs), inhibins/activins, TGFβs and Mullerian inhibiting substances [71]. Fifteen types of BMPs have been identified (found in both homodimer and heterodimer forms), which are divided into subfamilies according to their amino acid sequence. These groupings are as follows: BMP-2 and BMP-4, BMP-5 through BMP-8, and BMP-3 and GDF-10, which is a related growth factor [71]. While all of these BMPs have shown osteoinductivity; BMP-2 and BMP-7 especially, have exhibited equally effective abilities as their original predecessor, as reviewed in detail by Groeneveld et al. [71]. BMP-2 is the most studied BMP and as such, a significant database of information exists on its applications by a variety of biomaterials. BMP-2 was chosen for this project because of its aforementioned credentials, and because it has been employed by other members of this lab group previously [2,5,12,14,16,39], making it readily available. In addition to its effectiveness with osteoblasts and an osteoprecursor cell line (OPC1) [40], BMP-2 was shown to induce osteoblastic differentiation in non-osteoblast cells, such as pluripotent fibroblastic cell lines, C3H10T1/2, bone marrow stromal cell lines, W-20-17, ST2, MC3T3-G/PA6 cell lines, and C2C12 myoblastic cell lines [41].

When BMPs are implanted, they activate a set of cellular events, including chemotaxis of undifferentiated mesenchymal cells into the implant site and differentiation of these cells into chondroblasts and osteoblasts, removal of the calcified cartilage, and population of the new bone with bone marrow elements [70]. ALP expression is one of the phenotypic markers typically used to measure osteoblastic differentiation; other measurable markers include the ability to mineralize, the measurement of intact osteocalcin, osteonectin and osteopontin synthesized and secreted by the cells [40].

Extensive studies have been performed by other members of this group to develop carrier systems for effective delivery and sustained release of BMP-2 to local tissue sites [5,14,16,39,44]. BMP-2 was conjugated to the NiPAM based copolymers via the protein-reactive NASI groups, eliminating the need for additional crosslinkers, in the hopes of creating a controllable biomaterial carrier for sustained release of BMP-2. This system was effective in increasing BMP-2 retention in a rat intramuscular injection model as much as 100-fold [39], and increased retention is expected to yield a corresponding increase in osteoinductive activity (yet to be demonstrated). It is assumed that an osteoinductive event in vivo is limited by the responding cell population [16]. Therefore, by designing a biomaterial carrier that not only achieves sustained release and retention, but also enhances the number of cells available for response to the BMP, the osteoinductive potential at that site can be maximized. The RGD sequence was incorporated into the NiPAM/NASI copolymers for this reason. We intended to develop a material which would increase cell migration and proliferation at a specific site, thereby increasing the population of the cells available to respond to the co-injected BMP-2.

The ability of the GRGDS-conjugated surfaces to increase C2C12 cell adhesion and spreading was confirmed in Phase II of this project and described in earlier pages of this report. The ability of BMP-2 to induce osteoblastic activity in the C2C12 cells used in our studies was first explored on the TCPS well surfaces, using a concentration of 300 ng/mL and exposure times of 3 and 6 days. Since ALP is characteristically expressed by cells of osteoblastic lineage, the ALP assay was used as a measure of the extent of osteoblastic differentiation of the cells. Initial studies confirmed that cells cultured in an environment containing BMP exhibit a significant increase in ALP activity after 6 days. but not after 3 days. This data is summarized in Table 15. After 6 days, cells cultured on the TCPS surfaces, in medium containing BMP, expressed approximately 6 times the ALP activity (on average, taken from duplicate samples) than those cells cultured in medium without BMP.

Table 15 – BMP-2 induced ALP activity in C2C12 cells. Surfaces compared were TCPS, NiPAM/15.4%EMA (positive controls), NiPAM/3.8%NASI, NiPAM/3.8% NASI + 0.1 mg/mL GRGDS. Values are means ± SD of duplicate samples of enzyme/substrate reaction absorbances, measured at 405 nm, over 30 minutes and expressed as umol/mL of p-nitrophenol produced per hour. Cells were seeded at a density of ~1.7 x 10^4 cells/cm^2.

	3 Days BMP-2 Exposure		6 Days BMP-2 Exposure	
Surface	**- BMP**	**+ BMP**	**- BMP**	**+ BMP**
TCPS	0.151 ± .004	0.134 ± .089	0.038 ± .002	0.226 ± .001
NiPAM/15.4% EMA	0.139 ± .010	0.113 ± .003	0.070 ± .029	0.066 ± .003
NiPAM/3.8% NASI	0.090 ± .006	0.084 ± .016	0.119 ± .040	0.070 ± .009
GRGDS Conjugate	0.124 ± .003	0.122 ± .021	0.123 ± .054	0.111 ± .030

The presence of BMP-2 did not significantly increase ALP activity in cells cultured on other surfaces in this study (III:1). This may be due to the seeding density used; the results quoted above were obtained with an original seeding density of ~1.7 x 10^4 cells/cm^2. It was hypothesized that this cell density was too

few cells for them to be at a point where they could differentiate to the osteoblast lineage at the time of BMP introduction. As a result, the cells were proliferating during the incubation period with BMP-2, instead of being transformed.

A study, similar to the one discussed above, was designed to explore the effects of increasing the cell seeding density; also included in this study was a protein adsorption assay, meant to normalize the ALP activity values obtained with the number of cells responsible for that activity, per well. Unfortunately, the protein adsorption assay did not prove to be sensitive enough to accurately quantify the number of cells present in each sample well. Consequently, the ALP Activity continued to be expressed as μmol of p-nitrophenol/mL/hr, per well. The BMP-2 induced ALP activity of cells seeded onto TCPS, NiPAM/3.8%NASI and GRGDS-conjugated surfaces, using a higher cell density was displayed graphically in Figure 18.

After 3 days on the TCPS surfaces, cells cultured in medium containing BMP expressed ~28 times the ALP activity vs. those cells cultured in medium without BMP-2. For cells cultured on the GRGDS conjugated surfaces, the presence of BMP-2 in the medium increased ALP activity by a factor of 3.6. It was interesting to note that without BMP-2, the GRGDS conjugated surface tended to increase ALP activity when compared to the TCPS surface, but large SD did not allow for statistical significance. The ALP activity expressed by cells cultured on the NiPAM/3.8%NASI surfaces was significantly lower, in medium with and without BMP-2. After 6 days, the presence of BMP-2 increased ALP activity by factors of 7 and 2, for the TCPS and GRGDS conjugate surfaces, respectively. Again, the cells on the GRGDS conjugated surface had a

significantly higher ALP activity in the absence of BMP-2, when compared to the TCPS surface in the same environment.

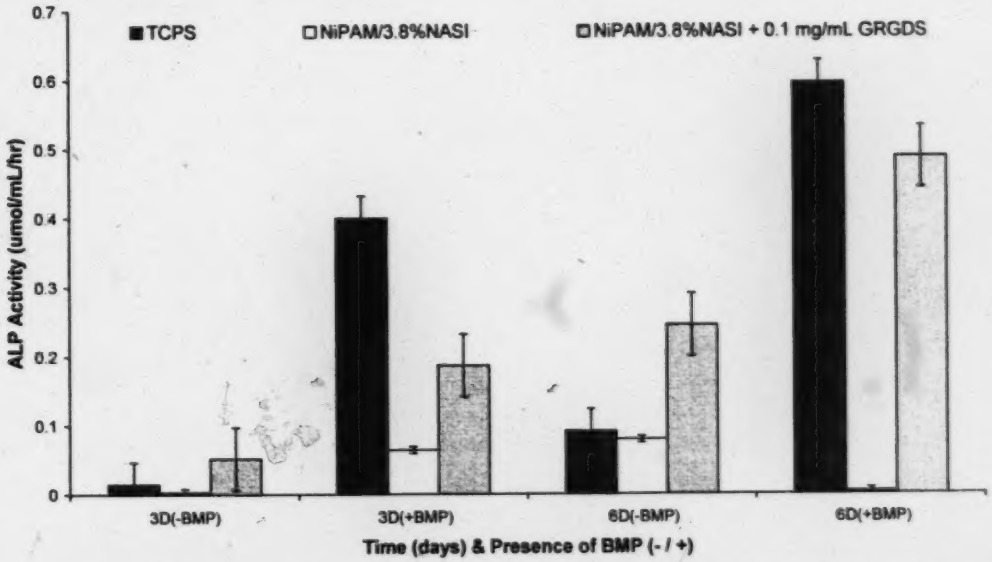

Figure 18 – Cell response to BMP-2 treatment, establishing that cells cultured on TCPS in medium containing BMP express higher levels of ALP activity (Study III:2). Original seeding density was ~2.3 x 10^4 cells/cm^2. Absorbances read for triplicate samples (405 nm) after 3 and 6 days exposure to BMP-2 were converted to concentrations of p-nitrophenol produced; values displayed were the mean ± SD, expressed as µmol/mL/hr. per well.

An important point to note was that the BMP-2-induced increase in ALP activity by cells cultured on the TCPS surfaces was evident at both the 3 and 6 day time points. As expected, BMP-2 responsiveness, i.e. increased ALP activity, was more pronounced after 6 days exposure; similar trends were reported by Yang et al. [41] and Shin et al. [43], who also studied the BMP-2 induced osteoblastic differentiation of C2C12 cells cultured in medium containing 300 ng/mL. These preliminary studies indicated that the measured increase in activity in cells cultured on TCPS surfaces was reproducible, and

that these surfaces were effective as positive controls for studying the ability of RGD-conjugated surfaces to retain cell responsiveness to BMP-2.

Once this positive control had been established, more extensive studies were performed, using varying concentrations of BMP-2 to establish a ALP – BMP-2 dose response. Cells were cultured on the same three surfaces as in previous experiments (TCPS, NiPAM/3.8%NASI, GRGDS conjugate) and exposed to BMP-2 concentrations of 0, 25, 100 and 250 ng/mL for 3 and 6 days. Although an exact seeding density was not available (we did not have access to neither a hemacytometer, nor a Coulter Counter for this particular experiment), the seeding density used for this experiment was higher than that used in previous experiments; it was estimated at approximately 2.6×10^4 cells/cm^2. The results of this experiment (III:3) were displayed in Figure 19.

After 3 days in culture, the ALP activity of cells on TCPS surfaces increased by factors of 7, 36 and 123 as the BMP concentration was increased from 0 to 25, 100 and 250 ng/mL, respectively. The results were similar after 6 days in culture. As the BMP-2 concentration in the culture medium was increased, the ALP activity of cells on TCPS surfaces increased by factors of 4, 9 and 24, respectively. A parameter used to characterize cellular response is IC_{50}. This value is typically defined as the concentration of a molecule that is required to induce half of the observed maximum response. In our hands, the IC_{50} value for BMP-2 responsiveness was taken as the BMP-2 concentration required to induce half of the maximum observed ALP activity. An IC_{50} value of ~125 ng/mL and 115 ng/mol BMP-2 was obtained from the dose response curves generated in our lab for 3 and 6 days exposure, respectively. These two values were considered to be similar, i.e. no significant difference.

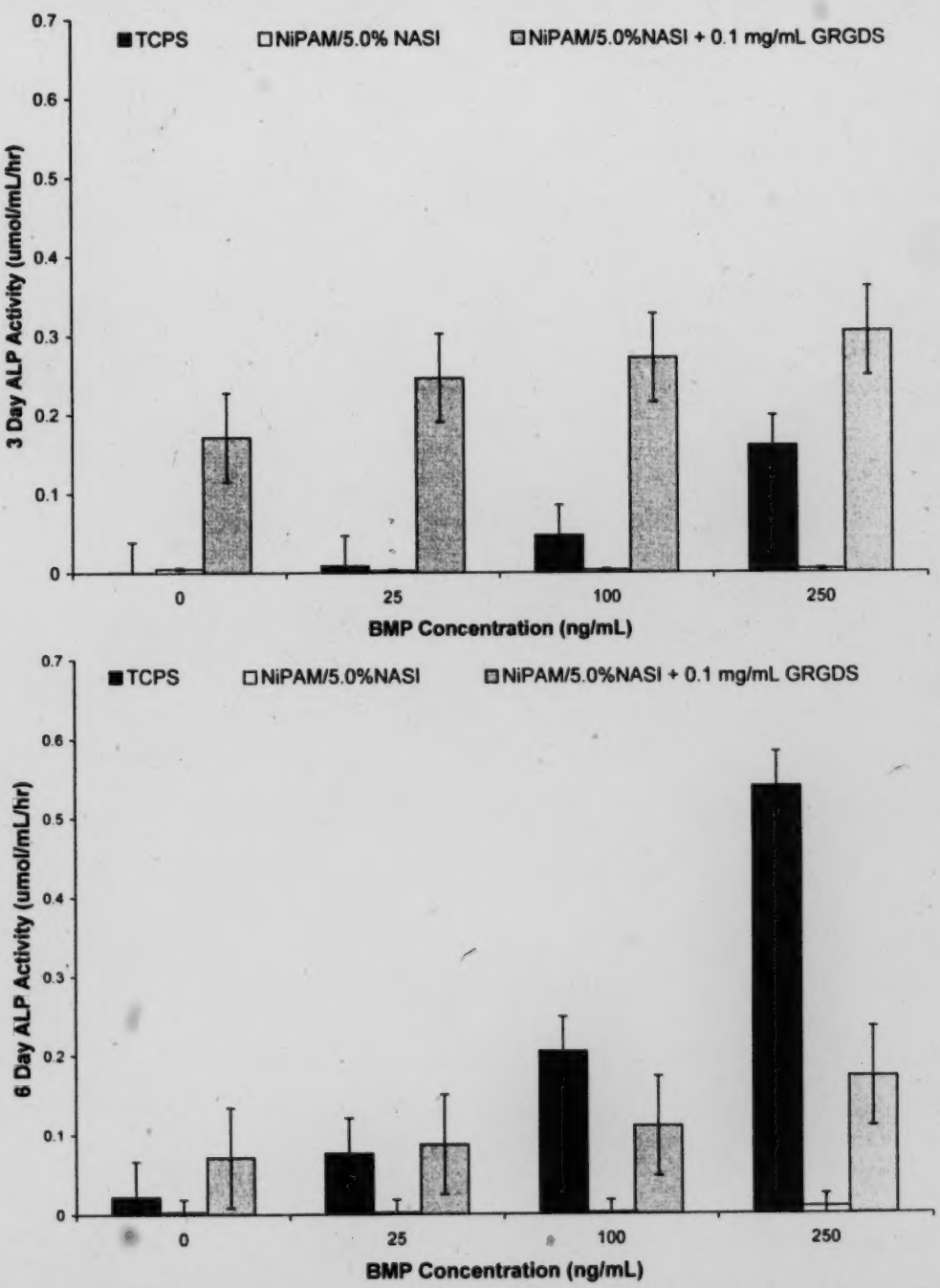

Figure 19 – ALP activity expressed by cells cultured in medium containing varying concentrations of BMP-2 on TCPS, NiPAM/3.8% NASI and GRGDS-conjugated surfaces. Absorbances were measured (405 nm) in triplicate after 3 (top) and 6 (bottom) days of BMP-2 exposure and converted to concentration of p-nitrophenol produced; values displayed are mean ± SD, expressed in μmol/mL/hr. per well (Study III:3).

The amount of BMP-2 required to induce osteoblastic differentiation varies for each cell type in culture; this is illustrated by the IC_{50} values obtained by other researchers who have examined the dose dependent cell response to BMP-2. For skeletal muscle myoblast cells (similar to C2C12 cells used in out studies), an IC_{50} of ~150 ng/mL was reported by Yamaguchi et al. [72], while Takuwa et al. reported an IC_{50} of ~125 mg/mL for MC3T3 cells [73]. For the MLB13MYC clone 14 cell, which is a prechondroblast-like cell line, Rosen et al. reported an IC_{50} value of ~100 ng/mL for the [74]. This dose dependent increase in BMP-2 induced ALP activity was also observed by Winn et al., who established and characterized an immortal human osteoprecursor cell line, OPC1. The OPC1 cell line was chosen for use in their extensive studies to characterize the ability of this particular type of cell line because of its tendency to exhibit the capacity to generate programmed osteoblastic differentiation in the presence of low dose BMP-2 [40]. Winn et al. varied the BMP-2 concentration in the culture medium (0, 10, 50 and 100 ng/mL) to generate a BMP-2 dose response curve for induced ALP activity after 4, 9 and 16 days exposure. An IC_{50} value of 71 ng/mL and 28 ng/mL was obtained for 4 and 9 days of BMP-2 exposure, respectively. While direct comparisons cannot be made between these other cell types and C2C12 cell lines, the IC_{50} values obtained for our C2C12 cells cultured on TCPS surfaces are similar to the IC_{50}s reported for other cell types. This further confirms that the C2C12 cell line was representative of the other cell models found in the bone biology literature; this provided credibility to our ALP activity results for cells cultured on GRGDS-conjugated surfaces.

B. Cell Response to BMP-2 When Cultured on GRGDS-Conjugated Surfaces

The results of Study III:3 (Figure 19) indicated that the cells cultured on GRGDS conjugated surfaces expressed increasing levels of ALP activity (by factors of 1.4, 1.6 and 1.8, compared to NiPAM/NASI surfaces) as the BMP-2 concentration was increased from 0 ng/mL, after 3 days exposure to BMP-2 treatment. After 6 days exposure, cells cultured on the GRGDS-conjugated surfaces, the ALP activity increased by factors of 1.2, 1.5 and 2.4, as the BMP-2 concentration increased from 0 to 25, 100 and 250 ng/mL, respectively (as compared to the NiPAM/NASI surfaces). While these numbers are of significance, the important observation in this study was the increased ALP activity on the GRGDS conjugated surfaces, as compared to TCPS, in the absence of BMP-2. In this particular study, after 3 days, ALP activity on the GRGDS-conjugated vs. the TCPS surfaces was increased by factors of 132, 29, 6 and 2 at BMP-2 concentrations of 0, 25, 100 and 250 ng/mL, respectively.

In general, the results of our studies confirmed that (i) the presence of BMP-2 in the culture medium did not inhibit the ability of the conjugated GRGDS to increase adhesion and spreading to the surface; and (ii) the presence of the conjugated GRGDS on the polymer surface did not inhibit the ability of BMP-2 to induce osteoblastic differentiation in adhered cells. In fact, as mentioned above, these studies indicated that cells cultured on the GRGDS-conjugated surfaces expressed higher levels of ALP activity, in the absence of BMP-2 than the cells cultured on TCPS surfaces (Figure 19).

There are no other studies performed to date, which have explored the feasibility of increasing osteoinductive activity at a local injection site by coinjecting BMP-2 with RGD/NiPAM polymers. It was expected that in the presence of BMP-2, the ALP activity

would be higher when more cells were present to respond (i.e. on the RGD surfaces vs. polymer surfaces); this was true for most experiments performed. The variability in results obtained from different experiments may be due, in part to the exact state of the cells at the time of harvesting and subsequent seeding on the respective surfaces. While a standard protocol was consistently used, the cell growth in the TCPS flasks was somewhat variable and the confluence of cells varied between 80 – 100% confluence at the time of harvest. This may have affected the state of the cells, their metabolic activity and/or their ability to respond to the BMP-2 treatment, once seeded onto the various surfaces.

It is not completely understood why the presence of the conjugated GRGDS peptide increased the ALP activity in the absence of BMP-2. It has been shown that BMP-2 induces the osteoblastic activity through two types of transmembrane receptors in C2C12 cells, BMP type I (BMPRI) and BMP type II (BMPRII) receptors [41]. Both Type I and Type II BMPs are able to bind ligand [70]. The BMPRI is further subclassified into BMPRIA and BMPRIB, and it was shown that the osteoinductive activity of BMP-2 is mediated through BMPRIA in C2C12 cells [41]. This BMP-2 signaling pathway triggers a chain of invents involving a number of Smad proteins, which are the functional signal transducers of the TGFβ/BMP family [71]. The Smad superfamily consists of three classes: (i) Class I (Smad 1 and 5), (ii) Class II (Smad 4) and (iii) Class III (Smads 6 and 7). Smad proteins are known to be associated with various nuclear transcription factors that bind to specific DNA sequences, some of which are involved in differentiation [43, 75-77]. After BMP-ligand binding, the type II receptor phosphorylates the type I receptor, which (now activated) proceeds to

phosphorylate Smad 1. Smads 1 and 5 form heteromeric Smad-Smad complexes with Smad 4, which are translocated into the nucleus where they then able to regulate molecular transcriptional responses of genes involved in osteoblastic differentiation directly [76,77]. A study done by Suzawa et al. examined the BMP signaling pathway and how ECM collagen signals converge with BMP actions [77]. They were able to show that signals activated by the $\alpha_2\beta_1$-integrin (which binds to type I collagen) could potentiate actions otherwise induced by BMP, through their direct effects on the Smad 1 transcriptional activity. The authors did not determine whether the RGD sequence in collagen was responsible for binding the $\alpha_2\beta_1$-integrin.

Integrins are a superfamily of integral membrane proteins (i.e. cell surface receptors), which mediate attachment to the ECM [76-79]. There are 16 α and 8 β transmembrane subunits which hereodimerize to produce more than 20 different receptors, all of which bind a variety of ligands that are components of ECM, such as collagen, fibronectin and vitronectin [78]. This redundancy allows integrins to elicit a large number of different cellular responses, depending on the specific type of integrin receptor expressed, the developmental stage of the cell and according to the composition of the surrounding ECM [28]. Many integrins have an affinity for the RGD sequence in their ECM ligand [79]; for example, the YGRGD peptide is known to engage the $\alpha_v\beta_3$ and $\alpha_5\beta_1$ integrins [80]. The noncallagenous proteins bone sialoprotein (BSP) and osteopontin (OP) contain RGD regions and bind tightly to hydroxyapatite, thereby being involved in bone cell-matrix attachment via cell surface integrins, such as $\alpha_v\beta_5$ [33]. This specific integrin has been found on osteoblasts (as well as $\alpha_1\beta_1$, $\alpha_2\beta_1$, $\alpha_3\beta_1$, $\alpha_5\beta_1$ and

$\alpha_8\beta_1$) and has been reported to mediate cell migration, adhesion and function in other cell systems as well [76].

In summary, we now know that ECM proteins, such as collagen, can bind to integrins, such as $\alpha_2\beta_1$, to stimulate several signaling molecules, which result in Smad 1 transcriptional activity leading to osteoblastic differentiation (without the need for BMP-2) [77]. Other bone ECM proteins, OP and BS, which contain the RGD sequence, can interact with the $\alpha_v\beta_5$ integrin, which is also known to mediate the osteoblastic differentiation [76]. Therefore, due to the ability of many integrins to bind a variety of ligands, it is possible that the RGD sequence on our polymer surfaces also interacts with the $\alpha_v\beta_5$ (or similar) integrin. Perhaps the increased ALP activity on the GRGDS-conjugated polymeric surfaces in the absence of BMP-2 is a result of the ability of the $\alpha_2\beta_1$ and/or $\alpha_v\beta_5$ integrins to bind a variety of ligands and elicit a similar response (i.e. osteoblastic differentiation). While it appears that BMP-2 is not necessary to induce osteoblastic differentiation in C2C12 cells, this may be specific to this particular cell line. Further studies will be required to determine whether the BMP-2-independent differentiation can be universally induced by the RGD surfaces.

C. Cell Density Effects on Cell Response to BMP-2

It was hypothesized that the cell seeding density (which varied from experiment to experiment) had a significant impact on the levels of ALP activity expressed by the cells cultured on the various surfaces, i.e. it affected the ability of the cells to respond to the BMP-2 treatment. A study was designed to assess this possibility, by seeding cells at three different densities on TCPS, NiPAM/15.4%EMA (Polymer U), NiPAM/3.8%NASI

(Polymer E) surfaces. Each surface was treated with either buffer or GRGDS at varying peptide concentrations (0.001, 0.01 and 0.1 mg/mL), as was used in previous studies. The densities chosen were to represent (i) low density, where no immediate differentiation was expected; (ii) intermediate density, which had reached confluence after one day, and was ready for differentiation; and (iii) high density, which had begun to differentiate immediately, thereby maintaining their original phenotype in the presence of BMP-2. The specific densities used were a) 1.3×10^4 cells/cm^2; b) 5.0×10^4 cells/cm^2; and c) 18.8×10^4 cells/cm^2. The results of this study are displayed in Figure 20.

Using the TCPS surface as a positive control, the ALP activity increased when the cell seeding density changed from 1.3 to 5.0×10^4 cells/cm^2, (ALP activity: 0.058 to 0.173 μmol PNP/mL/hr, respectively), but decreased at 18.8×10^4 cells/cm^2 (0.106 μmol PNP/mL/hr), in the presence of BMP-2. Consistent with previous studies, ALP activity was low for the cells cultured on the TCPS surfaces and not exposed to BMP-2 (~ 0.002 μmol PNP/mL/hr).

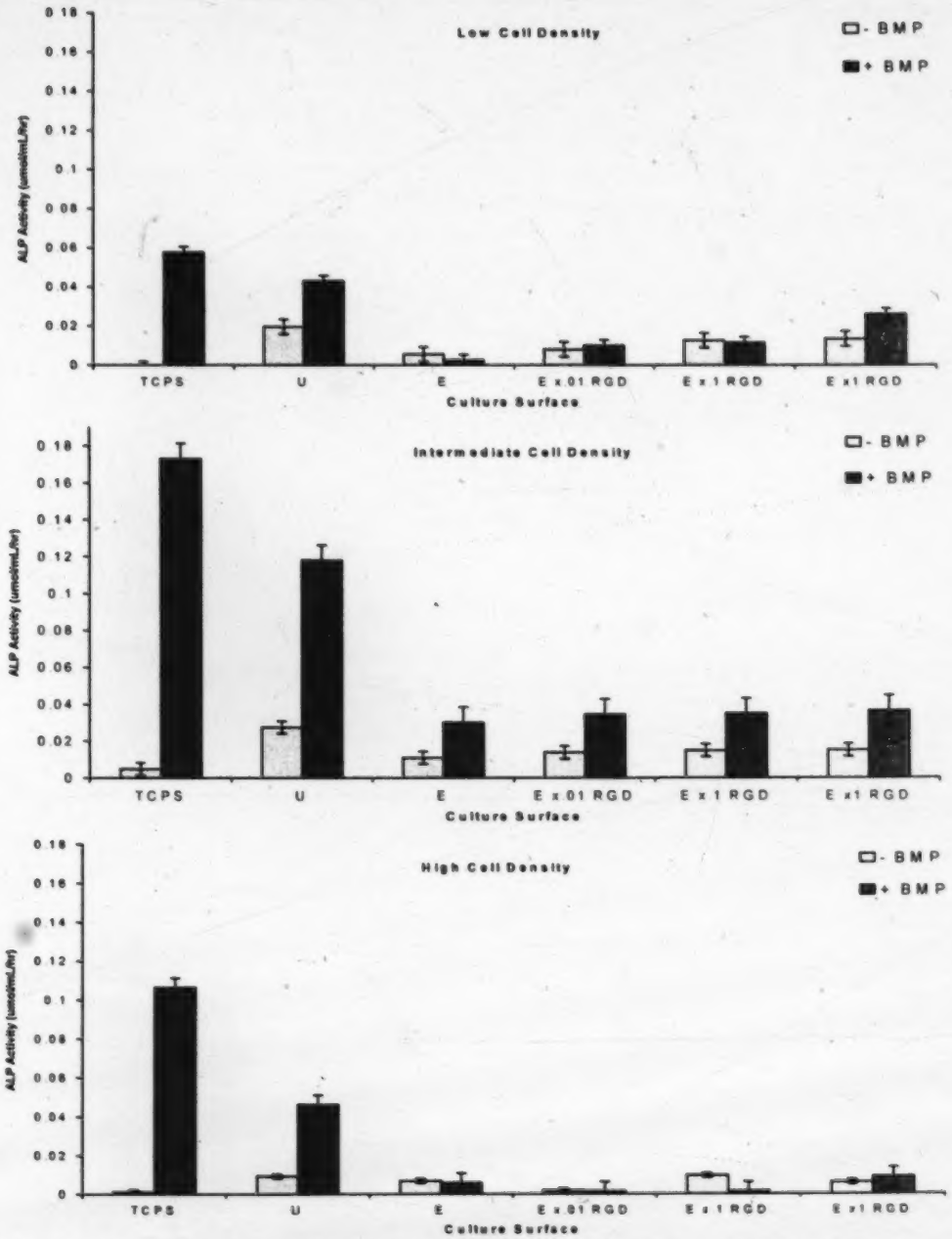

Figure 20 – Effects of cell seeding density on cell response to BMP-2 after 3 days of exposure. ALP activity is expressed in μmol p-nitrophenol/mL/hr. per well, for varying concentrations of GRGDS-conjugated surfaces (where x1 RGD = 0.1 mg/mL GRGDS). TCPS, NiPAM/15.4%EMA (Polymer U) and NiPAM/3.8%NASI (Polymer E) served as control surfaces. Low, intermediate and high seeding densities correspond to 1.3, 5.0 and 18.8 x 10^4 cells/cm^2. All densities were cultured in 48-well plates.

For most samples in this particular study, the ALP activity was slightly higher for cells cultured on the GRGDS-conjugated surfaces than the cells on the buffer-treated NiPAM/NASI surfaces. This was the case whether BMP-2 was present in the culture medium or not. At the lowest cell density, the ALP activity on GRGDS-conjugated surfaces was 4.1, 4.7 and 10.6 times greater (for GRGDS concentrations of 0.001, 0.01 and 0.1 mg/mL, respectively) than the activity on the NiPAM/NASI surfaces, for cells cultured in the presence of BMP-2. For all cell densities tested, in the absence of BMP-2, the ALP activity was higher for cells cultured on GRGDS-conjugated surfaces than the TCPS control surfaces. Even cells cultured on the lowest concentration of GRGDS-conjugated surfaces appeared to express higher ALP activity than the TCPS control. The increased ALP activity appeared to be GRGDS dose responsive, as it increased by factors of 4.2, 6.6 and 7.1, as the GRGDS concentration increased from 0.001 to 0.01 and 0.1 mg/mL, respectively, when compared to the TCPS surface.

The MTT assay was concurrently used in this study to confirm whether the presence of BMP-2 affected cell growth. The intermediate cell seeding density (5.0×10^4 cells/cm^2) was used for this particular experiment because it was hypothesized to be the most effective for BMP-2 induced ALP activity. This data was displayed in Figure 21. Cells were cultured under identical conditions to those whose ALP activity was measured, after 3 days exposure to BMP-2. As expected, the number of cells on the TCPS surfaces was considerably higher than all other surfaces tested. The presence of the GRGDS peptide on the conjugated surfaces continued to increase the number of cells adhered, as compared to the NiPAM/NASI surface, although not by a very large margin. As expected, the cell numbers were considerably less on the latter surfaces. The presence

of BMP-2 in the culture medium did not appear to significantly affect the number of cells adhered to each respective surface. More importantly, the BMP-2 treatment did not affect the cell number, indicating a lack of mitogenic effect of BMP-2 on the cells. These findings were consistent with the expected activity of BMP-2 to act as a morphogen (cell differentiation agent) and not a mitogen (cell proliferation agent).

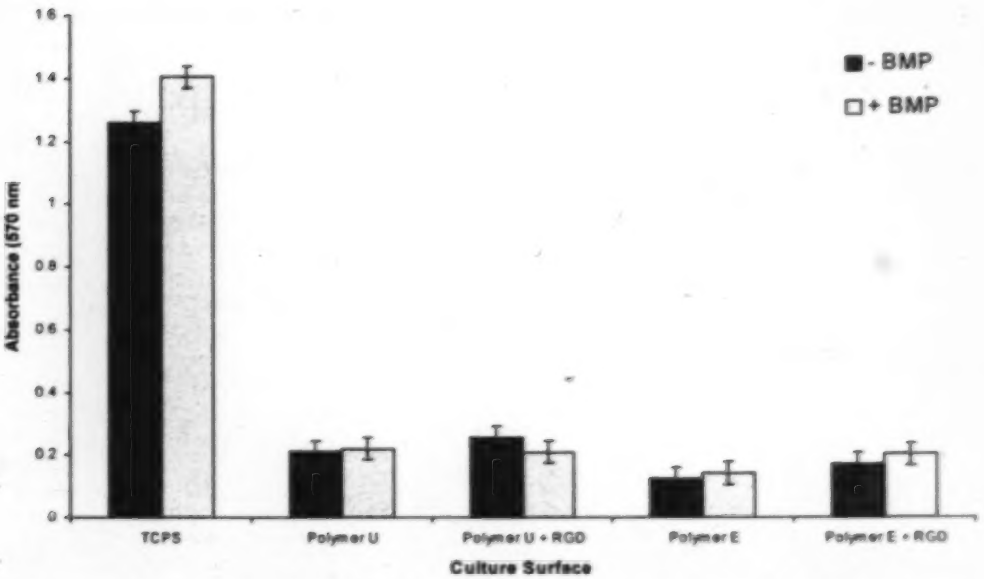

Figure 21 – Effects of BMP-2 exposure on cell growth, measured using the MTT assay. Cells seeded at 5.0 x 10^4 cells/cm^2 onto 48-well plates were incubated in and out of the presence of BMP-2 for 3 days, on TCPS, NiPAM/15.4%EMA (Polymer U), NiPAM/3.8%NASI (Polymer E) and RGD-conjugated (0.1 mg/mL GRGDS) surfaces. Values are expressed as mean ± SD absorbances, read at 570 nm.

In general, it was seen that in the presence of BMP-2, a higher cell number resulted in higher levels of ALP activity; this is just a natural consequence of having a higher number of cells to respond to BMP-2. This 'more is better' theory appeared to be true to a point, beyond which the ALP activity decreased, much the same as seen in the MTT data for cell proliferation rates, once they had reached confluence. This study designed to specifically address this cell density issue confirmed that cells which had

already reached multiple layer confluence when BMP-2 was introduced into the medium expressed lower levels of ALP activity, in general, than those cells which had not reached confluence. In addition, these studies showed that, when seeded at the appropriate density for optimal cell responsiveness (~5.0 x 10^4 cells/cm^2), the increased ALP activity on the GRGDS-conjugated surfaces was directly correlated to the concentration of peptide on the surface, both in and out of the presence of BMP-2 (Figure 20).

Typical of the myoblastic morphology, the cells seeded at the higher density had begun to form myotubules, and adopt an elongated shape, when the BMP-2 was introduced; the lower ALP activity levels is assumed to be correlated to a reduced cellular response in this case. It is hypothesized that because the cells seeded at the high density had already begun to differentiate, they were committed to the myoblastic phenotype and were not able to respond to the BMP-2 to the same extent as the uncommitted cells. This phenomenon was also observed by Winn et al., who reported that rhBMP-2 had no stimulatory effect on either differentiated osteoblasts obtained from human iliac bone or on a differentiated rat-derived osteoblast cell, ROB-C20 [40]. Groeneveld et al. also reported that the differentiation stage of a cell population was an important determinant of the effects of BMP, and that mature fibroblasts could not be induced to express osteogenic parameters after treatment with BMP-2 [71]. It was concluded from this study that there exists an optimum cell seeding density (~ 5.0 x 10^4 cells/cm^2), which will yield the maximum response to the BMP-2. Below this density, the cells are still in a state of rapid proliferation, therefore not 'primed' for BMP-2 induced osteoblastic differentiation, and above which, the cells are already committed to the myoblastic phenotype, therefore not able to respond to the BMP-2.

CONCLUSIONS

The ultimate goal of the research described within this report was to design a biomaterial to stimulate local bone regeneration. Specifically, we aimed to explore the feasibility of conjugating peptides containing the RGD sequence to NiPAM/NASI thermoresponsive polymers, to study the cell adhesion to these surfaces and the cellular response to BMP-2 treatment. These studies yielded promising results, beyond our expectations in some cases, from which we have been able to make several conclusions, which will have a significant impact on the future of bone tissue engineering.

Peptides containing the RGD sequence were successfully conjugated to NiPAM/NASI copolymers via the succinimide ester moieties in the NASI monomers. ^{1}H-NMR effectively confirmed that the peptide was in fact conjugated to the polymer and not free floating in a polymer solution. The peptide/polymer yield in the conjugates was directly correlated to the concentration of peptide in the conjugation reaction, decreasing from 3.8 to 0.7 peptides/polymer chain as the peptide concentration decreased from 2.5 to 0.5 mg/mL. RP-HPLC effectively quantified the conjugation reaction efficiency for RGD-peptides containing hydrophobic residues. The conjugation efficiency on the polymer films was determined to be ~10%.

When applied in the appropriate surface density, the NiPAM/NASI copolymers were found to support little or no C2C12 cell attachment. C2C12 cells cultured on these polymer surfaces remained round and suspended and did not express typical myoblastic morphology (i.e. attached, spread and elongated). This was irrespective of the number of cells seeded onto these surfaces. The bioactivity of the RGD sequence (as assessed by its ability to support cell adhesion) was retained through conjugation to the

NiPAM/NASI polymers. Cell adhesion to RGD-conjugated surfaces was significantly higher than adhesion on NiPAM/NASI surfaces and was comparable to adhesion on TCPS control surfaces. C2C12 cells which adhered to the RGD-conjugated surfaces exhibited typical myoblastic morphology, closely resembling the behavior of cells adhered to the TCPS control surfaces. The increased adhesion on the RGD-conjugated surfaces was directly correlated to the peptide surface density. Studies involving the inactive RGE peptide confirmed that the adhesion on the RGD-conjugated surfaces was biospecific.

BMP-2 treatment induced osteoblastic differentiation in C2C12 cells (as assessed by the induction of ALP activity). The increased ALP activity for cells cultured on TCPS surfaces was directly dependent on the concentration of BMP-2 in the tissue culture medium. The presence of BMP-2 did not affect the cell proliferation rate. The cell metabolic activity decreased once the cells reached confluence and the cell seeding density affected the cell response to the BMP-2 treatment. There appears to be an optimal seeding density, at which the cells are 'primed' for BMP-2 induced osteoblastic differentiation. At lower seeding densities, the cells are still proliferating when BMP-2 is introduced, resulting in a low response. At higher seeding densities, the cells have already begun to differentiate into their pre-designated phenotype when the BMP-2 is introduced, and are therefore not able to respond. In the absence of BMP-2 treatment, cells cultured on RGD-conjugated surfaces expressed higher levels of ALP activity than those cells cultured on TCPS surfaces. Most importantly, the presence of the conjugated RGD sequence induces osteoblast activity in C2C12 cells without the need for BMP-2 treatment.

FUTURE DIRECTION

The aim of this project was to develop a biomaterial, which would support and enhance osteoblast adhesion at a local injection site, while effectively delivering BMP-2 for sustained release. There are, of course, many issues to resolve and many factors to consider when attempting such an ambitious task. The studies described in this report have given us a fairly good, general understanding of the cell behavior, their response to the various surfaces, and to BMP-2 treatment. Having said this, the findings of this report are just one small step towards the ultimate goal of regenerating bone tissue, which will take many years of continued dedication and funding to achieve.

The single most significant finding of these studies was that the conjugated RGD sequence induces increased ALP activity in the absence of BMP-2 treatment. Extensive studies should be conducted to further explore this phenomenon, why it is occurring and if it is controllable. The involvement of integrins and Smad proteins in the BMP-2 signaling pathway is an intriguing area of study, which will need to be researched further, to optimize this system. More specifically, the effects of the specific cell type on these interactions should be explored. For subsequent *in vitro* studies, a cell line of osteoblastic lineage, such as the OPC1 line would be ideal, based on its ability to exhibit programmed osteoblast differentiation in the presence of low doses of BMP-2. The cell seeding densities may be the key to controlling the BMP-2 induced differentiation; the RGD-containing thermoreversible polymers will become essential for manipulating this parameter *in vivo*, i.e. recruiting an optimal cell population and density to the site.

In order for these RGD-containing polymers to be useful *in vivo*, the current system must be adapted to evolve from surface manipulation to a three-dimensional medium for osteoblast adhesion. A three-dimensional culture system will be more representative of in vivo conditions. Furthermore, the current surface conjugation coating technique is not practical for animal studies. To resolve this, it will be necessary to develop a better conjugation technique that can be scaled-up for animal studies. In order to recruit the optimal number of cells at the site of BMP-2 injection, it will be essential to maximize the number of RGD moieties at that site, which are available to interact with the cell population.

We have designed and developed a polymer system which uses the specific adhesive properties of the ubiquitous RGD sequence to augment the number of cells at specific site, which in turn results in increased osteoblast activity at that site. This system provides a small fragment in the foundation for a new era of biomaterials for use in regenerative medicine. While there are still many avenues to be explored, our RGD-containing polymer has the potential to make a significant impact on the field of bone tissue engineering.

REFERENCES

1. Kanis, J.A., (1996). Textbook of Osteoporosis, Blackwell Science Ltd., Cambridge Massachusetts, USA, pgs 213-216

2. Gittens, S.A.; Uludag, H. (2001). Growth factor delivery for bone tissue engineering. *Journal of Drug Targeting* Vol. Not known: 1-20

3. H.Reginster, J-Y.; Taquet, A.N.; Gosset, C. (1988). Therapy for osteoporosis: miscellaneous and experimental agents. *Endocrin. Metab. Clin. N.Amer.* 27:453-463

4. Trippel, S.B.; Coutts, R.D.; Einhorn, T.A.; Mundy, G.R.; Rosenfeld, R.G. (1996). Growth factors as therapeutic agents. *J. Bone Joint Surgery* 78A: 1272-1286

5. Uludag, H., D'Augusta, D., Golden, J., Timony, G., Riedel, R., Wozney, J.M. (2000). Implantation of recombinant human bone morphogenetic proteins with biomaterial carriers: A correlation between pharmacokinetics and osteoinduction in the rat ectopic model. *J Biomed Mater Res* 50:227-238

6. Yasko, A.W.; Lane, J.M.; Fellinger, E.J.; Rosen, V.; Wozney, J.M.; Wang, E.A. (1992). The healing of segmental bone defects, induced by recombinant human bone morphogenetic protein (rhBMP-2). A radiographic, histological, and biomechanical study in rats. *J Bone Joint Surg Am* 74:659-670

7. Gerhart, T.N.; Kirker-Head, C.A.; Kriz, M.J.; Holtrop, M.E.; Henning, G.E.; Hipp, J.; Schelling, S.H.; Wang, E. (1993). Healing segmental femoral defects in sheep using recombinant human bone morphogenetic protein. *Clin Orthop* 293:317-326

8. Cook, S.D.; Wolfe, M.W.; Salkeld, S.L.; Rueger, D.C. (1995). Effect of recombinant human osteogenic protein-1 on healing of segmental defects in non-human primates. *J Bone Joint Surg Am* 77:734-750

9. Bulstra, S. (1998) Experiences in human delayed non-unions using OP-1 (BMP-7). *Proceedings, First European Conference on Bone Morphogenetic Proteins*. Abstract 62.

10. Geesink, R.G.T.; Hoefnagels, N.H.M.; Bulstra, S.K. (1999). Osteogenic activity of OP-1 bone morphogenetic protein (BMP-7) in human fibular defect. *J Bone Joint Surg [Br]* 81B:710-718

11. Franceschi, R.T.; Wang, D.; Krebsbach, P.H.; Rutherford, R.B. (2000). Gene therapy for bone formation: In vitro and in vivo osteogenic activity of an adenovirus expressing BMP7. *J Cell Biochem* 78: 476-486

12. Uludag, H.; Gao, T.; Wohl, G.R.; Kantoci, D.: Zernicke, R.F. (2000). Bone affinity of a bisphosphonate-conjugated protein in vivo. *Biotech. Drug* 16: 258-267

13. Hubbell, J.A. (1995). Biomaterials in tissue engineering. *Bio/tech.* 13: 565-576

14. Winn, S.R.; Uludag, H.; Hollinger, J.O. (1998). Sustained release emphasizing recombinant human bone morphogenetic protein-2. *Advanced Drug Delivery Reviews* 31: 303-318

15. Hoffman, A.S. et al. (2000). Really smart bioconjugates of smart polymers and receptor proteins (Founder's Award, Sixth World Biomaterials Congress 2000). *J Biomed Mater Res* 52: 577-586

16. Uludag, H. (1998). Osteoinductive alternatives and bone substitutes. *Current Opinion in Orthopedics* 9:VI:31-37

17. Stile, R.A.; Burghardt, W.R.; and Healy, K.E. (1999). Synthesis and characterization of injectable poly(N-isopropylacrylamide)-based hyrogels that support tissue formation in vitro. *Macromolecules* 32:7370-7379

18. Chung, J.E.; Yokoyama, M.; Aoyagi, T.; Sakurai, Y.; and Okano, T. (1998). Effect of molecular architecture of hydrophobically modified poly(N-isopropylacrylamide) on the formation of thermoresponsive core-shell micellar drug carriers. *Journal of Controlled Release* 53; 119-130

19. Chung, J.E.; Yokoyama, M.; Yamato, M.; Aoyagi, T.; Sakurai, Y.; Okano, T. (1999). Thermo-responsive drug delivery from polymeric micelles constructed using block copolymers of poly(N-isopropylacrylamide) and poly(butylmethacrylate). *Journal of Controlled Release* 62:115-127

20. Chung, J.E.; Yokoyama, M.; Suzuki, K.; Aoyagi, T.; Sakurai, Y.; Okano, T. (1997). Reversibly thermo-responsive alkyl-terminated poly(N-isopropylacrylamide) core-shell micellar structures. *Colloids and Surfaces B: Biointerfaces* 9:37-48

21. Uludag, H.; Wong, M.; and Man, J. (2000). Reactivity of temperature-sensitive, protein-conjugating polymers prepared by a photopolymerization process. *Journal of Applied Science* 75:583-592

22. Uludag, H. and Fan, X. (2000). Synthesis and characterization of thermoreversible, protein-conjugating polymers based on N-isopropylacrylamide. Chapter 25, *American Chemical Society Symposium Series 752 for Controlled Drug Delivery*

23. Rollason, G.; Davies, J.E.; Sefton, M.V. (1993). Preliminary report on cell cultures on a thermally reversible copolymer. *Biomaterials* 14(2); 153-5

24. Chen, G.; Imanishi, Y.; Ito, Y. (1998). Effect of protein and cell behavior on pattern-grafted thermoresponsive polymer. *J Biomed Mater Res* 42:38-44

25. von Recum, H.A.; Wan Kim, S.; Kikuchi, A.; Okuhara, M.; Sakurai, Y.; Okano, T. (1998). Novel thermally reversible hydrogel as detachable cell culture substrate. *J Biomed Mater Res* 40:631-9

26. Collier, T.O.; Anderson, J.M.; Kikuchi, A.; Okano, T. (2002). Adhesion behavior of monocytes, macrophages and foreign body giant cells on poly(N-isopropylacrylamide) termperature-responsive surfaces. *J Biomed Mater Res* 59:136-143

27. DeFife, K.M.; Shive, M.S.; Hagen, K.M.; Clapper, D.L.: Anderson, J.M. (1999). Effects of photochemically immobilized polymer coatings on protein adsorption, cell adhesion and the foreign body reaction to silicone rubber. *J Biomed Mater Res* 44:298-307

28. Gronthos, S.; Simmons, P.J.; Graves, S.E.; Robey, P.G. (2001). Integrin-mediated interactions between human bone marrow stromal precursor cells and the extracellular matrix. *Bone* 28(2): 174-181

29. Dee, K.C.; Andersen, T.T.; Bizios, R. (1998). Design and function of novel osteoblast-adhesive peptides for chemical modification of biomaterials. *J Biomed Mater Res* 40: 371-7

30. Neff, J.A.; Caldwell, K.D.; Tresco, P.A. (1998). A novel method for surface modification to promote cell attachment to hydrophobic substrates. *J Biomed Mater Res* 40:511-9

31. Dobkowski, J.; Kolos, R.; Kaminski, J.; Kowalczynska, H.M. (1999). Cell adhesion to polymeric surfaces: Experimental study and simple theoretic approach. *J Biomed Mater Res* 47: 234-242

32. Hern, D.L.; Hubbell, J.A. (1998). Incorporation of adhesion peptides into nonadhesive hydrogels useful for tissue resurfacing. *J Biomed Mater Res* 39:266-276

33. Rezania, A.; Thomas, C.H.; Branger, A.B.; Waters, C.M.; Healey, K.E. (1997). The detachment strength and morphology of bone cells contacting materials modified with a peptide sequence found within bone sialoprotein. *J Biomed Mater Res* 37:9-19

34. Mann, B.K.; Tsai, A.T.; Scott-Burden, T.; West, J.L. (1999). Modification of surfaces with cell adhesion peptides alters extracellular matrix deposition. *Biomaterials* 20:2281-2286

35. Banerjee, P.; Irvine, D.J.; Mayes, A.M.; Griffith, L.G. (2000). Polymer latexes for cell-resistant and cell-interactive surfaces. *J Biomed Mater Res* 50:331-339

36. Porte-Durrieu, M.C.; Labrugere, C.; Villars, F.; Lefebvre, F.; Dutoya, S.; Guette, A.; Bordenave, L.; Baquey, C. (1999). Development of RGD peptides grafted onto silica surfaces: XPS characterization and human endothelial cell interactions. *J Biomed Mater Res* 46:368-375

37. Gobin, A.; Tsai, A.; Mann, B.; McIntire, L.; West, J. (2001). Cell migration through hydrogels containing adhesive and degradable peptide sequences. *2001 Society for Biomaterials – 27th Annual Meeting Transactions*. p208

38. Uludag, H.; Golden, J.; Palmer, R.; Wozney, J.M. (1999). Biotinated bone morphogenetic protein-2: In vivo and in vitro activity. *Biotechnol Bioeng* 65:668-672

39. Winn, S.R.; Randolph, G.; Uludag, H.; Wong, S.C.;, Hair, G.A.; Hollinger, J.O. (1999). Establishing an immortalized human osteoprecursor cell line: OPC1. *Journal of Bone and Mineral Research* 14:1721-1733

40. Yang, X., Matsuura, H., Fu, Y., Sugiyama, T., Miura, N. (2000). MFH-1 is required for bone morphogentic protein-2-induced osteoblastic differentiation of C2C12 myoblasts. *Federation of European Biochemical Societies Letters* 470: 29-34

41. Nishimura, R., Kato, Y., Chen, D., Harris, S.E., Mundy, G.R., Yoneda, T. (1998). Smad5 and DPC4 are key molecules in mediating BMP-2-induced osteoblastic differentiation of the pluripotent mesenchymal precursor cell line C2C12. *Journal of Biological Chemistry* 273(4): 1872-1879

42. Soo Shin, C., Lecanda, F., Sheikh, S., Weitzmann, L., Cheng, S., Civitelli, R. (2000). Relative abundance of different cadherins defines differentiation of mesenchymal precursors into osteogenic, myogenic, or adipogenic pathways. *Journal of Cellular Biochemistry* 78:566-577

43. Kirsch, T., Nickel, J., Sebald, W. (2000). BMP-2 antagonists emerge from alterations in the low-affinity binding epitope for receptor BMPR-II. *The European Molecular Biology Organization Journal* 19 (3): 3314-3324

44. Uludag, H.; Sefton, M.V. (1990). Colorimetric assay for cellular activity in microcapsules. *Biomaterials* 11:708-712

45. Janeway, C.M.L.; Xu, X.; Murphy, J.E.; Chaidaroglou, A.; Kantrowitz, E.R. (1993). Magnesium in the active site of escherichia coli alkaline phosphatase is important for both structural stabilization and catalysis. *Biochemistry* 32:1601-1609

46. Wen, J.; Arakawa, T.; Philo, J.S. (1996). Size-exclusion chromatography with on-line light scattering, absorbance and refractive index detectors for studying proteins and their interactions. *Anal. Biochem.* 240: 155-166

47. Uludag, H.; Kousinioris, N.; Gao, T.; Kantoci, D. (2000). Bisphosphonate conjugation to proteins as a means to impart bone affinity. *Biotechnol Prog.* 16:258-267

48. Stile, R.A.; Healy, K.E. (2001). Thermo-responsive peptide-modified hydrogels for tissue regeneration. *Biomacromolecules* 2:185-194

49. Smith, E.; Oxenford, C.; Somayagi, R.; Yang, J.; Uludag, H.; (2002). Conjugation of RGD-peptides to thermoreversible polymers. *Journal of Applied Polymer Science* (submitted)

50. Yang, J.; Singh, P.; Somayagi, V.; Uludag, H. (2000). End-functionalized thermosensitive polymers for protein conjugation. *Bioconjugate Chemistry* (submitted)

51. Bromberg, L.E.; Ron, E.S. (1998). Temperature-responsive gels and thermogelling polymer matrices for protein and peptide delivery. *Advanced Drug Delivery Review* 31:197-221

52. Pitt, C.G.; Shah, S.S. (1995). Manipulation of the rate of hydrolysis of polymer-drug conjugates: the degree of hydration. *Journal of Controlled Release* 33:397-403

53. Takezawa, T.; Mori, Y.; Yoshizato, K. (1990). Cell culture on a thermo-responsive polymer surface. *Biotechnology* 8:854-856

54. Yamada, N.; Okano, T.; Sakai, H.; Karikusa, F.; Sawasaki, Y.; Sakurai, Y. (1990). Thermo-responsive polymeric surface: Control of attachment and detachment of cultured cells. *Macromol. Chem. Rapid Commun.* 11:571-576

55. Okano, T.; Yamada, N.; Okuhara, M.; Sakai, H.; Sakurai, Y. (1995). Mechanism of cell detachment from temperature-modulated, hydrophilic-hydrophobic polymer surfaces. *Biomaterials* 16:297-303

56. Chen, G.; Ito, Y.; Imanishi, Y. (1997). Regulation of growth and adhesion of cultured cells by insulin conjugated with thermoresponsive polymers. *Biotechnol Bioeng* 53:339-344

57. Kwon, O.H.; Kikuchi, A.; Yamato, M.; Sakurai, Y.; Okano, T. (2000). Rapid cell sheet detachment from poly(N-isoproprylacrylamide)-grafted porous cell culture membranes. *J Biomed Mater Res* 50:82-89

58. Cook, A.D.; Hrkach, J.S.; Gao, N.N.; Johnson, I.M.; Pajvani, U.B.; Cannizzaro, S.M.; Langer, R. (1997). Characterization and development of RGD-peptide-modified poly(lactic acid-co-lysine) as an interactive resorbable biomaterial. *J Biomed Mater Res* 35(4); 513-523

59. Lin, H.; Sun, W.; Mosher, D.F. (1994). Synthesis, surface, and cell-adhesion properties of polyurethanes containing covalently grafted RGD-peptides. *J Biomed Mater Res* 28(3); 329-342

60. Rezania, A.; Healy, K.E. (1999). Biomimetic peptide surfaces that regulate adhesion, spreading, cytoskeletal organization, and mineralization of the matrix deposited by ssteoblast-like cells. *Biotechnol. Prog.* 15: 19-32

61. Massia, S.P.; Hubbell, J.A. (1991). An RGD spacing of 440 nm is sufficient for integrin $\alpha_v\beta_3$-mediated fibroblast spreading and 140 nm for focal contact and stress fiber formation. *J. Cell Biol.* 114:1089-1100

62. Freimoser, F.M.; Jakob, C.A.; Aebi, M.; Tuor, U. (1999). The MTT [3-(4,5-dimethylthiazol-2-yl)-2,5-diphenyltetrazolium bromide] assay is a fast and reliable method for colorimetric determination of fungal cell densities. *Applied and Environmental Microbiology* 65(8); 3727-3729

63. Geng, L.; Pfister, S.; Kraeft, S.; Rudd, C.E. (2001). Adaptor FYB (Fyn-binding protein) regulates inegrin-mediated adhesion ad mediator release: Differential involvement of the FYB SH3 domain. *PNAS* 98(20):11527-1532

64. Russel, C.A.; Vindelov, L.L. (1998). Optimization and comparison of the MTT assay and the 3H-TdR assay for the detection of IL-2 in helper T cell precursor assays. *J Immunol Methods* 217(1-2):165-175

65. Loster, K.; Schuler, C.; Heidrich, C.; Horstkorte, R.; Reutter, W. (1997). Quantification of cell-matrix and cell-cell adhesion using horseradish peroxidase. *Anal Biochem* 244:96-102

66. Yang, T.; Sinai, P.; Kain, S.R. (1996). An acid phophatase assay for quantifying the growth of adherent and nonadherent cells. *Anal Biochem* 241:103-108

67. Derhami, K.; Wolfaardt, J.F.; Wennerberg, A.; Scott, P.G. (2000). Quantifying the adherence of fibroblasts to titanium and its enhancement by substrate-attached material. *J Biomed Mater Res* 52:315-322

68. Kilpadi, K.L.; Chang, P.; Bellis, S.L. (2001). Hydroxyapatite binds more serum proteins, purified integrins and osteoblast precursor cells than titanium or steel. *J Biomed Mater Res* 57:258-267

69. Tamura, Y.; Takeuchi, Y.; Suzawa, M.; Fukumoto, S.; Kato, M.; Miyazono, K.; Fujita, T. (2001). Focal adhesion kinase activity is required for bone morphogenetic protein – smad1 signaling and osteoblastic differentiation in murine MC3T3-E1 cells. *Journal of Bone and Mineral Research* 16(10):1772-1779

70. Wozney, J.M.; Rosen, V. (1998). Bone morphogenetic protein and bone morphogenetic protein gene family in bone formation and repair. *Clinical Orthopaedics and Related Research* 346:26-37

71. Groenveld, E.H.J.; Burger, E.H. (2000). Bone morphogenetic proteins in human bone regeneration. *European Journal of Endocrinology* 142:9-21

72. Yamaguchi, A.; Katagiri, T.; Ikeda, T.; Wozney, J.M.; Rosen, V.; Wang, E.A.; Kahn, A.J.; Suda, T.; Yoshiki, S. (1991). Recombinant human bone morphogenetic protein-2 stimulates osteoblastic maturation and inhibits myogenic differentiation in vitro. *Journal of Cell Biology* 113(3):681-687

73. Takuwa, Y.; Ohse, C.; Wang, E.A.; Wozney, J.M.; Yamashita, K. (1991). Bone morphogenetic protein-2 stimulates alkaline phosphatase activity and collagen synthesis in cultured osteoblast-like cells. *Biochemical and Biophysical Research Communications* 174(1):96-101

74. Rosen, V.; Nove, J.; Song, J.J.; Thies, R.S.; Cox, K.; Wozney, J.M. (1994). Responsiveness of clonal limb bud cell lines to bone morphogenetic protein 2 reveals a sequential relationship between cartilage and bone cell phenotypes. *Journal of Bone and Mineral Research* 9(11):1759-1768

75. Weinstein, M.; Monga, S.P.S.; Liu, Y.; Brodie, S.G.; Tang, Y.; Li, C.; Mishra, L.; Deng, C. (2001). Smad proteins and hepatocyte growth factor control parallel regulatory pathways that converge on β1-integrin to promote normal liver development. *Molecular and Cellular Biology* 21(15):5122-5131

76. Lai, C.; Nishimura, R.; Teitelbaum, S.L.; Avioli, L.; Ross, F.P.; Cheng, S. (2000). Transforming growth factor-β up-regulates the β_5 integrin subunit expression via Sp1 and Smad signaling. *Journal of Biological Chemistry* 275(16):36400-36406

77. Suzawa, M.; Tamura, Y.; Fukumoto, S.; Miyazono, K.; Fujita, T.; Kato, S.; Takeuchi, Y. (2002). Stimulation of Smad1 transcriptional activity by ras-extracellular signal-regulated kinase pathway: A possible mechanism for collagen-dependent ssteoblastic differentiation. *Journal of Bone and Mineral Research* 17(2):240-247

78. Clark, E.A.; Brugge, J.S. (1995). Integrins and signal transduction pathways: The road taken. *Science* 268:233-239

79. Heidemann, S.R. (1993). A new twist on integrins and the cytoskeleton. *Science* 260: 1080-1082

80. Maheshwari, G.; Brown, G.; Lauffenburger, D.A.; Wells, A.; Griffith, L.G. (2000). Cell adhesion and motility depend on nanoscale RGD clustering. *Journal of Cell Science* 113: 1677-1686

APPENDIX A

^{1}H-NMR Spectra

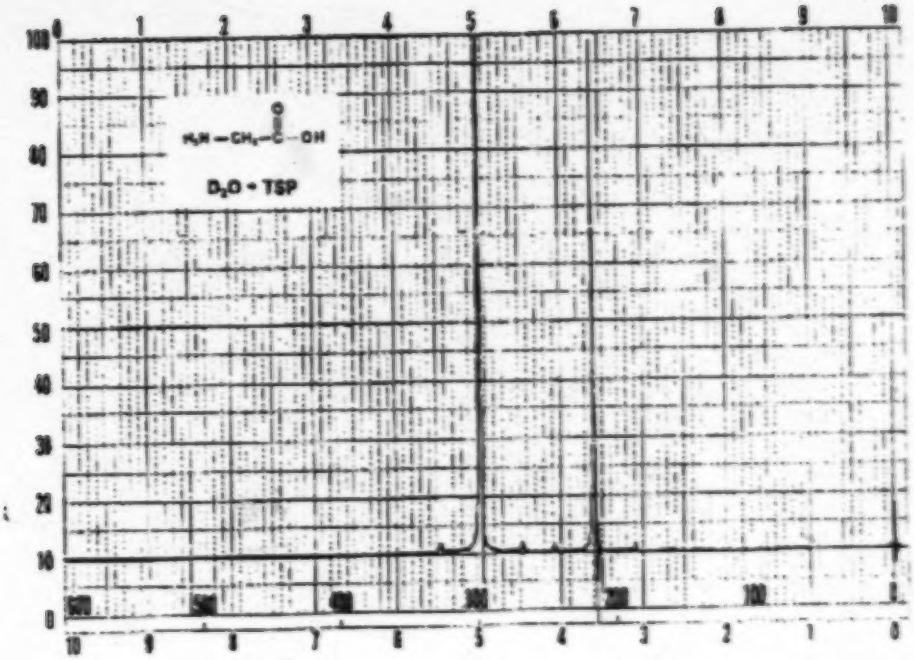

Figure A1 – Aldrich ^{1}H-NMR Spectrum for Glycine.

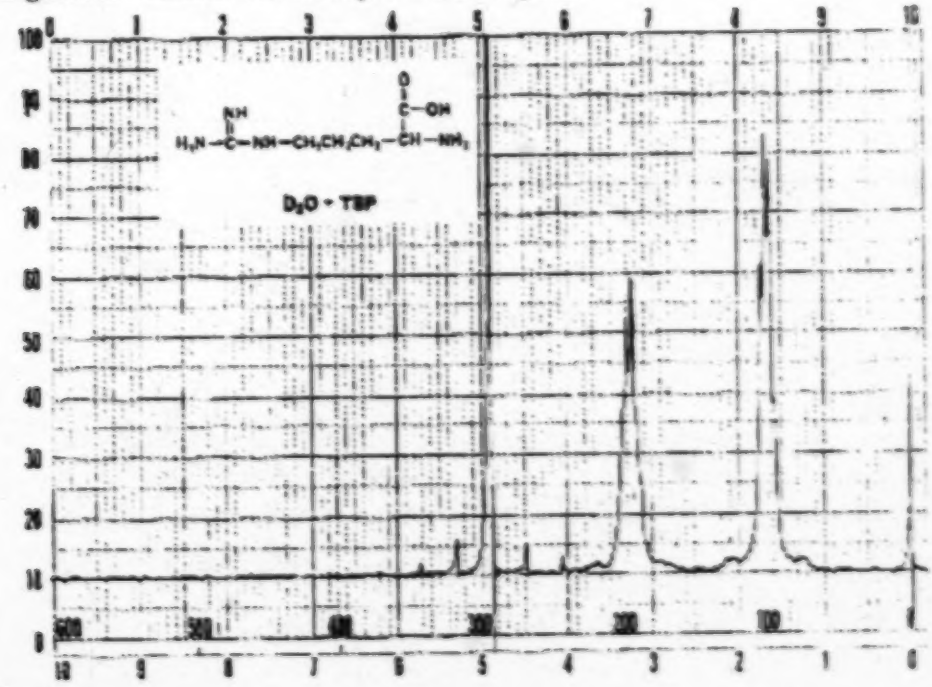

Figure A2 – Aldrich ^{1}H-NMR Spectrum for Arginine.

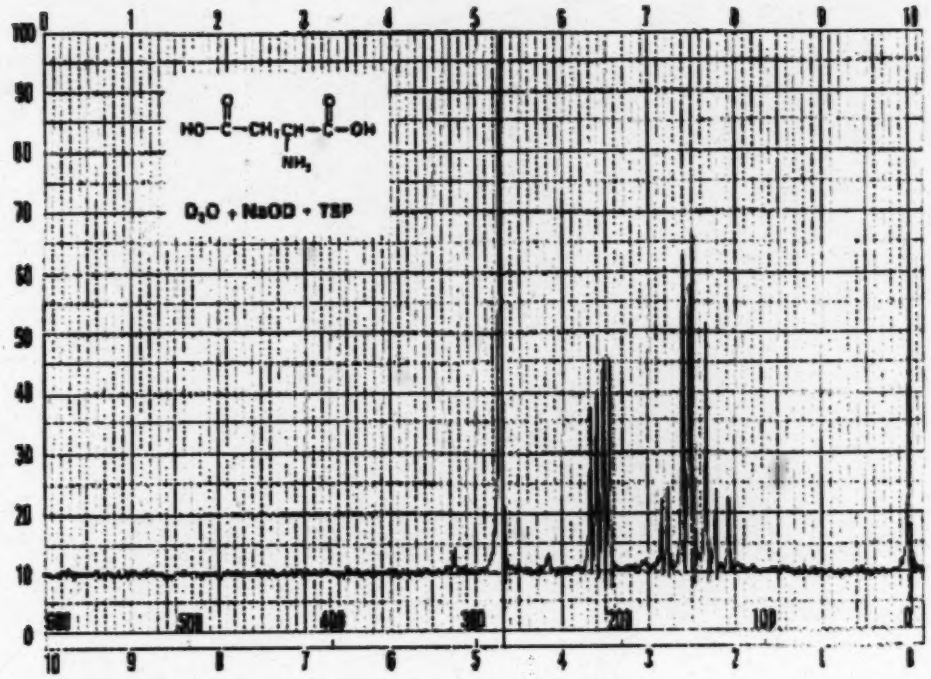

Figure A3 – Aldrich ^{1}H-NMR Spectrum for Aspartic Acid.

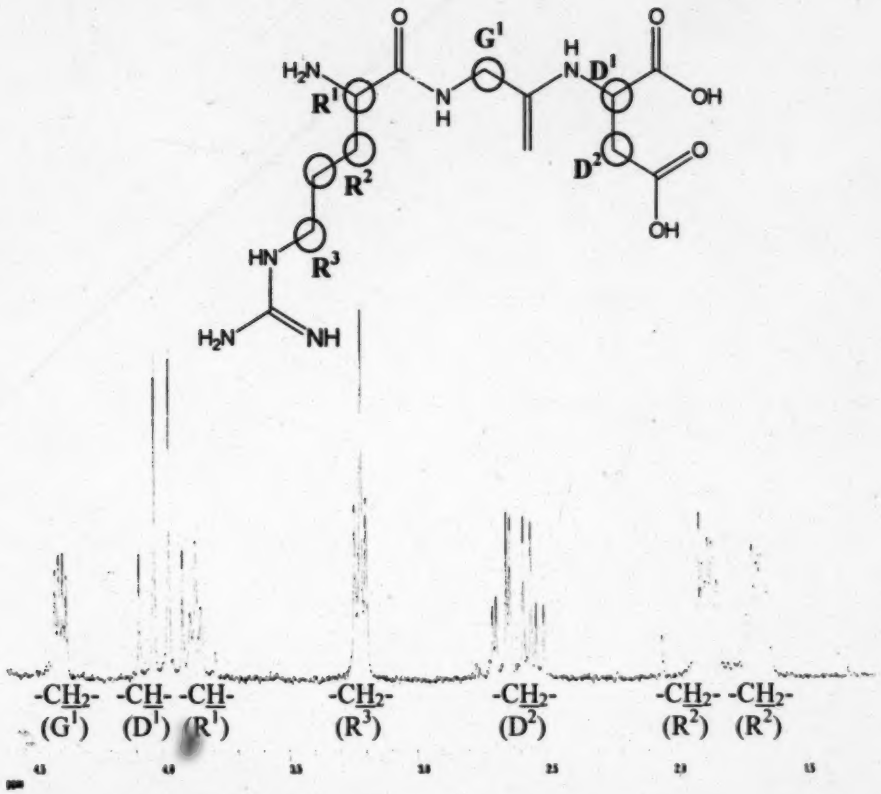

Figure A4 – ^{1}H-NMR Spectrum obtained in our lab for the RGD peptide. The chemical groups corresponding to each individual peak in this spectrum (as determined using the Aldrich spectra for Arginine, Glycine and Aspartic Acid, Figures A1, A2, A3, respectively) are illustrated in the diagram included above.